Faculty of Medicine and Dentistry

Department of Human Neurosciences

PhD in Clinical-Experimental Neuroscience and Psychiatry

XXXVI course

"NEUROIMAGING CORRELATES OF BRADYKINESIA IN PATIENTS WITH ESSENTIAL TREMOR"

Supervisor:

Prof. Matteo Bologna

PhD student:

Donato Colella

1325093

Academic Year 2023/2024

SAPIENZA
UNIVERSITÀ DI ROMA

Alla mia famiglia
A Irene

SUMMARY:

Abbreviations: Analysis of variance (ANOVA); Beck Depression Inventory (BDI-II); Basal Ganglia (BG); Blood Oxygenation Level-Dependent(BOLD); BTS Engineering(BTS); Cerebrospinal Fluid (CSF); coefficient of variation (CV); Dopamine Transporter (DAT); Dentate Nucleus (DN); Essential tremor (ET); Frontal Assessment Battery (FAB), FMRIB Automated Segmentation Tool (FAST); Functional Connectivity (FC); false discovery rate (FDR); FMRIB's Integrated Registration and Segmentation Tool (FIRST); FMRIB's Linear Image Registration Tool (FLIRT); FMRIB's Non-Linear Image Registration Tool (FNIRT); Field of View (FOV); FMRIB's Software Library (FSL); Fahn-Tolosa-Marin Tremor Rating Scale (FTMTRS); Grey Matter (GM); Globus Pallidus (GP); Internal Globus Pallidus (GPi); External Globus Pallidus (GPe); G root mean square squared (GRMS^2); Healthy Subjects(HS); Independent Component Analysis-Automatic Removal of Motion Artifacts (ICA-AROMA); Levodopa equivalent daily dose (LEDD); Movement Disorder Society-sponsored revision of the Unified Parkinson's Disease Rating Scale, part III (MDS-UPDRS-III); Montreal Neurological Institute (MNI); Montreal Cognitive Assessment (MoCA); Magnetization-Prepared Rapid Gradient-Echo (MPRAGE); MRI (Magnetic Resonance Imaging); Ordered subset expectation maximization (OSEM); Parkinson's disease (PD); Root-Mean-Square (RMS); resting-state functional magnetic resonance imaging (rs-fMRI); specific binding ratio (SBR); standard deviation (SD); Structural Imaging Evaluation of Normalized Atrophy (SIENAX); System SMART motion (SMART); Single-photon emission computed tomography (SPECT); Spatially Unbiased Infratentorial Template (SUIT); scans without evidence for dopaminergic deficit (SWEDD); Visual-motor coordination (VMC); White Matter (WM).

1. ABSTRACT

Essential tremor (ET) is a movement disorder characterized primarily by postural and kinetic tremor of the upper limbs. The presence of etiological variability and additional symptoms of uncertain significance configures it as heterogeneous clinical syndrome. In ET, movement slowness without sequence effect has objectively been documented by kinematic analysis of repetitive movements of the upper limb and fingers. When movement slowness (bradykinesia) or other soft neurological signs are present, the new tremor classification suggests the term ET-plus.

Bradykinesia is the cardinal symptom of Parkinson's disease (PD) and is typically related to basal ganglia (BG) dysfunction. Although the role of the cerebellum as a central tremor oscillator is well known in ET, the involvement of other brain areas, such as the BG, as determinants of bradykinesia is unclear. Recently, a dysfunction of brain networks was hypothesized as the substrate of bradykinesia in PD, and it is not excluded that the same occurs in ET.

In the present thesis, we will first provide an updated overview of altered voluntary movement execution in ET and discuss major findings from clinical and experimental studies.

In the experimental part of this thesis, we will show the results of two studies aimed at identifying voluntary movement abnormalities in ET patients using an optoelectronic kinematic system. Repetitive finger movements, the most useful task for bradykinesia assessment in PD clinical practice, were analysed. Various parameters were measured, including movement velocity, amplitude and velocity and amplitude reduction during movement repetition. Then, we will aim to demonstrate the possible neuroradiological substrates of bradykinesia in ET, correlating the kinematic parameters of finger movements to the results provided by dopamine transporter single-photon emission computed tomography (DAT-SPECT) in the first study and volumetric and functional magnetic resonance imaging (MRI) in the second. The data suggested a possible role of the BG and cerebellum in the genesis of impaired voluntary movement in ET, further confirming the heterogeneity of this neurological condition.

2. INTRODUCTION

According to the Consensus Statement on the Classification of Tremors of the Movement Disorder Society (MDS), ET is defined as an isolated tremor syndrome characterized by a bilateral action tremor of the upper limbs, lasting at least 3 years, with or without tremor in other locations (e.g., head, voice, lower limbs) and in the absence of other neurological signs, such as dystonia, ataxia or parkinsonism (Bhatia et al., 2018). The Task Force also introduced a new clinical entity called ET "plus", i.e., a tremor syndrome with the characteristics of ET, associated with neurological symptoms and signs defined as "soft", in doubtful relation to the tremor. These soft signs comprise an impaired tandem gait, a questionable dystonic posture, a memory impairment, or other mild neurologic signs of unknown significance that do not suffice to make an additional syndrome classification or diagnosis. ET with rest tremor is classified here (Bhatia et al., 2018). Upon the appearance of symptoms or signs after 3 years of observation, ET can be reclassified into a combined clinical syndrome or a specific etiological condition (Bhatia et al., 2018).

It is known that some ET patients can develop signs of parkinsonism over the years and show a higher incidence of a family history of PD (Tarakad and Jankovic, 2019; Thenganatt and Jankovic, 2016). The term ET-PD was often used in the literature, although not recognized in the classification, to include ET patients with symptoms of parkinsonian syndrome but cannot be classified as idiopathic PD (Waln et al., 2015). Several kinematic studies documented alterations of voluntary movement, including bradykinesia, even in ET patients (Bologna et al., 2020; Duval et al., 2006; Goubault et al., 2017). It is doubtful whether these alterations can be considered specific soft signs of ET-plus or whether they could instead predict the onset of parkinsonism (Algarni and Fasano, 2018; Tarakad and Jankovic, 2019). Moreover, neuroradiological data on the possible involvement of other structures beyond the cerebellum are inconsistent in ET. It is therefore not clear, for example, whether a dysfunction of the BG or brain networks could be responsible for the aforementioned motor alterations (Bologna et al., 2020b; Paparella et al., 2021b).

In the first part of this thesis, we will initially provide the results of clinical and kinematic studies documenting the alterations of voluntary movement in ET patients and, subsequently, the neuroradiological evidence of the possible areas involved.

In the second part, we will provide the results from two experimental studies, that investigated bradykinesia and its possible pathophysiological mechanisms in ET patients, correlating kinematic parameters of finger tapping movements to the radiological values of DAT-SPECT (i) and volumetric and functional MRI (ii).

2.1 Bradykinesia in Essential Tremor

Bradykinesia is one of the cardinal motor symptoms of PD and other parkinsonism. The term literally means slowness of movement, but is still used to refer to low-amplitude movements (hypokinesia) and no movement (akinesia) and is applicable to voluntary and spontaneous-automatic movements (Bologna et al., 2023). The current bradykinesia definition, in the context of diagnostic criteria for PD, includes slowness of movement and progressive reduction in speed and amplitude (or progressive hesitations or halts) performing repetitive movements (sequence effect) (Bologna et al., 2023, 2020b; Postuma et al., 2015a).

In ET bradykinesia is not systematically present. There are numerous medical reports, although controversial, on movement slowness in ET (Algarni and Fasano, 2018; Haubenberger and Hallett, 2018; Paparella et al., 2021b).

Several kinematic studies, based on different types of motor tasks, documented alterations in voluntary movement, including motor slowness without sequence effect. Montgomery et al. tested rapid wrist flexion-extension movements in ET and PD patients with tremor and found them slower than healthy subjects (HS) (Montgomery et al., 2000). Deuschl et al. documented a slowing of the total reach-to-grasp movements in ET with kinetic tremor (Deuschl, 2000). Slowness was found during the execution of prono-supination movements in ET (Duval et al., 2006), also with associated hypokinesia (Goubault et al., 2017). Costa et al. identified slowness and irregularity of oscillatory movements in ET and PD (Costa et al., 2010).

In clinical practice, however, the most used motor task to evaluate bradykinesia is represented by repetitive finger movements, and to date, few kinematic studies have used this task. Jimenez Jimenez et al. demonstrated a slow execution of finger tapping movements in ET patients, not secondary to the severity of the tremor (Jiménez-Jiménez et al., 2010). More recently, we documented in ET patients the presence of a motor slowness, not associated with the sequence effect typical of PD and not related to the severity of the postural and kinetic tremor (Bologna et al., 2020). ET patients showed intermediate velocity levels between PD patients and HS, with kinematic patterns common to both groups in the cluster analyses performed. We speculated that bradykinesia in ET should be interpreted, in the literary sense of the term, as a motor slowness without decrement and should be considered a soft sign detectable by laboratory techniques. Therefore, it could be expression of pathophysiological bases different from the sequence effect of PD and the action tremor of ET (Bologna et al., 2020).

Few longitudinal studies analysed the clinical evolution of ET patients to understand the underlying pathophysiology. A 3-year longitudinal study documented in ET patients a greater evidence of rest tremor, an extension of action tremor to other body sites and a subtle bradykinesia

(with hypokinesia) of finger tapping movements (not related to the tremor) (Angelini et al., 2023a). The greater frequency of soft signs after 3 years, without the appearance of further specific clinical signs, classified these patients as ET-plus and raised the question whether this entity was a different subtype or an evolutionary stage of ET toward to PD (Angelini et al., 2023a). The evidence of bradykinesia in ET patients could reflect a progressive involvement of the BG and possible interactions between the BG and the cerebellum (Angelini et al., 2023a; Paparella et al., 2021b). However, in none of these kinematic studies a DATscan examination was performed and therefore it is unknown whether a progressive dopaminergic involvement may be responsible for the motor alterations in ET (Waln et al., 2015).

2.2 Possible pathophysiological substrates of bradykinesia in ET

Bradykinesia in PD is classically related to the progressive depletion of dopaminergic neurons in the substantia nigra and to the consequent concentration of striatal dopamine in the circuitry of the BG (Fearnley and Lees, 1990; Kalia and Lang, 2015). The lack of dopamine effect on BG pathways leads to excessive inhibition of thalamo-cortical and brainstem motor systems, interfering with both preparation and execution phases of voluntary movement (Bologna et al., 2020b; Kalia and Lang, 2015).

Although the role of the cerebellum is well known, the involvement of the BG is unclear in ET. The 123I-Ioflupane DAT-SPECT exam represents a valid neuroradiological tool to identify a presynaptic nigrostriatal degeneration, typically found positive in PD but not in ET and other secondary parkinsonism (Benamer et al., 2000). However, recent DAT-SPECT studies, also based on semi-quantitative analyses (DaTQUANT), identified a mild dopaminergic involvement in ET patients. A study of 167 patients with isolated action tremor documented a reduced striatal uptake in 68% of them (Coria et al., 2012). Likewise, Isaias et al. reported a slight decrease in DAT efficiency in ET patients, intermediate between PD patients and HS (Isaias et al., 2008). In one study, two independent radiologists ‘‘blinded’’ to the clinical diagnosis examined 123I-ioflupane SPECT scans in 39 ET patients (22 with isolated ET, nine with ET and mild parkinsonism, and eight with ET–PD) and 13 HS, by a visual and semi-quantitative method. As expected, ET–PD patients had the lowest striatal uptake, but pure ET patients showed slightly lower striatal binding ratios than HS (Waln et al., 2015).

Other authors confirmed a mild dopaminergic deficit in ET, but only Schwartz et al. identified a correlation between levels of radioligand uptake and impairment of a visual motor task (VMC) (Schwartz et al., 2004).

Another imaging modality to study the dopaminergic system is represented by the transcranial ultrasound evaluation of the substantia nigra, which appears hyperechoic in PD patients (Berg, 2011). A hypercoegenicity of the substantia nigra has been documented in subgroups of ET patients (especially ET-PD patients), of lower intensity than in PD but more marked than in HS (Laučkaitė et al., 2014; Sprenger et al., 2016). Cardaioli et al. demonstrated how this radiological marker, monitored over 3 years of follow-up, could predict the development of early parkinsonian symptoms in ET patients. (Cardaioli et al., 2019).

As previously highlighted, bradykinesia in PD has traditionally been considered the consequence of a failure of BG output to the primary motor cortex (M1). However, recent evidence has better defined the role of other brain structures, including the cerebellum, in the pathophysiology of bradykinesia in PD (Bologna et al. 2020b). The same structures could be responsible for the alterations in voluntary movement in ET.

This hypothesis is particularly favorable in ET, as it has been clear for years that cerebellar dysfunction is responsible for the genesis of tremor in ET. Morphometric and resting state (rs) MRI studies showed structural and functional alterations of the cerebellum and correlated them with tremor features and severity in ET patients (Benito-León et al., 2019; Mueller et al., 2017). For example, Tikoo et al. documented, with a seed-based approach of the dentate nucleus (DN), a decreased DN functional connectivity (FC) with cortical, subcortical and cerebellar areas in ET patients, and a correlation between DN FC, clinical severity and kinematic amplitude of the tremor (Tikoo et al., 2020). However, various authors demonstrated the absence of a correlation between bradykinesia and tremor severity using kinematic techniques (Angelini et al., 2023a; Bologna et al., 2020; Jiménez-Jiménez et al., 2010). It is likely that motor slowness in ET may involve cerebellar mechanisms different from those of tremor. Interestingly, reduced motor speed could be found in other cerebellar pathologies (strokes, tumors, and degenerative pathologies). Strokes of the paravermian lobules IV/V and cerebellar nuclei are those most associated with slowing (Hallett et al., 1991; Konczak et al., 2010). These data support the cerebellar function of coding kinematic parameters, such as direction and speed of movement. The discharge activity of Purkinje cells regulates the speed of movement during multiple tasks (Ebner et al., 2011; Hewitt et al., 2011). So, their alteration could be responsible for the lack of this function and for the motor slowness in ET (Bologna et al., 2020; Louis et al., 2007).

Recently, additional interneural connections between the basal ganglia and cerebellum have been identified. It is likely that these structures interact with each other and with other cortical areas to optimize the execution of voluntary movement (Bostan and Strick, 2018). According with these results, several fMRI studies investigated a correlation between finger tapping task (the most used

motor task for the evaluation of voluntary movement in fMRI studies) and related brain structures in HS, including the primary sensorimotor cortices, supplementary motor area, premotor cortex, inferior parietal cortices, basal ganglia and anterior cerebellum (Turesky et al., 2018; Witt et al., 2008). A dysfunction of these networks should be implicated in the genesis of motor alterations in ET.

Buijink et al. found reduced activations in widespread cerebellar, frontal and parietal regions and the inferior olive nucleus during rhythmic finger tapping movements in ET patients. The hypoactivity of cerebellar cortex could facilitate a disinhibition of DN and, therefore, a dysfunction of other brain areas, responsible of tremor severity and impairment of finger tapping (Buijink et al., 2015).

Unfortunately, to date we do not have sufficient neuroradiological data on the alterations of voluntary movement in ET, and further studies are needed to better understand the underlying pathophysiological substrates.

2.3 The role of kinematic analysis in parkinsonian and non-parkinsonian conditions

The clinical assessment of bradykinesia in PD and atypical parkinsonisms is currently based on the specific assessment of dedicated clinical rating scales. MDS Unified Parkinson's Disease Rating Scale (MDS-UPDRS) part III is the most used scale in clinical motor evaluation (MDS-UPDRS Italian Validation Study Group et al., 2013). For limb bradykinesia, the examiner is asked to rate speed, amplitude, hesitations and halts or decrement during 10 repeated movements, and all these alterations provide the same influence on the final single score. Therefore, the assessment of bradykinesia could be affected by intra- and inter-individual variability and low reliability among all UPDRS items, with variable effects on therapeutic responses as well as in research protocols (Bologna et al., 2023, 2020b). To improve the reliability of bradykinesia rating, several technology-based tools have been proposed (Hasan et al., 2017). For example, kinematic optoelectronic systems can detect reflective markers positioned on specific points of the body during the execution of different motor tasks. With kinematic analysis protocols of repetitive finger tappings, it is possible to characterize specific components of voluntary movement (number of movements, speed, amplitude, rhythm, decrease in amplitude and speed of the movement, i.e. sequence effect) (Colella et al., 2021) and to provide continuous data on the type and severity of bradykinesia as well as on the therapeutic response in PD and atypical parkinsonisms (Bologna et al., 2016; Ling et al., 2012) . Mild bradykinesia and hypokinesia associated with sequence effect are present in the early stages of PD, but not in the advanced stages of PD where bradykinesia and hypokinesia are more marked (Bologna et al., 2016). Hypokinesia without decrement

distinguishes progressive supranuclear palsy from Parkinson's disease and multiple system atrophy (Djurić-Jovičić et al., 2016; Ling et al., 2012). Furthermore, it has been demonstrated how alterations of voluntary movement are also present in non-parkinsonian conditions, although not always clinically evident. A movement slowness was observed in hyperkinetic (i. e. ET, dystonia), iatrogenic, cerebellar disorders, motor neuron and cognitive disorders and in each of them bradykinesia was associated or not with further alterations of voluntary movement (Bologna et al., 2020a, 2020; Colella et al., 2021; Paparella et al., 2021a, 2020). Kinematic analysis could represent a valid tool to characterize bradykinesia in both axes (phenomenology and etiology), in line with new definition (Bologna et al., 2023). However, the phenomenology may be overlapping in different categories of patients, and it is not always possible to define the etiology on the bradykinesia features alone. Paparella et al. demonstrated how kinematic techniques allowed etiological differentiation between PD patients with moderate-severe bradykinesia and subjects with normal velocity values, although 30% of the subjects (PD, ET and HS) with mild-moderate abnormalities were precluded from an accurate diagnosis. Therefore, the kinematic components of bradykinesia must always be interpreted in association with other clinical information to define a correct diagnosis (Paparella et al., 2023).

Optoelectronic systems can provide objective information about tremor amplitude, frequency, body distribution and activation conditions, as well as tremor changes over time, and possible drug sensitivity of tremor (Angelini et al., 2023b). They could be useful to better characterize additional symptoms of ET-plus (with laboratory support) (Bhatia et al., 2018). Recently, Angelini et al documented the presence of soft signs, such as rest tremor and bradykinesia, in ET-plus patients through clinical and kinematic analyses. The findings of a more severe and widespread action tremor in patients with rest tremor and a non-concordant body asymmetry of rest tremor and bradykinesia could highlight different pathophysiological mechanisms in the genesis of the two soft signs (Angelini et al., 2024).

Despite their usefulness, kinematic techniques are not standardized. Each laboratory uses different methodologies and protocols and evaluates patients for clinical and research purposes, referring to its own database. Future clinical studies, carried out on larger groups of patients, will be necessary to better characterize motor abnormalities and validate these methods as standardized diagnostic tools (Angelini et al., 2023b; Paparella et al., 2023).

3. EXPERIMENTAL PART
3.1 STUDY 1: SUBTLE CHANGES IN CENTRAL DOPAMINERGIC TONE UNDERLIE BRADYKINESIA IN ESSENTIAL TREMOR

3.1.1 Abstract

Introduction: In this research, our primary objective was to explore the correlation between basal ganglia dopaminergic neurotransmission, assessed using 123I-FP-CIT DAT-SPECT, and finger movements abnormalities in patients with Essential Tremor (ET) and Parkinson's disease (PD). **Methods:** We enrolled 16 patients with ET, 17 with PD, and 18 HS. Each participant underwent comprehensive clinical evaluations, kinematic assessments of finger tapping. ET and PD patients underwent DAT-SPECT imaging. The DAT-SPECT scans were subjected to both visual and semi-quantitative analysis using DaTQUANT®. We then investigated the correlations between the clinical, kinematic, and DAT-SPECT data, in patients. **Results:** Our findings confirm that individuals with ET exhibited slower finger tapping than HS. Visual evaluation of radiotracer uptake in both striata demonstrated normal levels within the ET patient cohort, while PD patients displayed reduced uptake. However, there was notable heterogeneity in the quantification of uptake within the striata among ET patients. Additionally, we found a correlation between the amount of radiotracer uptake in the striatum and movement velocity during finger tapping in patients. Specifically, lower radioligand uptake corresponded to decreased movement velocity (ET: coef. = 0.53, p-adj = 0.03; PD: coef. = 0.59, p-adj = 0.01). **Conclusion:** The study's findings suggest a potential link between subtle changes in central dopaminergic tone and altered voluntary movement execution, in ET. These results provide further insights into the pathophysiology of ET. However, longitudinal studies are essential to determine whether the slight reduction in dopaminergic tone observed in ET patients represents a distinct subtype of the disease or could serve as a predictor for the clinical progression into PD.

3.1.2 Introduction

ET is a common movement disorder characterized by postural and kinetic tremor of the upper limbs (Bhatia et al., 2018). The presence of additional clinical symptoms, such as rest tremor or movement slowness (bradykinesia), in some cases presents challenges in differentiating it from PD (Algarni and Fasano, 2018; Tarakad and Jankovic, 2019). Various kinematic studies have demonstrated bradykinesia in ET patients (Angelini et al., 2023a; Bologna et al., 2020; Costa et al., 2010; Duval et al., 2006; Goubault et al., 2017; Jiménez-Jiménez et al., 2010; Montgomery et al., 2000), as movement slowness without sequence effect (Bologna et al., 2020). While the role of the BG in the pathophysiology of bradykinesia in PD is widely recognized (Berardelli et al., 2001; Bologna et al., 2020b), its possible involvement in ET patients is not as well-established (Paparella et al., 2021b).

A potentially valuable instrumental method for studying the nigrostriatal dopaminergic system is 123I-Ioflupane DAT-SPECT. Striatal dopamine transporter (DAT) radiotracer uptake indirectly assesses the extent of degeneration in dopaminergic terminals, indicative of PD and other parkinsonism (Benamer et al., 2000; Brogley, 2019). Although the DAT-SPECT scan is typically considered negative in ET patients, it is not entirely conclusive and may still present diagnostic uncertainties (Menéndez-González et al., 2014). When examining patients with isolated postural tremor, for example, DAT-SPECT revealed a slight reduction in radioligand uptake, albeit not statistically significant (Coria et al., 2012). Moreover, some studies have reported a significant decrease in dopamine transporter levels among patients with ET (Isaias et al., 2008; Schwartz et al., 2004). Currently, the availability of an automated software, i.e., DaTQUANT (GE Healthcare) enables a more precise semi-quantitative assessment of dopaminergic terminal loss (Brogley, 2019; Neill et al., 2021). DaTQUANT results have confirmed the presence of intermediate 123I-Ioflupane uptake values in ET patients, which are between those observed in PD patients and HS (Waln et al., 2015). However, it remains unclear whether this dopaminergic dysfunction correlates with the degree of bradykinesia observed in ET. Although Schwartz et al. found a correlation between reduced ligand uptake values and impaired visuo-motor coordination (VMC) task performance in ET patients (Schwartz et al., 2004) it is worth noting that the VMC task is not specifically designed to assess bradykinesia, unlike the finger tapping movements, commonly employed in clinical settings (Bologna et al., 2020, 2016).

The main objective of this study was to explore the potential association between changes in dopaminergic neurotransmission and the presence of bradykinesia in ET compared to PD and HS. To achieve this, we performed a kinematic analysis of repetitive finger tapping movements, allowing for an objective measurement of motor performance in ET patients. Furthermore, we quantitatively assessed the impairment of the dopaminergic system using DAT-SPECT imaging. Finally, we

investigated potential correlations between kinematic parameters of finger movements and radioligand uptake values measured through DaTQUANT. Data obtained in patients with ET were compared to those of PD patients and normal subjects.

3.1.3 Materials and methods

Participants

For this study, 16 ET patients, 17 PD patients, and 18 HS were consecutively recruited from the Department of Human Neurosciences at Sapienza University of Rome. ET and PD diagnoses were performed using the current clinical criteria (Bhatia et al., 2018; Postuma et al., 2015a). Notably, all PD patients enrolled in the study exhibited a tremor-dominant phenotype. We included ET patients, both with and without soft signs of parkinsonism, which encompasses pure ET and ET-plus patients (Bhatia et al., 2018). ET-plus patients presenting with additional soft signs, such as questionable dystonia, mild ataxia, or mild cognitive impairment, were excluded from the study. Patients with any other neurological or psychiatric conditions, as well as those with a history of taking anti-dopaminergic drugs, were also excluded. All patients underwent DAT-SPECT imaging as part of their diagnostic evaluation. We collected detailed demographic and clinical information for all participants. For ET patients, tremor-related therapy was discontinued at least 24 h before testing (Angelini et al., 2023a; Bologna et al., 2019, 2018; Paparella et al., 2023), (treatment details for ET patients are reported in Supplementary Table S1). PD patients were assessed in the practically defined OFF condition, i.e., after 12-hour withdrawal of dopaminergic therapy (Defer et al., 1999). The levodopa equivalent daily dose (LEDD) in PD is indicated in Table 1.

Movement Disorder Society-sponsored revision of the Unified Parkinson's Disease Rating Scale, part III (MDS-UPDRS-III) (MDS-UPDRS Italian Validation Study Group et al., 2013), to assess the severity of motor symptoms, as well as the Fahn-Tolosa-Marin Tremor Rating Scale (FTM-TRS) in patients with ET (Elble et al., 2012). Clinical assessments included the evaluation of cognitive and psychiatric aspects and included the Montreal Cognitive Assessment (MoCA) (Freitas et al., 2013), and the Frontal Assessment Battery (FAB) (Dubois et al., 2000). HS were included based on the following criteria: a negative neurological examination and no history of taking anti-dopaminergic drugs. Written informed consent was obtained from all participants, and the study procedures were approved by the local ethics committee. The research was conducted following the principles outlined in the Declaration of Helsinki.

Kinematic recordings and analysis

Bradykinesia was assessed through finger tapping movements. Participants sat comfortably on a chair and tapped their thumb on their index finger as fast as possible for 15 seconds, with a 60 second pause between movements to prevent fatigue (Angelini et al., 2023a; Bologna et al., 2020, 2016; Colella et al., 2021; Paparella et al., 2023, 2020). Kinematic recordings were obtained using 3 infrared cameras (sampling frequency: 120 Hz) from the SMART motion system by BTS Technology, Italy. The cameras detected reflective markers placed on the participant's thumb, index finger, and hand (acting as a reference plane). Considering our prior research, which consistently reported no significant influence of handedness on finger tapping execution, finger tapping assessment were conducted using the dominant hand for both ET patient and HS (Bologna et al., 2020, 2016; Paparella et al., 2023). In PD patients, the markers were placed on the most affected side (Bologna et al., 2018, 2016; Paparella et al., 2023). Offline movement analysis was performed using the SMART Analyzer software by BTS Engineering, Italy. Linear regression techniques were employed to determine the initial amplitude (degree) and velocity (degree/s) of the finger movement as well as the decrement in amplitude (degrees/number of movements) and velocity [(degrees/second)/number of movements] during repetitive movements. Again, the coefficient of variation (CV), calculated as the standard deviation divided by the mean value of the intertap intervals, was used to assess the motor rhythm. Higher CV values indicated less regular movement (Bologna et al., 2020, 2016; Colella et al., 2021). Tremor quantification in ET and PD patients was conducted by recording three 45-second epochs while patients were at rest or maintained anti-gravity posture with their arms extended forward (P1) flexed at the elbows (P2) (Angelini et al., 2023a; Bologna et al., 2020, 2019; Paparella et al., 2018a). The root-mean-square (RMS) of the accelerometer traces in the three dimensions of space was measured for each reference marker positioned on the upper limbs to assess tremor amplitude. The amplitude was then expressed in G-RMS^2. The peak dominant frequency (Hz) of the postural tremor spectrum was also measured (Bologna et al., 2020, 2019, 2015; Paparella et al., 2018a). Mean values between the two positions were considered for the subsequent analyses.

123I-FP-CIT (DAT-SPECT) acquisition and analysis

To minimize thyroid gland uptake, 400 mg of potassium perchlorate were administered to patients 30 min before intravenous injection of 185 MBq of 123I-FP-CIT Brain SPECT imaging was performed 3 h after the radiopharmaceutical injection using a dual-head gamma camera (Infinia, GE Healthcare, Milwaukee, USA) equipped with a low-energy parallel hole high-resolution (LEHR) collimator. The acquisition parameters included an angular step of 3 degrees, a 1.3 zoom factor, and a matrix size of 128 × 128. The energy window was set symmetrically to ± 10% of the 159-KeV 123I photopeak.

SPECT images were acquired and reconstructed using the iterative ordered subset expectation post hoc maximization (OSEM) algorithm, and attenuation correction was applied using Chang's method. Initially, a qualitative visual assessment of the presynaptic nigrostriatal system was performed based on the DATSPECT images by the same operator. Then, a semiquantitative evaluation of the striatal distribution of 123I-FP-CIT was carried out using the specific DaTQUANT software (GE Healthcare). This software enabled accurate and fully automated registration of patients' SPECT images onto a 3D-volume model of interest derived from a large database of healthy individuals who had undergone brain DAT-SPECT scans and were matched by age to the patients. Specific binding ratio (SBR) values for each patient were obtained using the DaTQUANT software, calculated as the mean counts in the specific striatal region minus the mean counts in the background region divided by the mean counts in the background region. SBR values were determined for both the right and left striatal regions (Ferrazzano et al., 2020).

Statistical analysis

Gender differences between groups were assessed using Fisher's exact test. The differences in demographic and other clinical features among the groups were evaluated through the Kruskal-Wallis test and post-hoc pairwise comparisons using the Wilcoxon rank sum test. For the comparison of kinematic parameters between ET patients, PD patients, and HS, separate one-way ANOVAs were conducted with the factor 'GROUP'. Kinematic variables were assessed in separate ANOVAs. Post hoc analyses were performed using Tukey's honestly significant difference (HSD) correction for multiple comparisons. To analyse the differences in DaTQUANT data we applied t-test comparisons. Spearman's correlation analysis was utilized to explore the relationship between clinical-demographic data and kinematic parameters or DaTQUANT parameters. Kinematic variables of interest were selected for finger tapping and tremor based on the results of group comparison analyses Pearson's correlation was used to examine the relationship between movement kinematics and SBR values in patients' contralateral putamen and caudate nuclei. Unless otherwise stated, results were presented as mean values (standard deviation - SD) or median (interquartile interval) for clinical and demographic data. The significance level was set at $p < 0.05$. To control the overall Type I error rate resulting from multiple comparisons, we applied the false discovery rate (FDR) correction method (Curran-Everett, 2000). Data analysis was performed using STATISTICA® software (TIBCO Software Inc., Palo Alto, California, US) and implemented in RStudio (Posit team (2023), Integrated Development Environment for R. Posit Software, PBC, Boston, MA. URL https://www. posit.co/.).

3.1.4 Results

Clinical and demographic data

No significant differences were observed in terms of age and gender distribution between the three groups (Table 1). A family history of tremor was present in 8 out of 16 ET patients (50%), whereas none of the participants in our study had a family history of parkinsonism. Kruskal Wallis for MoCA and FAB scores revealed significant group effect. Lower values were demonstrated for PD patients when compared to HS ($p = 0.014$) and ET ($p = 0.014$) for FAB scores, while MoCA post-hoc analysis did not display any significant result (Table 1). A significant difference ($p = 0.02$) was found in the MDS-UPDRS-III with PD patients exhibiting higher values than ET (Table 1). In ET patients, the MDS-UPDRS-III scores were mainly attributed to the presence of postural and kinetic tremor [median postural tremor scores in ET: 2.0 (1.0-2.0), in PD: 1.0 (1.0-2.0); median kinetic tremor scores in ET: 1.0 (0.0–1.0), in PD: 1.0 (0.0-1.75)]. Additionally, minimal subtle signs such as mild bradykinesia (6/16, 37.5%), incorrect posture (7/16, 47%), or minimal and uncertain rigidity of the upper limbs (5/16, 31.2%) contributed to the overall scores. On the other hand, the PD patients presented typical PD symptoms with rigidity, bradykinesia, and rest tremor, with a postural tremor in 13/17 patients (76.4%).

Kinematic analysis

The ANOVA showed a significant effect of the factor 'GROUP' on the number of movements ($F2,50 = 13.38$; $P < 0.001$), rhythm ($F2,50 = 3.41$; $P = 0.041$), amplitude ($F2,50 = 3.59$; $P = 0.035$) and velocity ($F2,50 = 17.85$; $P < 0.001$). Post-hoc analysis indicated that ET patients exhibited fewer movements compared to PD patients ($P = 0.003$) and HS ($P < 0.001$), while no difference was observed between PD patients and HS ($P = 0.269$) (Table 2). Velocity was significantly lower in the PD group ($p < 0.001$), and in ET compared to HS ($p = 0.002$). However, there was no significant difference in velocity between PD and ET patients (Table 2). The analyses for rhythm and amplitude showed no significant result. Comparison between PD and ET patients' kinematic assessment demonstrated no differences in resting tremor but a greater postural tremor magnitude in ET patients ($p = 0.046$, Table 1).

DAT-SPECT

As expected, visual evaluation of DAT-SPECT scans showed asymmetric dopaminergic uptake in PD patients, resulting in positive findings for all cases, while none of the ET patients demonstrated qualitative reduction of DAT binding. Again, the semiquantitative DaTQUANT analysis

demonstrated a statistically significant difference between the PD and ET groups for the striatum, putamen and caudate nuclei considering both SBR and z-scores values (Table 1).

Correlation analyses

Age correlated with the number of performed movements in PD patients (coef = -0.48, p-adj = 0.05) (Supplementary Table S2, Fig. 1). Conversely, no relationship was present between cognitive test scores or disease duration in ET and PD patients and finger tapping performance or tremor data (Supplementary Table S2-S3, Fig. 1). Also, there was no correlation between finger tapping velocity and postural and rest tremor magnitude, indicating that bradykinesia in ET and PD was not influenced by the presence of tremor (Supplementary Table S2-S3, Fig. 1). Pearson's correlation analysis revealed a linear relationship between the velocity of finger tapping and the degree of DAT integrity, as indicated by the semi-quantitative analysis using DaTQUANT, in the contralateral basal ganglia. This correlation was observed for velocity in both PD and ET groups with the putamen SBR data (ET: coef = 0.53, p-adj = 0.03; PD: coef = 0.59, p-adj = 0.01;) and in the PD group for the caudate nucleus data (coef = 0.49, p-adj = 0.05) (Supplementary Table S2-S3, Fig. 1).

However, no significant correlation was found between DaTQUANT data for the putamen and caudate nuclei, and MDS-UPDRS-III scores or the amplitude of postural and rest tremor in both ET and PD patients (Supplementary Table S2-S3, Fig. 1).

3.1.5 Discussion

Consistent with previous observations, the present study provides kinematic evidence of slowed finger tapping in ET patients compared to HS (Angelini et al., 2023a; Bologna et al., 2020). As expected, there was also kinematic evidence of reduced movement velocity during finger tapping in PD patients (Bologna et al., 2023). Again, the DAT-SPECT exams showed normal results in ET patients while altered findings in PD and the uptake values obtained through DaTQUANT analysis were consistently lower in the PD patient group compared to ET. Finally, we found a linear correlation between finger tapping movement velocity and the uptake values of the striatum, putamen and caudate nuclei as measured by the DaTQUANT demonstrated in both patients' groups.

Conversely, we did not find any correlation between DaTQUANT values and tremor in ET and in PD nor between finger tapping velocity and postural or kinetic tremor severity in patients, demonstrating that slowed movement velocity is not caused by the tremor itself (Bologna et al., 2020; Duval et al., 2006; Goubault et al., 2017). The first novel finding of the present paper is the correlation between kinematic parameters in patients and the results of DAT-SPECT and DaTQUANT analysis. As expected, qualitative DAT-SPECT examinations revealed dysfunction of the nigro-striatal system in

PD patients, whereas no visual abnormalities were observed in ET patients. This outcome was further supported by the semiquantitative DaTQUANT analysis, which demonstrated significantly lower overall uptake values in PD patients compared to the ET group (Brogley, 2019). Consistently with previous studies, ET patients evidenced normal DAT-SPECT scans based on visual interpretation (Kuya et al., 2018), while the DaTQUANT analysis revealed variations in DAT binding. These findings align with previous research indicating that reuptake values in patients with ET are lower than those in healthy individuals, but higher than in those with parkinsonian syndromes (Cuberas-Borrós et al., 2011; Isaias et al., 2010). The observed heterogeneity in DAT levels may reflect ET clinical and kinematic heterogeneity (Tarakad and Jankovic, 2019; Thenganatt and Jankovic, 2016), also confirming the pathophysiological link between ET and PD (Espay and Fasano, 2023; Minen and Louis, 2008; Pietracupa et al., 2021; Rajput et al., 2019). Notably, our findings revealed a significant correlation between velocity and the degree of dopaminergic reuptake in the caudate and putamen nuclei for both groups of patients. This correlation suggests that slower movement execution is associated with lower levels of dopaminergic reuptake in PD and ET. It has been well-established that nigrostriatal degeneration is the key factor contributing to bradykinesia in PD, and dopaminergic medications have shown significant efficacy in improving this symptom (Bologna et al., 2020). In contrast, the correlation between decreased movement velocity and dopaminergic dysfunction is less evident in ET, with the absence of clear clinical evidence of bradykinesia and the classical occurrence of qualitative negative DAT-SPECT scans. Although qualitative analysis of DAT-SPECT did not reveal dopamine dysfunction in our ET patients, the results of semiquantitative analyses and the correlations we found suggest a potential pathophysiological involvement of nigro-striatal circuits in some ET patients. However, this issue is still debated and requires further investigations (Erro et al., 2016). Our results are consistent with a previous study by Schwartz et al., who demonstrated a reduction in putamen uptake in 8 out of 10 ET patients with impaired VMC, showing a linear correlation between DAT binding and contralateral performance (Schwartz et al., 2004). However, finger tapping, which represents the most used task for assessing bradykinesia in clinical evaluations, is more suitable for defining possible relationship with dopaminergic dysfunction in the basal ganglia (BG), particularly the putamen, in ET patients. Notably, we have now observed a correlation between movement velocity and central dopaminergic tone in both groups of patients, further reinforcing the potential relationship between ET and PD. This finding may also possibly explain some ET patients progression to PD several years after the onset of symptoms (Bologna et al., 2023, 2020; Paparella et al., 2021c; Thenganatt and Jankovic, 2016). However, it remains unclear whether ET patients with subtle parkinsonian signs are prodromal PD cases not fully manifested or if they represent a distinct entity that can, in some cases, evolve into PD. In this regard, earlier research has also indicated that

ET may, to some extent, be a genetically-influenced condition, potentially falling under the category of repeat-expansion disorders, leading to a wide clinical overlap among various family members. This overlap includes some individuals affected by tremor-dominant PD and others by ET within the same family (Schneider et al., 2007). The discovery of patients with scans without evidence of dopaminergic deficit (SWEDD) adds complexity to this hypothesis. SWEDD can be observed not only in possible PD cases but also in those patients with no univocal parkinsonian signs (Schwingenschuh et al., 2010), including patients with adult onset dystonic tremor resembling parkinsonian tremor (Boecker et al., 2010; Hua and Lenz, 2005). Moreover, new concepts suggest that complex interactions within motor networks may be more important than single structure impairment in causing motor symptoms, particularly bradykinesia (Bologna et al., 2023, 2020b). It has been hypothesized that in PD the cerebellum and cortical motor areas may play a compensatory role in movement feedback and compensation for impaired BG function during the execution of continuous and repetitive movements (Bologna et al., 2023, 2020b). However, it is still unknown whether an altered interplay between BG and cerebellum is causing altered voluntary movement execution in ET patients. Future functional magnetic resonance imaging studies will be necessary to confirm these hypotheses and better understand the diverse pathophysiological substrates underlying this heterogeneous clinical syndrome. From a pathophysiological perspective, the results of our study could also be interpreted to gain insight into the mechanisms of action tremor in ET and PD. The cerebellum-thalamic-cortical circuit plays a key role in the pathophysiology of tremor in ET (Dirkx et al., 2018; Kosmowska and Wardas, 2021), while the contribution of the dopaminergic system in this condition is still unclear. Recent evidence suggest a dopamine modulation of cerebellar function through D3 receptors (Dirkx and Bologna, 2022). Rajput et al. found low dopamine levels in the caudate nucleus of ET patients (Rajput et al., 2019). Isaias and colleagues speculated on a connection between mild degeneration of the caudate nucleus's DAT and the onset of tremor in ET patients (Isaias et al., 2010, 2008). Hence, dopaminergic dysfunction should contribute to the development of tremor in ET patients. However, we did not find any correlation between tracer uptake and the severity of action tremor in ET and PD patients. Moreover, we did not observe any correlation between DAT-SPECT values and the motor clinical severity, as measured by MDS-UPDRS-III, in PD (Boecker et al., 2010; Curran-Everett, 2000; Hua and Lenz, 2005) and ET patients (Bologna et al., 2020). In PD, pallidal dopamine depletion was demonstrated to facilitate rest tremor severity, but postural tremor appears to have mainly a nondopaminergic basis (Berardelli et al., 2013; Guerra et al., 2023). Therefore, further investigations are required to clarify whether effective dopaminergic alterations can influence cerebellar activity in the pathophysiology of action tremor in PD and ET. Another innovative aspect of the study lies in the results obtained from the kinematic analysis of finger

tapping, which provides valuable support to the clinical evaluation and diagnosis of patients by detecting specific movement parameters that are not easily recognized during a standard outpatient visit (Bologna et al., 2020). In this regard, bradykinesia in PD patients is usually associated with hypokinesia (i.e., reduced movement amplitude) and, especially in the initial stages, with sequence effect, i.e., a progressive decrease in amplitude and speed during the execution of repetitive movements (Bologna et al., 2016; Paparella et al., 2021b). However, our sample of PD patients did not show a sequence effect, probably due to the subtype enrolled in this study (Bologna et al., 2016). This study primarily included patients with PD who exhibited a tremor-dominant phenotype. During the initial phase, these patients presented diagnostic challenges, resembling ET, necessitating DAT-SPECT investigation. To the best of our knowledge, our study is the first to specifically investigate with objective techniques the bradykinesia features in patients with PD exhibiting a tremor-dominant phenotype. Overall, the results demonstrate that the sequence effect may lack in this subgroup of patients, as already described in patients with advanced PD (Bologna et al., 2023, 2016). Some possible confounding should be considered when interpreting the results of our study. Because we specifically tested finger tapping movements, we consider it unlikely that altered voluntary movement execution in ET is due to action tremor, which instead may possibly have a greater impact on proximal arm movements (Bologna et al., 2020; De Biase et al., 2022; Paparella et al., 2023). As previously observed (Angelini et al., 2023a; De Biase et al., 2022), in this study we found no correlation between action tremor severity and movement velocity during finger tapping in patients. Furthermore, concerning the ET group, we did not enroll patients with subtle dystonic symptoms, thus we can exclude that impaired motor performance was due, at least in part, to dystonia (Lofredi et al., 2023; Paparella et al., 2021b). Concerning possible study limitations, the sample size was small, which may reduce the generalizability of our findings. Additionally, the assessment demonstrated a slight but significant cognitive reduction in PD patient (Hua and Lenz, 2005; Schwingenschuh et al., 2010). However, we excluded a significant confounding effect on motor assessment because this study did not include subjects with cognitive performance below the normal range. Furthermore, the correlation analysis did not show any impact of these tests on motor performance. Finally, DATSPECT was not acquired for HC, and this did not allow investigation of the relationship between movement kinematics and SBR values in the HC group. Further investigations should better delineate this issue, also considering that that mild parkinsonian syndromes may be present in up to 25% of elderly persons without PD (Postuma et al., 2015a).

3.1.6 Conclusion

Our study confirmed the presence of movement slowness in ET patients which correlates with subtle dopaminergic dysfunction. These results align with recent evidence indicating a significant overlap in the pathophysiology of some disorders of movement, including ET and PD. We believe that the observation of shared phenomenological manifestations (lack of sequence effect of in PD patients with tremor-dominant phenotype as in ET) and partially overlapping pathophysiological mechanisms (role of central dopaminergic tone) that contribute to altered movement execution in both ET and PD supports the rationale for adopting the term ’bradykinesia’ in reference to movement slowness in both conditions, as has been recently suggested (Bologna et al., 2023). Further studies, ideally incorporating kinematic techniques, are needed to understand better the role of dopaminergic dysfunction in the pathophysiology of bradykinesia in ET, PD, and other movement disorders.

3.2 STUDY 2: THE ROLE OF CEREBELLUM AND BASAL GANGLIA FUNCTIONAL CONNECTIVITY IN ALTERED VOLUNTARY MOVEMENT EXECUTION IN ESSENTIAL TREMOR

3.2.1 Abstract

Background: Substantial evidence highlights the role of the cerebellum in the pathophysiology of tremor in essential tremor (ET), although its potential involvement in altered movement execution in this condition remains unclear.

Objective: This study aims to explore potential correlations between the cerebellum and basal ganglia functional connectivity and voluntary movement execution abnormalities in ET, objectively assessed with kinematic techniques.

Methods: A total of 20 patients diagnosed with ET and 18 healthy subjects were enrolled in this study. Tremor and repetitive finger tapping were recorded using an optoelectronic kinematic system. All participants underwent comprehensive 3T-MRI examinations, including 3D-T1 and blood-oxygen-level dependent (BOLD) sequences during resting state. Morphometric analysis was conducted on the 3D-T1 images, while a seed-based analysis was performed to investigate the resting-state functional connectivity (rsFC) of dorsal and ventral portions of the dentate nucleus and the external and internal segments of the globus pallidus. Finally, potential correlations between rsFC alterations in patients and clinical as well as kinematic scores were assessed.

Results: Finger tapping movements were slower in ET than in healthy subjects. Compared to healthy subjects, patients with ET exhibited altered FC of both dentate and globus pallidus with cerebellar, basal ganglia, and cortical areas. Interestingly, both dentate and pallidal FC exhibited positive correlations with movement velocity in patients, differently from that we observed in healthy subjects, indicating the higher the FC, the faster the finger tapping.

Conclusion: The findings of this study indicate the possible role of both cerebellum and basal ganglia in the pathophysiology of altered voluntary movement execution in patients with ET.

.

3.2.2 Introduction

Essential tremor (ET) is a neurological condition clinically characterized by bilateral action tremor of the upper limb lasting for at least 3 years (Bhatia et al., 2018). Previous neurophysiological studies have demonstrated an altered voluntary movement execution, manifested as movement slowness (bradykinesia) in a significant proportion of ET patients (Bologna et al., 2023, 2020; Duval et al., 2006; Goubault et al., 2017; Jiménez-Jiménez et al., 2010; Paparella et al., 2021b).

It is widely acknowledged that dysfunction within the cerebello-thalamo-cortical circuit plays a significant role in the pathophysiology of ET (Benito-León and Labiano-Fontcuberta, 2016; Fanning and Kuo, 2023; Haubenberger and Hallett, 2018; Helmich et al., 2013; Muthuraman et al., 2012). Resting-state functional magnetic resonance imaging (rs-fMRI) studies have consistently demonstrated impaired functional connectivity (FC) between the cerebellum and both cortical and subcortical regions in ET patients (Bédard et al., 2022; Mueller et al., 2017; Nicoletti et al., 2020; Pietracupa et al., 2021; Tikoo et al., 2020). The dentate nucleus (DN), which is the primary cerebellar output, projects to the thalamus and cortical areas. DN is composed by dorsal (motor) and ventral (associative) domains (Shozo Matano, 2001). The dorsal domain receives projection from the lateral cerebellum and is connected via ventro-lateral nuclei of thalamus with motor cortical areas (motor cortex, premotor cortex, supplementary motor area, somatosensory cortex) whereas the ventral domain is connected via dorsomedial thalamus nuclei with associative cortices (prefrontal cortex, intraparietal and inferior parietal cortex) (Hoover and Strick, 1999; Middleton and Strick, 2001, 1997). Both domains are connected with striatum via intralaminar nuclei of thalamus (Hoshi et al., 2005). Alterations in DN-FC, both within and outside the cerebellum, is also present in ET (Fanning and Kuo, 2023). Tikoo et al., found a correlation between DN functional disconnection and the severity of tremors as well as cognitive impairment in ET patients (Tikoo et al., 2020). Given the key role of the cerebellum in ET pathophysiology, it is plausible to suggest that DN dysfunction may also play a role in the pathophysiology of abnormalities of voluntary movement execution in ET patients (Bologna et al., 2020; Buijink et al., 2015; Wu and Hallett, 2013). This hypothesis is supported by the observation that various kinematic parameters, particularly movement direction and velocity, are encoded in cerebellar neural activity. In particular, the spike firing of Purkinje cells, the main output of the cerebellar cortex, is thought to control movement velocity across multiple tasks (Bologna et al., 2020). Furthermore, several studies have shown that degenerative cerebellar disease, cerebellar tumors and ischemic lesions may be associated with slowed movement execution (bradykinesia) (Bologna et al., 2020b; Paparella et al., 2021b). Additional mechanisms, however, may involve a wider cerebral network, including not only the cerebellum and interconnected cortical motor areas but also the basal ganglia (BG). In this regard, the globus pallidus (GP) serves as the central output

hub within the basal ganglia circuitry, essential for efficient and fast voluntary movement execution (Jahanshahi et al., 2015; Redgrave et al., 2010). GP is distinct in two parts, the internal (GPi) is deputed of motor output of BG; and the external (GPe) is a regulatory relay in BG circuit, classically acknowledged in the indirect pathway (Jaeger and Kita, 2011). GP has been implicated in fine regulation of movement velocity and amplitude, regulating frequency and synchronicity of oscillation in motor network (Blenkinsop et al., 2017; Nishibayashi et al., 2011; Villalobos et al., 2022). ET patients demonstrated reduced structural connectivity within the GP, caudate, and supplementary motor area (SMA) (Caligiuri et al., 2017). Hence, together with the cerebellum, the BG may also contribute to the pathophysiology of altered voluntary movement execution in ET, as recently proposed (Colella et al., 2023).

To the best of our knowledge, there is a no research study investigating the relationship between quantitative kinematic measurements of voluntary movement execution, and the activity of brain networks in individuals with ET. Moreover, no previous studies have thoroughly examined possible changes in connectivity within (or between) the cerebellum and BG, focusing on GP network activity as main voluntary movement BG output, and their potential implications in ET pathophysiology. Therefore, the primary objective of this study is to investigate the morphometric and functional changes of the cerebellum and BG in ET patients and to explore the correlations between these changes and kinematic measures of altered movement execution observed during repetitive finger tapping tasks, which are widely employed in clinical practice to evaluate bradykinesia (Bologna et al., 2020, 2016). By conducting this study, we aim to gain deeper insights into the role of the cerebellum and basal ganglia in the pathophysiology of movement execution alterations in ET.

3.2.3 Material and methods

Participants and clinical assessment

This study included 20 ET patients (3 females) with a mean age of 67.7±13.4 years and a disease duration of 13.9±9.9 years. ET patients were consecutively enrolled from the Movement Disorder Outpatient Clinic at the Department of Human Neurosciences, Sapienza University of Rome, Italy. The control group consisted of 18 healthy subjects (HS) (6 females) with a mean age of 62.8±7.8 years. The clinical diagnosis of ET was based on the established clinical diagnostic criteria (Bhatia et al., 2018). ET patients with clinically detectable soft-signs (ET-plus patients with rest tremor, questionable dystonia and ataxia) and psychiatric conditions were excluded from the study. Clinical evaluations of the patients were conducted by a neurologist with expertise in movement disorders. To minimize any potential confounding effects of medication, all patients discontinued their medications

48 hours prior to the experiment. Five out of 20 subjects exhibited head tremor, yet this did not lead to significant artifacts, as also demonstrated by ICA-AROMA analysis. Clinical assessment of ET patients was performed using the Fahn-Tolosa-Marin Tremor Rating Scale (FTMTRS) (Elble et al., 2012) and the Movement Disorder Society -sponsored revision of the Unified Parkinson's Disease Rating Scale, motor section (MDS-UPDRS-III) (MDS-UPDRS Italian Validation Study Group et al., 2013). All participants also underwent the Montreal Cognitive Assessment (MoCA) (Freitas et al., 2013) and the Beck Depression Inventory (BDI-II) (Beck, 1961) to define the cognitive profile and depressive symptoms. Study participants underwent the kinematic evaluation and MRI session on two separate days, within one week. All enrolled subjects provided written informed consent for the use of their data for research purposes. The study protocol was approved by the institutional ethics committee and conducted in accordance with the principles outlined in the Declaration of Helsinki.

Kinematic recordings and analysis

The kinematic assessment was conducted using an optoelectronic system (SMART motion system, BTS Engineering, Italy), which consisted of three infrared cameras operating at a frequency of 120 Hz. Reflective markers of negligible weight were attached to the participant's hand, with three markers placed at the wrist and two markers on the distal phalanx of the thumb and index finger to evaluate finger tapping movements. Participants were comfortably seated in a chair and instructed to perform 'as wide and fast as possible' repetitive opposition movement of the thumb and index finger (finger tapping). Each trial lasted for 15 seconds, and the task was repeated three times for each hand. A rest interval of 60 seconds was provided between trials to prevent fatigue(Bologna et al., 2020, 2016; Colella et al., 2021).

The kinematic recordings were analyzed using dedicated software (SMART Analyzer, BTS, Milan, Italy). This software utilized an automatized algorithm and linear regression techniques to calculate the relevant kinematic variables, including the number of movements, amplitude (in degrees), velocity (in degrees per second), as well as amplitude and velocity decrement during 15 seconds of repetitive finger movements. Additionally, the coefficient of variation (CV) was also measured to quantify movement rhythm. The CV was calculated by dividing the standard deviation by the mean value of the inter-tap intervals, with higher CV values indicating less rhythmic repetitive movements (Bologna et al., 2020, 2016; Colella et al., 2021). In ET, we performed also postural tremor analysis. To this aim, we used two markers placed on each hand. Three 45-sec recordings of postural tremor were obtained with the upper limbs positioned forward to the chest (Angelini et al., 2022; Bologna et al., 2020; Paparella et al., 2020, 2018b; Passaretti et al., 2022). Tremor analysis was performed using

the same dedicated software (SMART Analyzer, BTS Engineering, Italy). The magnitude of tremor was analyzed by measuring the root-mean-square (RMS) of the acceleration traces of the reference marker (on the second metacarpal bone) in 3D space and then was expressed in GRMS^2. Power spectra were quantified by means of fast Fourier transformation (Angelini et al., 2023a; Bologna et al., 2020; Paparella et al., 2020, 2018b; Passaretti et al., 2022). We then measured the dominant frequency peak (Hz) of postural tremor.

MRI Acquisition

Participants underwent a multimodal 3T-MRI scan using a 12-channel head coil for parallel imaging (Verio, Siemens AG). The MRI protocol included a high-resolution 3-dimensional T1-weighted MPRAGE (3D T1) sequence with 176 contiguous sagittal slices, 1-mm thick (TR = 1900 ms, TE = 2.93 ms, flip angle = 9˚, matrix = 256 × 256, FOV = 260 mm^2). T2-weighted images were also acquired (TR = 3320 ms, TE = 10/103 ms, FOV = 220 mm^2, 384 × 384 matrix, 25 4-mm thick slices, 30% gap). Additionally, blood oxygenation level-dependent (BOLD) single-shot echo-planar images were acquired (TR = 3000 ms, TE = 30 ms, flip angle = 89˚, 64 × 64 matrix, 50 slices, 140 volumes, acquisition time = 7 min, voxel size 3 mm^3). During the MRI scan, participants were instructed to lie down with their eyes closed and remain awake.

MRI Analysis

Structural and functional data were pre-processed using FMRIB's Software Library (FSL), version 6.0.1 (http://fsl.fmrib.ox.ac.uk/fsl).

Structural MRI.

Three-dimensional (3D) T1-weighted images were skull stripped using FSL's Brain Extraction Tool (BET) followed by segmentation into grey matter (GM) white matter (WM) and cerebrospinal fluid (CSF) via FMRIB automated segmentation tool (FAST). Brain tissue volumes, normalized for head size, were estimated with SIENAX.(Smith et al., 2002) Volumes of subcortical grey matter structures were calculated by FMRIB's Integrated Registration and Segmentation Tool (FIRST), part of FSL (http://fsl.fmrib.ox.ac.uk/fsl/fslwiki/FIRST).

To calculate cerebellar volume on the 3D T1 images, we used the spatially unbiased infratentorial template toolbox (SUIT), version 3.4 (http://www.diedrichsenlab.org/imaging.suit.htm), implemented in SPM12 (http://www.fil.ion.ucl.ac.uk/spm) running under MATLAB R2020. The

following steps were performed with SUIT: 1) extraction of each subject's cerebellum from 3DT1 anatomical images; 2) normalization of the isolated cerebellum to the SUIT atlas template space using the affine transformation matrix and non-linear flow field; in particular, in the present work the *suit_normalize_dentate* module of SUIT normalization was used to ensure accurate individual isolation of the DN; 3) reslicing the cerebellum, in order to preserve the volume of cerebellar lobules in the SUIT atlas template space. Lastly, the obtained SUIT atlas was realigned back to the native subject space. For each subject, we parceled and computed 28 cerebellar lobules and 6 nuclei (dentate, interposed and fastigial). Left and right cerebellar volumes were computed as the sum of lobules I–IV, V, VI, Crus I, Crus II, VIIa, VIIIa, VIIIb, IX, and X and used for further statistical analyses. Left and right dentate volumes were also extracted.

Functional MRI

Preprocessing of functional data included the following steps: removal of the first three volumes to allow the signal to reach equilibrium; spatial smoothing at 6 mm full width at half maximum Gaussian kernel; movement removal with independent component analysis- automatic removal of motion artifacts (ICA-AROMA) (Pruim et al., 2015) application of a band-pass filter [0.008-0.09 Hz] to exclude physiological artifacts; and further movement and artifact correction via WM and CSF signal regression. A two-step procedure for the linear/non-linear registration of subject functional images on standard space was implemented using FMRIB's linear image registration tool (FLIRT) and FMRIB's non-linear registration tool (FNIRT).

Seed Description

For seed-based analyses, regions of interest (ROIs) were created using 2-mm-radius spheres centered on reference MNI coordinates. For DN, dorsal and ventral seeds, corresponding to motor and non-motor functional territories, were defined following previous studies (Anteraper et al., 2019; Bernard et al., 2014) (right dorsal: x= 12, y= -57, z= -30; left dorsal: x= -12, y= -57, z= -30; right ventral: x= 17, y= -65, z= -35; left ventral: x= -17, y= -65, z= -35).

For the GP, GPe and GPi seeds, corresponding to the inhibitory indirect and excitatory direct pathways, were defined according to Tarcijonas et al. (Tarcijonas et al., 2020) (right GPe: x= 17, y= 4, z= 1; left GPe: x= −15, y= 4, z= −4; right GPi: x= 15, y= −1, z= −2; left GPi: x= −17, y= −3, z= −4).

For each subject, left and right dorsal and ventral DN as well as left and right GPe and GPi were combined in bilateral masks and transformed into the functional space using both linear and non-

linear deformations. Seed-based analyses were performed using FSL's FMRI Expert Analysis Tool (FEAT). For each subject, the mean time series was calculated within each of the selected 4 ROIs and used as seeds in the analyses. Voxel-wise maps of FC were calculated between each seed and the rest of the brain for each individual participant via a general linear model (GLM).

Statistical analysis

Statistical analysis was performed using SPSS software (IBM SPSS Statistics, Version 25.0. Armonk, NY: IBM Corp.). Age was compared using the Mann-Whitney U test, while gender was compared using the Fisher's exact test between the patient and control groups.

Kinematic data

In a preliminary analysis, paired sample t-tests were used to compare the kinematic variables of tremor and finger tapping movements of two sides of the body in both groups (ET and HS). After demonstrating no difference between sides in either group, we calculated the averages of kinematic variables of both sides and used them for group comparison by unpaired sample t-tests. The Bonferroni correction, was to account for multiple comparisons when conducting t-tests, thereby minimizing the risk of type I errors.

MRI Structural data

Group differences in terms of GM and WM volumes, volumes of deep grey matter structures, left and right cerebellar volumes and DN were tested via non-parametric test (Mann-Whitney U test), Bonferroni corrected (21-ROIs; corrected alpha level 0.002).

MRI Functional data

Maps of dorsal and ventral DN- and GPe and GPi-FC were assessed voxel-wise in the single groups of patients and HS (one-sample t-test), and between groups (two sample unpaired t-test), via non-parametric tests (FSL randomise, 5000 permutations), including age, sex, and GM volume as covariates of no interest.

Results were corrected using false discovery rate (FDR) correction (Benjamini and Hochberg, 1995) for multiple comparisons ($p < 0.05$). The minimum cluster extent was set at 100 voxels.

Correlation between kinematic and MRI data

In both HS and ET patients' groups, voxel-wise correlations between either dorsal and ventral DN- or GPe and GPi-FC maps and finger tapping velocity were non parametrically performed (FSL randomize, 5000 permutations), with age and gender as covariates of no interest. For ET patients we also included tremor severity (GRMS^2) as covariate of no interest. Results were corrected using false discovery rate (FDR) correction (Benjamini and Hochberg, 1995) for multiple comparisons ($p < 0.05$). The minimum cluster extent was set at 100 voxels.

As a supplementary analyses, we also performed voxel-wise correlations between DN and GPe and GPi FC maps and essential tremor severity (see Supplementary Materials for further details).

3.2.4 Results

Clinical and demographic data

There were no significant differences between ET patients and HS in terms of age ($p=0.10$), gender distribution ($p=0.71$), and MOCA scores ($p=0.11$). The demographic and clinical characteristics of the subjects are presented in Table 3.

In the ET group, the FTMTRS score was 17.7±10.8, and the MDS-UPDRS-III score was 6.2±3.0, with the main influence coming from the postural and kinetic tremor components (as assessed by items 3.14 and 3.15). However, none of the patients exhibited other clinically-detectable symptoms that would warrant an alternative diagnosis (Postuma et al., 2015a).

Kinematic data

ET subjects had postural upper limb tremor characterized by an average frequency of 6.07 Hz ± 1.22 and an amplitude of 0.38 GRMS^2 ± 0.21. The analysis of finger tapping revealed that ET patients had a reduced number of movements and lower velocity in their finger tapping movements compared to HS (number of movements: 41.00±13.36 vs. 54.63±13.76, $p<0.01$; velocity: 951.51±187.51 vs. 1126.35±142.92, $p<0.01$). The analysis of finger tapping movements also indicated a tendency for ET patients to exhibit lower amplitude compared to HS (amplitude: 47.49±8.61 vs. 53.41±8.05, $p<0.05$). However, it is important to note that this difference did not reach statistical significance after applying the Bonferroni correction for multiple comparisons. Finally, no significant differences were observed in terms of rhythm, and amplitude and velocity slope (sequence effect) between ET and HS ($p>0.05$) (Table 4).

MRI

In terms of structural MRI findings, no significant differences were observed in the volumes of whole brain GM and WM, cerebellum, and deep gray matter structures between ET patients and HS ($p>0.05$) (Table 5).

Maps of dorsal and ventral DN- and GPe and GPi-FC in the single groups of patients and HS were reported in the Supplementary Materials (Suppl. Fig. 1, Suppl. Fig.2, Suppl. Table 4 and Suppl. Table 5).

DN

In the between group comparison, ET patients, compared to HS, exhibit higher FC ($p < 0.05$ FDR corrected) between dorsal DN and several regions, including cerebellum (left lobules VI, VIIb, VIIIa, VIIIb, crus I and II, right lobules I-IV, V and vermis), thalamus and BG, bilateral pre and post-central gyri and bilateral temporal and insular cortices. Additionally, they demonstrate lower FC between dorsal DN and precuneus, right inferior and middle temporal gyri, parieto-occipital cortices and orbitofrontal regions (Fig. 2, Table 6).

ET patients also showed higher FC when compared to HS between ventral DN and several regions including the cerebellum (left lobule VI and VIIb, right lobules I-IV, lobule V and VI, bilateral crus I and II and vermis), thalamus, BG, insular and temporal cortices, supramarginal gyri and orbitofrontal regions. Additionally, ET patients exhibited lower FC between ventral DN and brainstem, temporal regions including para-hippocampal gyri and left hippocampus (Fig. 2, Table 6).

GP

In the between group comparison, ET patients showed higher FC ($p < 0.05$ FDR corrected) between the GPe and several regions including the cerebellum (right lobule IX, crus I and left lobule X), brainstem, right putamen, right occipital and parietal regions, insular cortex, bilateral frontal pole and inferior frontal gyri. Additionally, ET patients exhibited lower FC, compared to HS, between GPe and the cerebellum (right lobule VIIb, crus I and II), left superior and middle frontal gyri, left frontal medial cortex and right middle and inferior temporal gyri (Fig. 2, Table 7).

Furthermore, ET compared to HS showed higher FC between the GPi and the cerebellum (bilateral crus I, lobules VI, VIIb, VIIIa, VIIIb, IX, left crus II and lobule X), brainstem, right putamen, right temporal pole and insular cortex, precuneus, parieto-occipital regions, pre- and post-central gyri, middle and inferior frontal gyri and orbitofrontal regions. Additionally, ET exhibited lower FC between GPi and right temporal regions and brainstem (Fig. 2, Table 7).

Correlation between kinematic and MRI data

DN

In HS, dorsal DN-FC with the cerebellum (lobules V-VI, left lobules I-IV, left crus I and II and vermis), brainstem and occipital fusiform cortex was positively correlated with finger tapping velocity. Instead, dorsal DN-FC with left thalamus, lateral occipital cortices, precuneus and left frontal cortex was negatively correlated with finger tapping velocity (Fig. 3, Table 8).

In ET patients, dorsal DN-FC with the cerebellum (lobules I-IV and right lobule V), brainstem, BG, left occipital pole, parietal operculum cortex bilaterally, insular and temporal cortices as well as pre and postcentral gyri was positively correlated with finger tapping velocity.

No correlation was found between ventral DN- FC and finger tapping velocity neither in HS nor in ET patients (Fig. 3, Table 8).

GP

In HS, GPe-FC with left putamen and insular cortex was positively correlated with finger tapping velocity. Additionally, GPe-FC with left caudate, pallidum and thalamus, right putamen, hippocampus and amygdala, insular and temporal cortices and right precentral gyrus was negatively correlated with finger tapping velocity (Fig. 3, Table 8).

In ET patients, GPe-FC with several cerebellar regions (lobules I-IV, left lobules V, VI, VIIb, VIIIa and crus I), putamen, left caudate, insular cortex, temporo-parietal regions, supplementary motor area, pre and post-central gyri and frontal cortices was positively correlated with finger tapping velocity. Additionally, GPe-FC with frontal pole, cingulate and paracingulate gyri exhibited a negative correlation between with finger tapping velocity (Fig. 3, Table 8).

In HS, GPi-FC with left putamen and pallidum, paracingulate gyrus and left insular cortex was positively correlated with finger tapping velocity.

In ET patients, GPi-FC with the cerebellum (bilateral crus I, right crus II and lobule VI), right putamen, brainstem, insular and temporal cortices, left postcentral gyrus, right superior and middle frontal gyri was positively correlated with finger tapping velocity (Fig. 3, Table 8).

For ET patients, we also found significant correlations between dorsal and ventral DN and GPe and GPi-FC and essential tremor severity (FMTRS scores). Results are reported in the Supplementary Materials (Suppl. Fig. 3 and Suppl. Table 6).

3.2.5 Discussion

The objective of this study was to explore the potential relationship between the structural and functional characteristics of the cerebellum and BG and objective measures of altered voluntary movement execution in individuals with ET. By doing so, we aimed to better understand the pathophysiology of altered movement execution in ET. Our findings confirm that individuals with ET exhibit altered execution of repetitive finger tapping, characterized by bradykinesia (slowness of movement), without the presence of other abnormalities (Bologna et al., 2023), as identified through kinematic analysis. Our morphometric analysis did not reveal any significant changes in global, cerebellar and pallidal volumes between individuals with ET and HS, accordingly with previous studies (Holtbernd and Shah, 2021; Luo et al., 2019). Although some earlier studies have demonstrated white matter alterations related to ET (Pietracupa et al., 2019), a consistent reproducible pattern of atrophy has not been conclusively demonstrated in this condition (Holtbernd and Shah, 2021; Luo et al., 2019). Interestingly, our data demonstrate a trend to volume reduction in bilateral GP of ET patients, in line with previous observations of bilateral GP iron deposition (Novellino et al., 2013). However, patients exhibited complex patterns of altered FC involving both the cerebellum and the BG. Interestingly, impaired movement execution, i.e., a lower movement velocity, was associated with decreased DN and GP-FC with cerebellar areas, striatum and sensorimotor areas.

Slowed Voluntary Movement Execution in ET

The present study shows that ET patients perform sequential finger movement at lower speed that normal subjects. We have previously interpreted this finding as a consequence of a cerebellum involvement (Angelini et al., 2023a; Bologna et al., 2020; Paparella et al., 2021b; Passaretti et al., 2022), based on experimental observation demonstrating that the cerebellum encodes various kinematic parameters, including movement velocity, and that cerebellar diseases may be associated with movement slowness (bradykinesia) (Bologna et al., 2020b; Paparella et al., 2021b).

Increased Cerebellar Activity, and DN Motor Shift in ET

The first novel finding to be discussed is the evidence of increased activity of the cerebellar internal circuitry in ET patients, involving both anterior and posterior lobules. Also, we provide evidence of an altered FC between the cerebellum and various cortical areas, likely mediated by pathways that traverse the thalamic nuclei (Fang et al., 2016; Hoover and Strick, 1999; S. Matano, 2001; Middleton and Strick, 2001, 1997). In detail, we found that ET patients show increased FC between the DN and both anterior and posterior cerebellar lobules. This finding is in line with the evidence of involvement of both anterior and posterior cerebellar lobules in ET, as demonstrated by Buijink and colleagues

(Buijink et al., 2015). ET patients demonstrated increased FC of dorsal DN with areas part of habitual motor network including thalamus, BG and bilateral somatosensory cortices, while demonstrating reduced functional connectivity with multimodal associative cortices. Intriguingly, a similar pattern is evidenced for the ventral portion of the DN, classically deputed to associative connections.

These findings are consistent with previous studies and support the notion of impaired connectivity between the cerebellum and multimodal associative areas, which may contribute to ET pathophysiology (Benito-León et al., 2019; Fang et al., 2015; Lenka et al., 2017; Pietracupa et al., 2021; Tikoo et al., 2020). Moreover, these results evidence a shift of DN towards increased connectivity with motor network areas. This shift may reflect deregulated increased connectivity for dorsal DN, but also a neural plasticity adaptation concerning ventral DN connectivity, that in normal condition has a main associative role.

Increased GPi Connectivity in ET

Equally important, our study highlights the significance of FC abnormalities of both the DN and the striatum as well as between the cerebellar hemispheres responsible for sensory-motor integration (specifically the antero-lateral hemispheric cerebellar lobules) and the GP (Tikoo et al., 2020). The GPe, important relay nuclei in the indirect BG pathway, demonstrated increased connectivity with cerebellar areas and striatum, while demonstrating alternatively increased and decreased connectivity with multiple cortical areas. The GPi, serving as the primary output structure of the BG, demonstrated increased FC with components of habitual motor network such as cerebellar lobules, brainstem, striatum and somatosensory motor cortices, as well as different neocortical areas. The observation of enhanced FC of GP, especially within the habitual motor network, can be interpreted in two distinct ways. Firstly, it might indicate a primary pathological manifestation of altered GP activity, or it could potentially be a compensatory mechanism, in an effort to counterbalance the uncontrolled activation of the cerebellum (Alamy et al., 1995; Connolly et al., 2015; Filion and Tremblay, 1991; Johnson et al., 2021; Obeso et al., 2008). Remarkably, high-frequency, desynchronized GP activity and increased connectivity with cerebellum and cortical motor areas have been observed in both patients and animal models of Parkinson's disease (PD) (Alamy et al., 1995; Connolly et al., 2015; Filion and Tremblay, 1991; Johnson et al., 2021; Obeso et al., 2008). These findings have, in some instances, been associated with poorer motor performance or the progression of motor symptoms in patients. In ET patients augmented GP connectivity was associated with poorer cognitive performance (Benito-León et al., 2019; Wang et al., 2018), but scarce evidences regard motor manifestation in ET and GP activity. The presence of similar abnormalities in GP connectivity patterns in ET patients raises

intriguing questions regarding shared neurophysiological mechanisms between ET and PD, particularly concerning voluntary motor execution.

Reduced Voluntary Movement Velocity in ET Associates with Weaker Motor Network FC

When considering the correlations between neuroimaging and kinematic data, our study revealed that decreased finger tapping velocity in ET patients was associated with weaker FC between both dorsal DN and GPi with the motor network encompassing the cerebellar (antero-lateral cerebellar hemispheres)-thalamo-striatal-sensorimotor cortex. GPe exhibited a peculiar relation with finger tapping velocity in ET. In fact while in HS GPe-FC within habitual motor network and temporo-insular cortices had mainly negative correlation with movement velocity, in ET GPe-FC with the same structures was demonstrated to be positive, involving also GPe-FC with cerebellar areas. Repetitive motor tasks, such as finger tapping, require precise and coordinated activation and inhibition of brain regions involved in motor control. Our findings underscore the significance of both cerebellar and BG activity in facilitating optimal motor performance. Proper activity in these structures enables enhanced movement velocity while minimizing reliance on higher cortical structures for movement preparation and planning. As a result, both cerebellar and BG facilitates efficient motor execution (Jahanshahi et al., 2015; Redgrave et al., 2010). Hence, we observed increased connectivity of GP and DN portions with cerebellar and motor network areas in ET patients and a positive correlation between the GP- and DN-FC and faster voluntary movement execution. This suggests a potential compensatory role of observed findings, in an attempt to counterbalance the reduced voluntary motor performance in ET patients. Adjunctively, connectivity outside habitual motor network, especially with temporo-insular areas, was correlated with better motor performance, thus reinforcing the hypothesis of a compensatory origin of the observed findings. Increased activity within the motor network as well as a recruitment of non-motor areas in an effort to improve motor performance can constitute a compensatory network, that in an overloading context can potentially lead to imbalances in global brain activity with detrimental effects.

Previous studies demonstrated altered FC in cerebellar and pallidal networks, also correlating with poorer motor and non-motor performances, but none of them focused on their role in altered voluntary movement execution in ET patients (Benito-León et al., 2019; Buijink et al., 2015; Fang et al., 2016, 2015; Nicoletti et al., 2020; Tikoo et al., 2020; Wang et al., 2018). Dopamine transporter studies demonstrated reduced striatal dopaminergic uptake in certain subgroups of ET patients (Isaias et al., 2010, 2008), and our study recently correlated it with lower finger tapping velocity (Colella et al., 2023). Dopaminergic dysfunction can lead to secondary changes in cerebellar activity, in order to sustain motor performance in striatum (putamen)-thalamus-M1 circuit hypofunction, as observed in

PD (Wu and Hallett, 2013). The potential relationships between alterations in central dopaminergic tone and FC changes between the BG and cerebellum should be object of further exploration in future studies.

Confounding Effect of Tremor and Potential Study Limitations

An important aspect to discuss is the potential confounding effect of tremor on movement related results. The present results extend observations by previous studies that alterations in FC within the cerebellar-thalamus-sensorimotor network is associated with the severity of tremor (Fang et al., 2016; Tikoo et al., 2020). More in detail, Tikoo et al demonstrated that tremor severity, tremor amplitude and peak frequency were significantly associated with altered FC of the dentate nucleus with cerebellar areas, sensorimotor cortex and thalamus/BG, respectively as confirmed by our supplementary analyses on clinical tremor severity. In particular, positive correlation with tremor severity included the FC of ventral DN with cerebellar and cortical areas, as well as the GPe-FC with other BG structures, while negative correlation involved both dorsal DN- and GPi-FC with widespread cortical areas. Hence, it could be argued that the results of the present study might reflect the severity of the tremor rather than the impairment of voluntary movement. Importantly, however, in our analysis, we have considered tremor as a covariate of non-interest, thus excluding the possibility that it may have influenced our results. Moreover, a recent study evidenced that movement velocity in ET is not influenced by tremor amplitude, and tremor does not correlate with subtle dopaminergic changes in ET (Colella et al., 2023). Thus, we can infer that, like tremor, the underlying pathophysiological mechanisms of impaired movement execution in ET cannot be solely attributed to a singular anatomical structure. Rather, a complex interplay of partially overlapping brain areas contributes to the generation of both tremor and altered movement execution in ET.

This study has some limitations. Firstly, our sample size is relatively small, although it is consistent with the majority of fMRI studies on ET (Holtbernd and Shah, 2021; Pietracupa et al., 2021), and is composed by a prevalence of men. It is important to consider that ET is a highly heterogeneous condition from a clinical perspective, and our study predominantly focused on patients with intermediate forms of the disease. Therefore, future research is needed to validate the findings of this study on larger and more diverse patient cohorts to further elucidate the potential role played by clinical heterogeneity. Moreover, we excluded patients presenting with ET soft signs, since, especially questionable dystonia, could influence kinematic measures, and alter functional connectivity (Brinker et al., 2023; Isaias et al., 2010). Another limitation is the absence of DAT imaging for clinical confirmation of the diagnosis. However, it is important to note that the clinical diagnosis of ET was based on the most recent diagnostic criteria, which do not require DAT imaging

(Bhatia et al., 2018). Finally, another potential limitation of the study is that we solely examined repetitive finger movements and did not assess movements of different types or involving other body segments. Consequently, the generalizability of our observations to other types of movements remains uncertain.

3.2.6 Conclusion

Our study contributes to a better understanding of the pathophysiology of ET by highlighting the role of the cerebellum, BG and cerebral cortex within a dysfunctional network. In this regard, functional alterations in the networks may not only influences the generation of tremor but also contributes to impaired motor execution in ET. The results of this study could hold significance within the current research landscape, which is increasingly focused on identifying specific ET subtypes or even distinct individual diseases within the broader spectrum of ET. Such an approach would aid in early recognition of patients who may progress to develop parkinsonian syndromes and shed light on potential diverse underlying causes.

4. PATHOPHYSIOLOGICAL IMPLICATIONS

Our two studies provided new pathophysiological information on voluntary movement abnormalities in ET. Bradykinesia, literally defined as motor slowness, is linked specifically to nigrostriatal dysfunction in PD (Kalia and Lang, 2015), but in ET the clinical and DAT alterations can only be investigated by quantitative analyses (Bologna et al., 2020; Brogley, 2019). We demonstrated how in ET patients a slight slowness detectable by kinematic analysis can be correlated to low DaTQUANT striatal values. These results allow us to classify these patients as ET and not parkinsonism (Bhatia et al., 2018), but at the same time, they underline a possible involvement of the substantia nigra also in ET (Tarakad and Jankovic, 2019) . However, recent studies in PD have shown a greater involvement of brain networks than of a single structure like the BG, and the same could be found in ET (Bologna et al., 2020b; Paparella et al., 2021b).

In the second study, we found increased DN and GPi FC with cerebellar lobules, thalamus, BG, and sensory-motor areas. These results confirm in ET an abnormal cerebellar activity within the motor network (as highlighted by DN FC) (Benito-León et al., 2019; Tikoo et al., 2020), but also a pathological involvement of the GP, primitive or compensatory to the cerebellar dysfunction (Alamy et al., 1995; Filion and Tremblay, 1991; Obeso et al., 2008). This altered connectivity could determine the onset of motor alterations in ET, in line with previous studies (Buijink et al., 2015; Tikoo et al., 2020). In our ET patients, the DN and GP FC with antero-lateral cerebellar hemispheres, thalamus, BG, sensorimotor and non-motor cortical areas correlated positively with the velocity of finger tapping (lower velocity was associated with lower connectivity of the interested areas). Furthermore, in HS we documented a negative correlation of GPe FC within motor network and temporo-insular cortices with motor speed, which was instead positive in the group of ET patients, involving also GPe-FC with cerebellar areas. In HS, coordination and inhibition of brain network components are necessary during the execution of repetitive movements and generally do not require the constant participation of associative cortices, responsible for movement planning. We supposed that in ET the cerebellum and BG cooperate synergistically in a compensative way to facilitate correct motor performance, also with the contribution of non-motor cortical areas (Jahanshahi et al., 2015; Redgrave et al., 2010).

In addition to the well-known role of the cerebellum, we demonstrated here a pathological involvement of the basal ganglia in terms of mild dopaminergic depletion and altered pallidal connectivity in ET patient. If the BG and cerebellum interact with each other during the motor execution, their alteration could determine a motor network dysfunction and facilitate the onset of motor slowness in ET. It was discovered how the cerebellum and basal ganglia communicate bidirectionally with two main pathways: the first thalamo-striatal and the second, which projects from

the Subthalamic Nucleus (STN) to the cerebellar cortex and pontine nuclei (Bostan and Strick, 2018). In PD, dopaminergic degeneration seems to cause secondary changes in cerebellar activity as a compensatory effect of the hypofunction in the cortical striato-thalamic circuit to maintain motor function as normal as possible (Wu et al., 2011, 2009; Wu and Hallett, 2013). However, recent anatomical studies have suggested the presence of cerebellar projections directed to the substantia nigra pars compacta, with the role of modulating striatal dopamine levels and facilitating the processes of motor initiation and execution (Washburn et al., 2024). The discovery of these additional cerebellar connections is truly relevant if we consider that a cerebellar dysfunction could reduce striatal dopamine levels and influence the activity of the basal ganglia. Thus, the mild dopaminergic in ET deficit could represent a primitive alteration as happens in PD, but, more likely, it may be secondary to the typical cerebellar dysfunction of ET. The pathological mechanism through this dysfunction can influence these neural projections is still unclear. In the literature there are conflicting data on the development of degenerative processes in ET, although a reduction in the number of Purkinje cells or axonal anatomical alterations have been identified (Tarakad and Jankovic, 2019). According with other studies, we found no qualitative evidence of dopaminergic denervation (Benamer et al., 2000) or cerebral and cerebellar morphological changes in our ET patients (Holtbernd and Shah, 2021; Luo et al., 2019). It is possible that a cerebellar alteration, not macroscopic and not yet identified, for example an altered oscillatory activity such as for tremor (Bosch et al., 2023; Guerra et al., 2024; Raethjen and Deuschl, 2012), could modulate striatal dopamine levels (evident only quantitatively) in ET. The increased brain connectivity, as demonstrated by rs-fMRI, may have a compensatory effect on the abnormal cerebellar activity, to further facilitate the connection with the substantia nigra and basal ganglia, and to involve other brain structures during the motor execution. If this compensatory activity become ineffective, kinematic motor slowness could be detectable.

These observations further confirm the hypothesis that movement slowness in ET can be generated by different brain areas in the context of a network impairment, rather than a dysfunction of single anatomical structure (Paparella et al., 2021b). Of interest, there was no association between tremor severity and dopaminergic deficit, although tremor negatively correlated with increased DN and GPi FC with widespread cortical areas (Tikoo et al., 2020). The mechanisms by which a different involvement of the BG and cerebellum determine bradykinesia rather than tremor are not yet known and require further subsequent studies.

5. GENERAL CONCLUSIONS

Motor slowness without sequence effect represents a typical feature of ET patients and must be distinguished terminologically from the bradykinesia of PD (Bologna et al., 2023, 2020b). Components of brain networks, rather than a single area, are involved in different ways in the genesis of impaired voluntary movement and postural tremor in ET. Basal ganglia, cerebellum and cortical areas don't act independently of each other, but instead they are highly interconnected. We speculated that mild dopamine depletion and BG and cerebellar dysfunction, in the context of a network failure, may synergistically determine bradykinesia in ET (Bologna et al., 2020b; Paparella et al., 2021b). Kinematic analysis techniques are confirmed as a valid tool for quantifying non-clinically relevant motor alterations. The evidence of a soft sign such as motor slowness categorized our patients as ET-plus by neurophysiological (though not clinical) evidence (Bologna et al., 2020). The term ET-plus has been highly criticized, as it could only represent a state condition, without significant clinical and research implications. The phenotypic identification of the various types of ET-plus does not allow an unambiguous pathophysiological interpretation (Erro et al., 2022; Louis, 2020). However, in line with previous studies, our kinematic and neuroradiological findings support the pathophysiological relationship between this subtype of ET-plus and PD, and do not exclude its possible future evolution towards a clinical picture of parkinsonism (ET-PD) (Angelini et al., 2024, 2023a). Therefore, in accordance with the current convention of ET (Bhatia et al. 2018), ET-plus with subtle bradykinesia constitutes a heterogeneous clinical syndrome and, in the absence of objective clinical manifestations, cannot be identified as an additional etiological entity. Longitudinal studies with clinical and radiological follow-up evaluations are necessary to better identify the progression of these patients and to provide further information to direct them towards the correct diagnosis and therapy (Angelini et al., 2024, 2023a).

In conclusion, our results confirmed the great clinical heterogeneity and the pathophysiological complexity of ET. We demonstrated how the combination of different methodologies can significantly help to understand the pathophysiology of ET, but the identification of future reproducible biomarkers could be necessary to enhance diagnostic accuracy and to better classify these ET patients, from the early stages of the disease.

6. REFERENCES

Alamy, M., Pons, J.C., Gambarelli, D., Trouche, E., 1995. A defective control of small-amplitude movements in monkeys with globus pallidus lesions: an experimental study on one component of pallidal bradykinesia. Behav. Brain Res. 72, 57–62. https://doi.org/10.1016/0166-4328(96)00048-4

Algarni, M., Fasano, A., 2018. The overlap between Essential tremor and Parkinson disease. Parkinsonism Relat. Disord. 46, S101–S104. https://doi.org/10.1016/j.parkreldis.2017.07.006

Angelini, L., Paparella, G., Cannavacciuolo, A., Costa, D., Birreci, D., De Riggi, M., Passaretti, M., Colella, D., Guerra, A., Berardelli, A., Bologna, M., 2024. Clinical and kinematic characterization of parkinsonian soft signs in essential tremor. J. Neural Transm. 131, 941–952. https://doi.org/10.1007/s00702-024-02784-0

Angelini, L., Paparella, G., De Biase, A., Maraone, A., Panfili, M., Berardelli, I., Cannavacciuolo, A., Di Vita, A., Margiotta, R., Fabbrini, G., Berardelli, A., Bologna, M., 2023a. Longitudinal study of clinical and neurophysiological features in essential tremor. Eur. J. Neurol. 30, 631–640. https://doi.org/10.1111/ene.15650

Angelini, L., Terranova, R., Lazzeri, G., Van Den Berg, K.R.E., Dirkx, M.F., Paparella, G., 2023b. The role of laboratory investigations in the classification of tremors. Neurol. Sci. 44, 4183–4192. https://doi.org/10.1007/s10072-023-07108-w

Anteraper, S.A., Guell, X., Taylor, H.P., D'Mello, A., Whitfield-Gabrieli, S., Joshi, G., 2019. Intrinsic Functional Connectivity of Dentate Nuclei in Autism Spectrum Disorder. Brain Connect. 9, 692–702. https://doi.org/10.1089/brain.2019.0692

Beck, A.T., 1961. An Inventory for Measuring Depression. Arch. Gen. Psychiatry 4, 561. https://doi.org/10.1001/archpsyc.1961.01710120031004

Bédard, P., Panyakaew, P., Cho, H.-J., Hallett, M., Horovitz, S.G., 2022. Multimodal imaging of essential tremor and dystonic tremor. NeuroImage Clin. 36, 103247. https://doi.org/10.1016/j.nicl.2022.103247

Benamer, H.T.S., Patterson, J., Grosset, D.G., Booij, J., de Bruin, K., van Royen, E., Speelman, J.D., Horstink, M.H.I.M., Sips, H.J.W.A., Dierckx, R.A., Versijpt, J., Decoo, D., Van Der Linden, C., Hadley, D.M., Doder, M., Lees, A.J., Costa, D.C., Gacinovic, S., Oertel, W.H., Pogarell, O., Hoeffken, H., Joseph, K., Tatsch, K., Schwarz, J., Ries, V., 2000. Accurate differentiation of parkinsonism and essential tremor using visual assessment of [123I]-FP-CIT SPECT imaging: The [123I]-FP-CIT study group. Mov. Disord. 15, 503–510. https://doi.org/10.1002/1531-8257(200005)15:3<503::AID-MDS1013>3.0.CO;2-V

Benito-León, J., Labiano-Fontcuberta, A., 2016. Linking Essential Tremor to the Cerebellum: Clinical Evidence. The Cerebellum 15, 253–262. https://doi.org/10.1007/s12311-015-0741-1

Benito-León, J., Sanz-Morales, E., Melero, H., Louis, E.D., Romero, J.P., Rocon, E., Malpica, N., 2019. Graph theory analysis of resting-state functional magnetic resonance imaging in essential tremor. Hum. Brain Mapp. 40, 4686–4702. https://doi.org/10.1002/hbm.24730

Benjamini, Y., Hochberg, Y., 1995. Controlling the False Discovery Rate: A Practical and Powerful Approach to Multiple Testing. J. R. Stat. Soc. Ser. B Methodol. 57, 289–300. https://doi.org/10.1111/j.2517-6161.1995.tb02031.x

Berardelli, A., Rothwell, J.C., Thompson, P.D., Hallett, M., 2001. Pathophysiology of bradykinesia in Parkinson's disease. Brain J. Neurol. 124, 2131–2146.

Berardelli, A., Wenning, G.K., Antonini, A., Berg, D., Bloem, B.R., Bonifati, V., Brooks, D., Burn, D.J., Colosimo, C., Fanciulli, A., Ferreira, J., Gasser, T., Grandas, F., Kanovsky, P., Kostic, V., Kulisevsky, J., Oertel, W., Poewe, W., Reese, J.-P., Relja, M., Ruzicka, E., Schrag, A., Seppi, K., Taba, P., Vidailhet, M., 2013. EFNS/MDS-ES recommendations for the diagnosis of Parkinson's disease. Eur. J. Neurol. 20, 16–34. https://doi.org/10.1111/ene.12022

Berg, D., 2011. Substantia nigra hyperechogenicity is a risk marker of Parkinson's disease: yes. J. Neural Transm. 118, 613–619. https://doi.org/10.1007/s00702-010-0565-6

Bernard, J.A., Peltier, S.J., Benson, B.L., Wiggins, J.L., Jaeggi, S.M., Buschkuehl, M., Jonides, J., Monk, C.S., Seidler, R.D., 2014. Dissociable functional networks of the human dentate nucleus. Cereb. Cortex N. Y. N 1991 24, 2151–2159. https://doi.org/10.1093/cercor/bht065

Bhatia, K.P., Bain, P., Bajaj, N., Elble, R.J., Hallett, M., Louis, E.D., Raethjen, J., Stamelou, M., Testa, C.M., Deuschl, G., the Tremor Task Force of the International Parkinson and Movement Disorder Society, 2018. Consensus Statement on the classification of tremors. from the task force on tremor of the International Parkinson and Movement Disorder Society: IPMDS Task Force on Tremor Consensus Statement. Mov. Disord. 33, 75–87. https://doi.org/10.1002/mds.27121

Blenkinsop, A., Anderson, S., Gurney, K., 2017. Frequency and function in the basal ganglia: the origins of beta and gamma band activity. J. Physiol. 595, 4525–4548. https://doi.org/10.1113/JP273760

Boecker, H., Weindl, A., Brooks, D.J., Ceballos-Baumann, A.O., Liedtke, C., Miederer, M., Sprenger, T., Wagner, K.J., Miederer, I., 2010. GABAergic Dysfunction in Essential Tremor: An ^{11}C-Flumazenil PET Study. J. Nucl. Med. 51, 1030–1035. https://doi.org/10.2967/jnumed.109.074120

Bologna, M., Berardelli, I., Paparella, G., Ferrazzano, G., Angelini, L., Giustini, P., Alunni-Fegatelli, D., Berardelli, A., 2019. Tremor Distribution and the Variable Clinical Presentation of Essential Tremor. The Cerebellum 18, 866–872. https://doi.org/10.1007/s12311-019-01070-0

Bologna, M., Espay, A.J., Fasano, A., Paparella, G., Hallett, M., Berardelli, A., 2023. Redefining Bradykinesia. Mov. Disord. Off. J. Mov. Disord. Soc. 38, 551–557. https://doi.org/10.1002/mds.29362

Bologna, M., Guerra, A., Colella, D., Cioffi, E., Paparella, G., Di Vita, A., D'Antonio, F., Trebbastoni, A., Berardelli, A., 2020a. Bradykinesia in Alzheimer's disease and its neurophysiological substrates. Clin. Neurophysiol. 131, 850–858. https://doi.org/10.1016/j.clinph.2019.12.413

Bologna, M., Guerra, A., Paparella, G., Giordo, L., Alunni Fegatelli, D., Vestri, A.R., Rothwell, J.C., Berardelli, A., 2018. Neurophysiological correlates of bradykinesia in Parkinson's disease. Brain 141, 2432–2444. https://doi.org/10.1093/brain/awy155

Bologna, M., Leodori, G., Stirpe, P., Paparella, G., Colella, D., Belvisi, D., Fasano, A., Fabbrini, G., Berardelli, A., 2016. Bradykinesia in early and advanced Parkinson's disease. J. Neurol. Sci. 369, 286–291. https://doi.org/10.1016/j.jns.2016.08.028

Bologna, M., Paparella, G., Colella, D., Cannavacciuolo, A., Angelini, L., Alunni-Fegatelli, D., Guerra, A., Berardelli, A., 2020. Is there evidence of bradykinesia in essential tremor? Eur. J. Neurol. 27, 1501–1509. https://doi.org/10.1111/ene.14312

Bologna, M., Paparella, G., Fasano, A., Hallett, M., Berardelli, A., 2020b. Evolving concepts on bradykinesia. Brain 143, 727–750. https://doi.org/10.1093/brain/awz344

Bologna, M., Rocchi, L., Leodori, G., Paparella, G., Conte, A., Kahn, N., Fabbrini, G., Berardelli, A., 2015. Cerebellar Continuous Theta Burst Stimulation in Essential Tremor. The Cerebellum 14, 133–141. https://doi.org/10.1007/s12311-014-0621-0

Bosch, T.J., Espinoza, A.I., Singh, A., 2023. Cerebellar oscillatory dysfunction during lower-limb movement in Parkinson's disease with freezing of gait. Brain Res. 1808, 148334. https://doi.org/10.1016/j.brainres.2023.148334

Bostan, A.C., Strick, P.L., 2018. The basal ganglia and the cerebellum: nodes in an integrated network. Nat. Rev. Neurosci. 19, 338–350. https://doi.org/10.1038/s41583-018-0002-7

Brinker, D., Granert, O., Gövert, F., Tödt, I., Baumann, A., Zeuner, K.E., Wolke, R., Deuschl, G., Becktepe, J.S., 2023. Grey matter correlates of dystonic soft signs in essential tremor. Parkinsonism Relat. Disord. 112, 105457. https://doi.org/10.1016/j.parkreldis.2023.105457

Brogley, J.E., 2019. DaTQUANT: The Future of Diagnosing Parkinson Disease. J. Nucl. Med. Technol. 47, 21–26. https://doi.org/10.2967/jnmt.118.222349

Buijink, A.W.G., Broersma, M., van der Stouwe, A.M.M., van Wingen, G.A., Groot, P.F.C., Speelman, J.D., Maurits, N.M., van Rootselaar, A.F., 2015. Rhythmic finger tapping reveals cerebellar dysfunction in essential tremor. Parkinsonism Relat. Disord. 21, 383–388. https://doi.org/10.1016/j.parkreldis.2015.02.003

Caligiuri, M.E., Arabia, G., Barbagallo, G., Lupo, A., Morelli, M., Nisticò, R., Novellino, F., Quattrone, Andrea, Salsone, M., Vescio, B., Cherubini, A., Quattrone, Aldo, 2017. Structural connectivity differences in essential tremor with and without resting tremor. J. Neurol. 264, 1865–1874. https://doi.org/10.1007/s00415-017-8553-5

Cardaioli, G., Ripandelli, F., Paolini Paoletti, F., Nigro, P., Simoni, S., Brahimi, E., Romoli, M., Filidei, M., Eusebi, P., Calabresi, P., Tambasco, N., 2019. Substantia nigra hyperechogenicity in essential tremor and Parkinson's disease: a longitudinal study. Eur. J. Neurol. 26, 1370–1376. https://doi.org/10.1111/ene.13988

Colella, D., Guerra, A., Paparella, G., Cioffi, E., Di Vita, A., Trebbastoni, A., Berardelli, A., Bologna, M., 2021. Motor dysfunction in mild cognitive impairment as tested by kinematic analysis and transcranial magnetic stimulation. Clin. Neurophysiol. 132, 315–322. https://doi.org/10.1016/j.clinph.2020.10.028

Colella, D., Passaretti, M., Frantellizzi, V., Silvia De Feo, M., Cannavacciuolo, A., Angelini, L., Birreci, D., Costa, D., Paparella, G., Guerra, A., De Vincentis, G., Berardelli, A., Bologna, M., 2023. Subtle changes in central dopaminergic tone underlie bradykinesia in essential tremor. NeuroImage Clin. 40, 103526. https://doi.org/10.1016/j.nicl.2023.103526

Connolly, A.T., Jensen, A.L., Bello, E.M., Netoff, T.I., Baker, K.B., Johnson, M.D., Vitek, J.L., 2015. Modulations in oscillatory frequency and coupling in globus pallidus with increasing parkinsonian severity. J. Neurosci. Off. J. Soc. Neurosci. 35, 6231–6240. https://doi.org/10.1523/JNEUROSCI.4137-14.2015

Coria, F., Gimenez-Garcia, M., Samaranch, L., Mora, F.J., Sampol-Bas, C., Pastor, P., 2012. Nigrostriatal dopaminergic function in subjects with isolated action tremor. Parkinsonism Relat. Disord. 18, 49–53. https://doi.org/10.1016/j.parkreldis.2011.08.025

Costa, J., González, H.A., Valldeoriola, F., Gaig, C., Tolosa, E., Valls-Solé, J., 2010. Nonlinear dynamic analysis of oscillatory repetitive movements in Parkinson's disease and essential tremor: Nonlinear Dynamics of Repetitive Movements. Mov. Disord. 25, 2577–2586. https://doi.org/10.1002/mds.23334

Cuberas-Borrós, G., Lorenzo-Bosquet, C., Aguadé-Bruix, S., Hernández-Vara, J., Pifarré-Montaner, P., Miquel, F., Álvarez-Sabin, J., Castell-Conesa, J., 2011. Quantitative Evaluation of Striatal I-123-FP-CIT Uptake in Essential Tremor and Parkinsonism. Clin. Nucl. Med. 36, 991–996. https://doi.org/10.1097/RLU.0b013e3182291a7b

Curran-Everett, D., 2000. Multiple comparisons: philosophies and illustrations. Am. J. Physiol.-Regul. Integr. Comp. Physiol. 279, R1–R8. https://doi.org/10.1152/ajpregu.2000.279.1.R1

De Biase, A., Paparella, G., Angelini, L., Cannavacciuolo, A., Colella, D., Cerulli Irelli, E., Giallonardo, A.T., Di Bonaventura, C., Berardelli, A., Bologna, M., 2022. Tremor and Movement Slowness Are Two Unrelated Adverse Effects Induced by Valproate Intake. Mov. Disord. Clin. Pract. 9, 1062–1073. https://doi.org/10.1002/mdc3.13560

Defer, G.-L., Widner, H., Mari□, R.-M., R□my, P., Levivier, M., Conference Participants: Conference Participants: G. L. Defer, MD (Caen, France, Chairman of the CAPSIT-PD committee), and M. Levivier, MD, PhD (Brussels, Belgium, coordinator of the NIPD program) served as moderators for all the sessions. They, together with H. Widner, MD, PhD (Lund, Sweden); R. M. Mari□, MD, PhD (Caen, France); Ph. R□my, MD, PhD (Cr□teil, France) served as coordinators and cowriters for the dyskinesia/dystonia, cognitive and behavioral, and imaging sections, respectively. P. C, 1999. Core assessment program for surgical interventional therapies in Parkinson's disease (CAPSIT-PD). Mov. Disord. 14, 572–584. https://doi.org/10.1002/1531-8257(199907)14:4<572::AID-MDS1005>3.0.CO;2-C

Deuschl, G., 2000. Essential tremor and cerebellar dysfunction Clinical and kinematic analysis of intention tremor. Brain 123, 1568–1580. https://doi.org/10.1093/brain/123.8.1568

Dirkx, M.F., Bologna, M., 2022. The pathophysiology of Parkinson's disease tremor. J. Neurol. Sci. 435, 120196. https://doi.org/10.1016/j.jns.2022.120196

Dirkx, M.F., Zach, H., Bloem, B.R., Hallett, M., Helmich, R.C., 2018. The nature of postural tremor in Parkinson disease. Neurology 90, e1095–e1103. https://doi.org/10.1212/WNL.0000000000005215

Djurić-Jovičić, M., Petrović, I., Ječmenica-Lukić, M., Radovanović, S., Dragašević-Mišković, N., Belić, M., Miler-Jerković, V., Popović, M.B., Kostić, V.S., 2016. Finger tapping analysis in patients with Parkinson's disease and atypical parkinsonism. J. Clin. Neurosci. 30, 49–55. https://doi.org/10.1016/j.jocn.2015.10.053

Dubois, B., Slachevsky, A., Litvan, I., Pillon, B., 2000. The FAB: A frontal assessment battery at bedside. Neurology 55, 1621–1626. https://doi.org/10.1212/WNL.55.11.1621

Duval, C., Sadikot, A.F., Panisset, M., 2006. Bradykinesia in patients with essential tremor. Brain Res. 1115, 213–216. https://doi.org/10.1016/j.brainres.2006.07.066

Ebner, T.J., Hewitt, A.L., Popa, L.S., 2011. What Features of Limb Movements are Encoded in the Discharge of Cerebellar Neurons? The Cerebellum 10, 683–693. https://doi.org/10.1007/s12311-010-0243-0

Elble, R., Comella, C., Fahn, S., Hallett, M., Jankovic, J., Juncos, J.L., LeWitt, P., Lyons, K., Ondo, W., Pahwa, R., Sethi, K., Stover, N., Tarsy, D., Testa, C., Tintner, R., Watts, R., Zesiewicz, T., 2012. Reliability of a new scale for essential tremor. Mov. Disord. 27, 1567–1569. https://doi.org/10.1002/mds.25162

Erro, R., Schneider, S.A., Stamelou, M., Quinn, N.P., Bhatia, K.P., 2016. What do patients with scans without evidence of dopaminergic deficit (SWEDD) have? New evidence and continuing controversies. J. Neurol. Neurosurg. Psychiatry 87, 319–323. https://doi.org/10.1136/jnnp-2014-310256

Erro, R., Sorrentino, C., Russo, M., Barone, P., 2022. Essential tremor plus rest tremor: current concepts and controversies. J. Neural Transm. 129, 835–846. https://doi.org/10.1007/s00702-022-02516-2

Espay, A.J., Fasano, A., 2023. The Existential Essentialism in Tremor Nosology − 7 Pitfalls, 2 Remedies, and a Path Ahead. Mov. Disord. Clin. Pract. 10. https://doi.org/10.1002/mdc3.13622

Fang, W., Chen, H., Wang, H., Zhang, H., Liu, M., Puneet, M., Lv, F., Cheng, O., Wang, X., Lu, X., Luo, T., 2015. Multiple Resting-State Networks Are Associated With Tremors and Cognitive Features in Essential Tremor. Mov. Disord. Off. J. Mov. Disord. Soc. 30, 1926–1936. https://doi.org/10.1002/mds.26375

Fang, W., Chen, H., Wang, H., Zhang, H., Puneet, M., Liu, M., Lv, F., Luo, T., Cheng, O., Wang, X., Lu, X., 2016. Essential tremor is associated with disruption of functional connectivity in the ventral intermediate Nucleus--Motor Cortex--Cerebellum circuit. Hum. Brain Mapp. 37, 165–178. https://doi.org/10.1002/hbm.23024

Fanning, A., Kuo, S.-H., 2023. Clinical Heterogeneity of Essential Tremor: Understanding Neural Substrates of Action Tremor Subtypes. The Cerebellum. https://doi.org/10.1007/s12311-023-01551-3

Fearnley, J.M., Lees, A.J., 1990. STRIATONIGRAL DEGENERATION: A CLINICOPATHOLOGICAL STUDY. Brain 113, 1823–1842. https://doi.org/10.1093/brain/113.6.1823

Ferrazzano, G., Frantellizzi, V., De Bartolo, M.I., De Feo, M.S., Conte, A., Fabbrini, G., De Vincentis, G., Berardelli, A., 2020. Isolated head tremor: A DAT-SPECT and somatosensory

temporal discrimination study. Parkinsonism Relat. Disord. 81, 56–59. https://doi.org/10.1016/j.parkreldis.2020.10.015

Filion, M., Tremblay, L., 1991. Abnormal spontaneous activity of globus pallidus neurons in monkeys with MPTP-induced parkinsonism. Brain Res. 547, 142–151.

Freitas, S., Simões, M.R., Alves, L., Santana, I., 2013. Montreal Cognitive Assessment: Validation Study for Mild Cognitive Impairment and Alzheimer Disease. Alzheimer Dis. Assoc. Disord. 27, 37–43. https://doi.org/10.1097/WAD.0b013e3182420bfe

Goubault, E., Nguyen, H.P., Ayachi, F.S., Bogard, S., Duval, C., 2017. Do Bradykinesia and Tremor Interfere in Voluntary Movement of Essential Tremor Patients? Preliminary Findings. Tremor Hyperkinetic Mov. 7, 459. https://doi.org/10.5334/tohm.341

Guerra, A., D'Onofrio, V., Ferreri, F., Bologna, M., Antonini, A., 2023. Objective measurement versus clinician-based assessment for Parkinson's disease. Expert Rev. Neurother. 23, 689–702. https://doi.org/10.1080/14737175.2023.2229954

Guerra, A., Paparella, G., Passaretti, M., Costa, D., Birreci, D., De Biase, A., Colella, D., Angelini, L., Cannavacciuolo, A., Berardelli, A., Bologna, M., 2024. Theta-tACS modulates cerebellar-related motor functions and cerebellar-cortical connectivity. Clin. Neurophysiol. 158, 159–169. https://doi.org/10.1016/j.clinph.2023.12.129

Hallett, M., Berardelli, A., Matheson, J., Rothwell, J., Marsden, C.D., 1991. Physiological analysis of simple rapid movements in patients with cerebellar deficits. J. Neurol. Neurosurg. Psychiatry 54, 124–133. https://doi.org/10.1136/jnnp.54.2.124

Hasan, H., Athauda, D.S., Foltynie, T., Noyce, A.J., 2017. Technologies Assessing Limb Bradykinesia in Parkinson's Disease. J. Park. Dis. 7, 65–77. https://doi.org/10.3233/JPD-160878

Haubenberger, D., Hallett, M., 2018. Essential Tremor. N. Engl. J. Med. 378, 1802–1810. https://doi.org/10.1056/NEJMcp1707928

Helmich, R.C., Toni, I., Deuschl, G., Bloem, B.R., 2013. The Pathophysiology of Essential Tremor and Parkinson's Tremor. Curr. Neurol. Neurosci. Rep. 13, 378. https://doi.org/10.1007/s11910-013-0378-8

Hewitt, A.L., Popa, L.S., Pasalar, S., Hendrix, C.M., Ebner, T.J., 2011. Representation of limb kinematics in Purkinje cell simple spike discharge is conserved across multiple tasks. J. Neurophysiol. 106, 2232–2247. https://doi.org/10.1152/jn.00886.2010

Holtbernd, F., Shah, N.J., 2021. Imaging the Pathophysiology of Essential Tremor-A Systematic Review. Front. Neurol. 12, 680254. https://doi.org/10.3389/fneur.2021.680254

Hoover, J.E., Strick, P.L., 1999. The organization of cerebellar and basal ganglia outputs to primary motor cortex as revealed by retrograde transneuronal transport of herpes simplex virus type 1. J. Neurosci. Off. J. Soc. Neurosci. 19, 1446–1463. https://doi.org/10.1523/JNEUROSCI.19-04-01446.1999

Hoshi, E., Tremblay, L., Féger, J., Carras, P.L., Strick, P.L., 2005. The cerebellum communicates with the basal ganglia. Nat. Neurosci. 8, 1491–1493. https://doi.org/10.1038/nn1544

Hua, S.E., Lenz, F.A., 2005. Posture-Related Oscillations in Human Cerebellar Thalamus in Essential Tremor Are Enabled by Voluntary Motor Circuits. J. Neurophysiol. 93, 117–127. https://doi.org/10.1152/jn.00527.2004

Isaias, I.U., Canesi, M., Benti, R., Gerundini, P., Cilia, R., Pezzoli, G., Antonini, A., 2008. Striatal dopamine transporter abnormalities in patients with essential tremor. Nucl. Med. Commun. 29, 349–353. https://doi.org/10.1097/MNM.0b013e3282f4d307

Isaias, I.U., Marotta, G., Hirano, S., Canesi, M., Benti, R., Righini, A., Tang, C., Cilia, R., Pezzoli, G., Eidelberg, D., Antonini, A., 2010. Imaging essential tremor. Mov. Disord. 25, 679–686. https://doi.org/10.1002/mds.22870

Jaeger, D., Kita, H., 2011. Functional connectivity and integrative properties of globus pallidus neurons. Neuroscience 198, 44–53. https://doi.org/10.1016/j.neuroscience.2011.07.050

Jahanshahi, M., Obeso, I., Rothwell, J.C., Obeso, J.A., 2015. A fronto–striato–subthalamic–pallidal network for goal-directed and habitual inhibition. Nat. Rev. Neurosci. 16, 719–732. https://doi.org/10.1038/nrn4038

Jiménez-Jiménez, F.J., Rubio, L., Alonso-Navarro, H., Calleja, M., Pilo-de-la-Fuente, B., Plaza-Nieto, J.F., Benito-León, J., García-Ruiz, P.J., Agúndez, J.A.G., 2010. Impairment of rapid repetitive finger movements and visual reaction time in patients with essential tremor: Motor performance in essential tremor. Eur. J. Neurol. 17, 152–159. https://doi.org/10.1111/j.1468-1331.2009.02784.x

Johnson, L.A., Aman, J.E., Yu, Y., Escobar Sanabria, D., Wang, J., Hill, M., Dharnipragada, R., Patriat, R., Fiecas, M., Li, L., Schrock, L.E., Cooper, S.E., Johnson, M.D., Park, M.C., Harel, N., Vitek, J.L., 2021. High-Frequency Oscillations in the Pallidum: A Pathophysiological Biomarker in Parkinson's Disease? Mov. Disord. Off. J. Mov. Disord. Soc. 36, 1332–1341. https://doi.org/10.1002/mds.28566

Kalia, L.V., Lang, A.E., 2015. Parkinson's disease. The Lancet 386, 896–912. https://doi.org/10.1016/S0140-6736(14)61393-3

Konczak, J., Pierscianek, D., Hirsiger, S., Bultmann, U., Schoch, B., Gizewski, E.R., Timmann, D., Maschke, M., Frings, M., 2010. Recovery of Upper Limb Function After Cerebellar Stroke:

Lesion Symptom Mapping and Arm Kinematics. Stroke 41, 2191–2200. https://doi.org/10.1161/STROKEAHA.110.583641

Kosmowska, B., Wardas, J., 2021. The Pathophysiology and Treatment of Essential Tremor: The Role of Adenosine and Dopamine Receptors in Animal Models. Biomolecules 11, 1813. https://doi.org/10.3390/biom11121813

Kuya, K., Ogawa, T., Shinohara, Y., Ishibashi, M., Fujii, S., Mukuda, N., Tanabe, Y., 2018. Evaluation of Parkinson's disease by neuromelanin-sensitive magnetic resonance imaging and ^{123}I-FP-CIT SPECT. Acta Radiol. 59, 593–598. https://doi.org/10.1177/0284185117722812

Laučkaitė, K., Rastenytė, D., Šurkienė, D., Vaidelytė, B., Dambrauskaitė, G., Sakalauskas, A., Vaitkus, A., Gleiznienė, R., 2014. Ultrasonographic (TCS) and clinical findings in overlapping phenotype of essential tremor and Parkinson's disease (ET-PD). BMC Neurol. 14, 54. https://doi.org/10.1186/1471-2377-14-54

Lenka, A., Bhalsing, K.S., Panda, R., Jhunjhunwala, K., Naduthota, R.M., Saini, J., Bharath, R.D., Yadav, R., Pal, P.K., 2017. Role of altered cerebello-thalamo-cortical network in the neurobiology of essential tremor. Neuroradiology 59, 157–168. https://doi.org/10.1007/s00234-016-1771-1

Ling, H., Massey, L.A., Lees, A.J., Brown, P., Day, B.L., 2012. Hypokinesia without decrement distinguishes progressive supranuclear palsy from Parkinson's disease. Brain 135, 1141–1153. https://doi.org/10.1093/brain/aws038

Lofredi, R., Scheller, U., Mindermann, A., Feldmann, L.K., Krauss, J.K., Saryyeva, A., Schneider, G., Kühn, A.A., 2023. Pallidal Beta Activity Is Linked to Stimulation-Induced Slowness in Dystonia. Mov. Disord. 38, 894–899. https://doi.org/10.1002/mds.29347

Louis, E.D., 2020. "Essential Tremor Plus": A Problematic Concept: Implications for Clinical and Epidemiological Studies of Essential Tremor. Neuroepidemiology 54, 180–184. https://doi.org/10.1159/000502862

Louis, E.D., Faust, P.L., Vonsattel, J.-P.G., Honig, L.S., Rajput, A., Robinson, C.A., Rajput, A., Pahwa, R., Lyons, K.E., Ross, G.W., Borden, S., Moskowitz, C.B., Lawton, A., Hernandez, N., 2007. Neuropathological changes in essential tremor: 33 cases compared with 21 controls. Brain 130, 3297–3307. https://doi.org/10.1093/brain/awm266

Luo, R., Pan, P., Xu, Y., Chen, L., 2019. No reliable gray matter changes in essential tremor. Neurol. Sci. Off. J. Ital. Neurol. Soc. Ital. Soc. Clin. Neurophysiol. 40, 2051–2063. https://doi.org/10.1007/s10072-019-03933-0

Matano, Shozo, 2001. Brief communication: Proportions of the ventral half of the cerebellar dentate nucleus in humans and great apes. Am. J. Phys. Anthropol. 114, 163–165. https://doi.org/10.1002/1096-8644(200102)114:2<163::AID-AJPA1016>3.0.CO;2-F

Matano, S., 2001. Brief communication: Proportions of the ventral half of the cerebellar dentate nucleus in humans and great apes. Am. J. Phys. Anthropol. 114, 163–165. https://doi.org/10.1002/1096-8644(200102)114:2<163::AID-AJPA1016>3.0.CO;2-F

MDS-UPDRS Italian Validation Study Group, Antonini, A., Abbruzzese, G., Ferini-Strambi, L., Tilley, B., Huang, J., Stebbins, G.T., Goetz, C.G., Barone, P., Bandettini di Poggio, M., Fabbrini, G., Di Stasio, F., Tinazzi, M., Bovi, T., Ramat, S., Meoni, S., Pezzoli, G., Canesi, M., Martinelli, P., Maria Scaglione, C.L., Rossi, A., Tambasco, N., Santangelo, G., Picillo, M., Morgante, L., Morgante, F., Quatrale, R., Sensi, M., Pilleri, M., Biundo, R., Nordera, G., Caria, A., Pacchetti, C., Zangaglia, R., Lopiano, L., Zibetti, M., Zappia, M., Nicoletti, A., Quattrone, A., Salsone, M., Cossu, G., Murgia, D., Albanese, A., Del Sorbo, F., 2013. Validation of the Italian version of the Movement Disorder Society—Unified Parkinson's Disease Rating Scale. Neurol. Sci. 34, 683–687. https://doi.org/10.1007/s10072-012-1112-z

Menéndez-González, M., Tavares, F., Zeidan, N., Salas-Pacheco, J.M., Arias-Carrión, O., 2014. Diagnoses behind patients with hard-to-classify tremor and normal DaT-SPECT: a clinical follow up study. Front. Aging Neurosci. 6, 56. https://doi.org/10.3389/fnagi.2014.00056

Middleton, F.A., Strick, P.L., 2001. Cerebellar projections to the prefrontal cortex of the primate. J. Neurosci. Off. J. Soc. Neurosci. 21, 700–712. https://doi.org/10.1523/JNEUROSCI.21-02-00700.2001

Middleton, F.A., Strick, P.L., 1997. Cerebellar output channels. Int. Rev. Neurobiol. 41, 61–82. https://doi.org/10.1016/s0074-7742(08)60347-5

Minen, M.T., Louis, E.D., 2008. Emergence of Parkinson's disease in essential tremor: A study of the clinical correlates in 53 patients. Mov. Disord. 23, 1602–1605. https://doi.org/10.1002/mds.22161

Montgomery, E.B., Baker, K.B., Lyons, K., Koller, W.C., 2000. Motor initiation and execution in essential tremor and Parkinson's disease. Mov. Disord. 15, 511–515. https://doi.org/10.1002/1531-8257(200005)15:3<511::AID-MDS1014>3.0.CO;2-R

Mueller, K., Jech, R., Hoskovcová, M., Ulmanová, O., Urgošík, D., Vymazal, J., Růžička, E., 2017. General and selective brain connectivity alterations in essential tremor: A resting state fMRI study. NeuroImage Clin. 16, 468–476. https://doi.org/10.1016/j.nicl.2017.06.004

Muthuraman, M., Heute, U., Arning, K., Anwar, A.R., Elble, R., Deuschl, G., Raethjen, J., 2012. Oscillating central motor networks in pathological tremors and voluntary movements. What

makes the difference? NeuroImage 60, 1331–1339. https://doi.org/10.1016/j.neuroimage.2012.01.088

Neill, M., Fisher, J.M., Brand, C., Lei, H., Sherman, S.J., Chou, Y.-H., Kuo, P.H., 2021. Practical Application of DaTQUANT with Optimal Threshold for Diagnostic Accuracy of Dopamine Transporter SPECT. Tomography 7, 980–989. https://doi.org/10.3390/tomography7040081

Nicoletti, V., Cecchi, P., Pesaresi, I., Frosini, D., Cosottini, M., Ceravolo, R., 2020. Cerebello-thalamo-cortical network is intrinsically altered in essential tremor: evidence from a resting state functional MRI study. Sci. Rep. 10, 16661. https://doi.org/10.1038/s41598-020-73714-9

Nishibayashi, H., Ogura, M., Kakishita, K., Tanaka, S., Tachibana, Y., Nambu, A., Kita, H., Itakura, T., 2011. Cortically evoked responses of human pallidal neurons recorded during stereotactic neurosurgery. Mov. Disord. 26, 469–476. https://doi.org/10.1002/mds.23502

Novellino, F., Cherubini, A., Chiriaco, C., Morelli, M., Salsone, M., Arabia, G., Quattrone, A., 2013. Brain iron deposition in essential tremor: A quantitative 3-tesla magnetic resonance imaging study. Mov. Disord. 28, 196–200. https://doi.org/10.1002/mds.25263

Obeso, J.A., Rodríguez-Oroz, M.C., Benitez-Temino, B., Blesa, F.J., Guridi, J., Marin, C., Rodriguez, M., 2008. Functional organization of the basal ganglia: therapeutic implications for Parkinson's disease. Mov. Disord. Off. J. Mov. Disord. Soc. 23 Suppl 3, S548-559. https://doi.org/10.1002/mds.22062

Paparella, G., Angelini, L., De Biase, A., Cannavacciuolo, A., Colella, D., Di Bonaventura, C., Giallonardo, A.T., Berardelli, A., Bologna, M., 2020. Clinical and Kinematic Features of Valproate-Induced Tremor and Differences with Essential Tremor. Cerebellum Lond. Engl. https://doi.org/10.1007/s12311-020-01216-5

Paparella, G., Cannavacciuolo, A., Angelini, L., Costa, D., Birreci, D., Alunni Fegatelli, D., Guerra, A., Berardelli, A., Bologna, M., 2023. May Bradykinesia Features Aid in Distinguishing Parkinson's Disease, Essential Tremor, And Healthy Elderly Individuals? J. Park. Dis. 13, 1047–1060. https://doi.org/10.3233/JPD-230119

Paparella, G., Ceccanti, M., Colella, D., Cannavacciuolo, A., Guerra, A., Inghilleri, M., Berardelli, A., Bologna, M., 2021a. Bradykinesia in motoneuron diseases. Clin. Neurophysiol. 132, 2558–2566. https://doi.org/10.1016/j.clinph.2021.08.006

Paparella, G., Fasano, A., Hallett, M., Berardelli, A., Bologna, M., 2021b. Emerging concepts on bradykinesia in non-parkinsonian conditions. Eur. J. Neurol. 28, 2403–2422. https://doi.org/10.1111/ene.14851

Paparella, G., Ferrazzano, G., Cannavacciuolo, A., Cogliati Dezza, F., Fabbrini, G., Bologna, M., Berardelli, A., 2018a. Differential effects of propranolol on head and upper limb tremor in patients with essential tremor and dystonia. J. Neurol. 265, 2695–2703. https://doi.org/10.1007/s00415-018-9052-z

Passaretti, M., De Biase, A., Paparella, G., Angelini, L., Cannavacciuolo, A., Colella, D., Berardelli, A., Bologna, M., 2022. Worsening of Essential Tremor After SARS-CoV-2 Infection. Cerebellum Lond. Engl. https://doi.org/10.1007/s12311-022-01366-8

Pietracupa, S., Bologna, M., Bharti, K., Pasqua, G., Tommasin, S., Elifani, F., Paparella, G., Petsas, N., Grillea, G., Berardelli, A., Pantano, P., 2019. White matter rather than gray matter damage characterizes essential tremor. Eur. Radiol. 29, 6634–6642. https://doi.org/10.1007/s00330-019-06267-9

Pietracupa, S., Bologna, M., Tommasin, S., Berardelli, A., Pantano, P., 2021. The Contribution of Neuroimaging to the Understanding of Essential Tremor Pathophysiology: a Systematic Review. The Cerebellum 21, 1029–1051. https://doi.org/10.1007/s12311-021-01335-7

Postuma, R.B., Berg, D., Stern, M., Poewe, W., Olanow, C.W., Oertel, W., Obeso, J., Marek, K., Litvan, I., Lang, A.E., Halliday, G., Goetz, C.G., Gasser, T., Dubois, B., Chan, P., Bloem, B.R., Adler, C.H., Deuschl, G., 2015a. MDS clinical diagnostic criteria for Parkinson's disease. Mov. Disord. Off. J. Mov. Disord. Soc. 30, 1591–1601. https://doi.org/10.1002/mds.26424

Pruim, R.H.R., Mennes, M., Buitelaar, J.K., Beckmann, C.F., 2015. Evaluation of ICA-AROMA and alternative strategies for motion artifact removal in resting state fMRI. NeuroImage 112, 278–287. https://doi.org/10.1016/j.neuroimage.2015.02.063

Raethjen, J., Deuschl, G., 2012. The oscillating central network of Essential tremor. Clin. Neurophysiol. 123, 61–64. https://doi.org/10.1016/j.clinph.2011.09.024

Rajput, A.H., Rajput, E.F., Bocking, S.M., Auer, R.N., Rajput, A., 2019. Parkinsonism in essential tremor cases: A clinicopathological study. Mov. Disord. 34, 1031–1040. https://doi.org/10.1002/mds.27729

Redgrave, P., Rodriguez, M., Smith, Y., Rodriguez-Oroz, M.C., Lehericy, S., Bergman, H., Agid, Y., DeLong, M.R., Obeso, J.A., 2010. Goal-directed and habitual control in the basal ganglia: implications for Parkinson's disease. Nat. Rev. Neurosci. 11, 760–772. https://doi.org/10.1038/nrn2915

Schneider, S.A., Edwards, M.J., Mir, P., Cordivari, C., Hooker, J., Dickson, J., Quinn, N., Bhatia, K.P., 2007. Patients with adult-onset dystonic tremor resembling parkinsonian tremor have

scans without evidence of dopaminergic deficit (SWEDDs). Mov. Disord. 22, 2210–2215. https://doi.org/10.1002/mds.21685

Schwartz, M., Groshar, D., Inzelberg, R., Hocherman, S., 2004. Dopamine-transporter imaging and visuo-motor testing in essential tremor, practical possibilities for detection of early stage Parkinson's disease. Parkinsonism Relat. Disord. 10, 385–389. https://doi.org/10.1016/j.parkreldis.2004.03.004

Schwingenschuh, P., Ruge, D., Edwards, M.J., Terranova, C., Katschnig, P., Carrillo, F., Silveira-Moriyama, L., Schneider, S.A., Kägi, G., Palomar, F.J., Talelli, P., Dickson, J., Lees, A.J., Quinn, N., Mir, P., Rothwell, J.C., Bhatia, K.P., 2010. Distinguishing SWEDDs patients with asymmetric resting tremor from Parkinson's disease: A clinical and electrophysiological study. Mov. Disord. 25, 560–569. https://doi.org/10.1002/mds.23019

Smith, S.M., Zhang, Y., Jenkinson, M., Chen, J., Matthews, P.M., Federico, A., De Stefano, N., 2002. Accurate, Robust, and Automated Longitudinal and Cross-Sectional Brain Change Analysis. NeuroImage 17, 479–489. https://doi.org/10.1006/nimg.2002.1040

Sprenger, F.S., Wurster, I., Seppi, K., Stockner, H., Scherfler, C., Sojer, M., Schmidauer, C., Berg, D., Poewe, W., 2016. Substantia nigra hyperechogenicity and Parkinson's disease risk in patients with essential tremor. Mov. Disord. 31, 579–583. https://doi.org/10.1002/mds.26515

Tarakad, A., Jankovic, J., 2019. Essential Tremor and Parkinson's Disease: Exploring the Relationship. Tremor Hyperkinetic Mov. 8, 589. https://doi.org/10.5334/tohm.441

Tarcijonas, G., Foran, W., Haas, G.L., Luna, B., Sarpal, D.K., 2020. Intrinsic Connectivity of the Globus Pallidus: An Uncharted Marker of Functional Prognosis in People With First-Episode Schizophrenia. Schizophr. Bull. 46, 184–192. https://doi.org/10.1093/schbul/sbz034

Thenganatt, M.A., Jankovic, J., 2016. The relationship between essential tremor and Parkinson's disease. Parkinsonism Relat. Disord. 22, S162–S165. https://doi.org/10.1016/j.parkreldis.2015.09.032

Tikoo, S., Pietracupa, S., Tommasin, S., Bologna, M., Petsas, N., Bharti, K., Berardelli, A., Pantano, P., 2020. Functional disconnection of the dentate nucleus in essential tremor. J. Neurol. 267, 1358–1367. https://doi.org/10.1007/s00415-020-09711-9

Turesky, T.K., Olulade, O.A., Luetje, M.M., Eden, G.F., 2018. An fMRI study of finger tapping in children and adults. Hum. Brain Mapp. 39, 3203–3215. https://doi.org/10.1002/hbm.24070

Villalobos, N., Almazán-Alvarado, S., Magdaleno-Madrigal, V.M., 2022. Elevation of GABA levels in the globus pallidus disinhibits the thalamic reticular nucleus and desynchronized cortical beta oscillations. J. Physiol. Sci. 72, 17. https://doi.org/10.1186/s12576-022-00843-3

Waln, O., Wu, Y., Perlman, R., Wendt, J., Van, A.K., Jankovic, J., 2015. Dopamine transporter imaging in essential tremor with and without parkinsonian features. J. Neural Transm. 122, 1515–1521. https://doi.org/10.1007/s00702-015-1419-z

Wang, L., Lei, D., Suo, X., Li, N., Lu, Z., Li, J., Peng, J., Gong, Q., Peng, R., 2018. Resting-state fMRI study on drug-naive patients of essential tremor with and without head tremor. Sci. Rep. 8, 10580. https://doi.org/10.1038/s41598-018-28778-z

Washburn, S., Oñate, M., Yoshida, J., Vera, J., Bhuvanasundaram, R., Khatami, L., Nadim, F., Khodakhah, K., 2024. The cerebellum directly modulates the substantia nigra dopaminergic activity. Nat. Neurosci. https://doi.org/10.1038/s41593-023-01560-9

Witt, S.T., Laird, A.R., Meyerand, M.E., 2008. Functional neuroimaging correlates of finger-tapping task variations: An ALE meta-analysis. NeuroImage 42, 343–356. https://doi.org/10.1016/j.neuroimage.2008.04.025

Wu, T., Hallett, M., 2013. The cerebellum in Parkinson's disease. Brain 136, 696–709. https://doi.org/10.1093/brain/aws360

Wu, T., Long, X., Zang, Y., Wang, L., Hallett, M., Li, K., Chan, P., 2009. Regional homogeneity changes in patients with Parkinson's disease. Hum. Brain Mapp. 30, 1502–1510. https://doi.org/10.1002/hbm.20622

Wu, T., Wang, L., Hallett, M., Chen, Y., Li, K., Chan, P., 2011. Effective connectivity of brain networks during self-initiated movement in Parkinson's disease. NeuroImage 55, 204–215. https://doi.org/10.1016/j.neuroimage.2010.11.074

7. TABLES

Table1: Demographic, clinical, DaTQUANT data of patients with essential tremor (ET), Parkinson's disease (PD) and healthy subjects (HS)

	ET	***PD***	***HS***	***P***
Age, years	73.00 (68.50, 78.75)	73.00 (64.00, 78.00)	68.00 (65.00, 72.50)	0.222
Sex, Female n, %	7 (43.8)	5 (29.4)	5 (25.0)	0.469
Disease duration, years	9.00 (6.50, 12.00)"	3.00 (2.00, 6.00)		0.049
FAB	17.00 (16.75, 18.00)	16.00 (16.00, 17.00)***, #**	17.00 (16.00, 18.00)	**0.009**
MOCA	26.0 (25.0, 26.0)	25.0 (23.0, 27.0)	27.5 (26.0, 28.3)	**0.029**
MDS-UPDRS III	9.50 (5.75, 17.50)	22.0 (16.0, 28.0)		**0.006**
Bradykinesia subscores	3.00 (0.0, 7.25)	9.00 (5.00, 13.00)		**0.006**
Tremor subscores	5.00 (2.75, 7.25)	7.00 (5.00, 9.00)		0.524
Rigidity subscores	0.00 (0.00, 1.00)	2.00 (0.00, 4.00)		**0.007**
FTM-TRS	19.5 (13.00, 27.00)			
LEDD, mg/die		242.5 (113-375)		
Rest tremor				
Frequence, Hz	5.79 (1.24)	5.67 (1.01)		0.998
Magnitude, RMS	0.36 (0.58)	0.45 (0.79)		0.738
Postural tremor				
Frequence, Hz	5.01(1.45)	5.15 (1.05)		0.680
Magnitude, RMS	1.72 (2.55)	0.48 (0.73)		0.042
DaT-QUANT				
Striatum SBR	3.04 (0.51)	1.86 (0.72)		**<0.001**
Putamen SBR	2.80 (0.52)	1.70 (0.75)		**<0.001**
Caudate SBR	3.28 (0.62)	2.18 (0.70)		**<0.001**
Striatum z- score	1.35 (1.02)	-0.87 (1.65)		**<0.001**
Putamen z-score	1.39 (0.88)	-0.79 (2.00)		**<0.001**
Caudate z-score	1.06 (1.30)	-0.55 (1.20)		**0.001**

The data are presented as mean (standard deviation) or median and interquartile range for non-parametric comparisons, if not otherwise specified. P-values results from groups comparisons, when group comparison resulted from Kruskal-Wallis analysis, post-hoc test Wilcoxon rank results were indicated if significant as: ***** for comparison with ET, **#** for comparison with HS FAB: Frontal Assessment Battery; MOCA: Montreal Cognitive Assessment; MDS-UPDRS III: Movement Disorder Society Unified Parkinson's Disease Rating Scale; RMS: root-mean-square; SBR: striatal binding ratio.

Table 2. Kinematic variables of finger tapping in patients with essential tremor (ET), Parkinson's disease (PD) and healthy subjects (HS).

Empty Cell	***ET***	***PD***	***HC***	$F_{(2, 50)}$	***P***	P_1	P_2	P_3
N° movements	32.71 (8.91)	47.80 (13.25)	54.33 (14.45)	13.38	**<0.001**	**0.003**	**<0.001**	0.269
Rhythm	0.11 (0.06)	0.12 (0.05)	0.08 (0.03)	3.41	0.041	0.723	0.216	0.037
Amplitude	52.81 (10.14)	43.60 (11.96)	51.98 (11.14)	3.59	0.035	0.055	0.973	0.068
Amplitude Slope	−0.26 (0.27)	−0.16 (0.13)	−0.14 (0.17)	1.81	0.174	0.321	0.176	0.949
Velocity	897.60 (161.12)	774.30 (154.84)	1103.96 (188.16)	17.85	**<0.001**	0.104	**0.002**	**< 0.001**
Velocity Slope	-5.81 (4.30)	-3.47 (3.26)	-4.48 (4.45)	1.38	0.260	0.231	0.593	0.731

The rhythm is expressed as the coefficient of variation of the inter-tap intervals. The amplitude is expressed in degrees. The amplitude slope is expressed in degrees per number of movements. The velocity is expressed in degrees per second. The velocity slope is expressed in degrees per second per number of movements. Means and standard deviation are reported for each parameter for the three groups, with significant values in bold. F-values and P-values of ANOVAs, and P-values of the post-hoc Tukey's HSD test, P_1 = comparison between ET and PD, P_2 = comparison between ET and HS, P_3 = comparison between PD and HS. Abbreviations: PD: Idiopathic Parkinson's Disease, ET: Essential Tremor, HS: Healthy Subjects.

Table 3: Demographic and clinical characteristics of patients with essential tremor (ET) and healthy subjects (HS)

	ET	HS	p- value
Age, years	67.7 (13.4)	62.8 (7.8)	0.10
Gender, Female/Male	3/17 (20)	6/12 (18)	0.71
Disease duration, years	13.9 (9.9)	NA	NA
MOCA	26.4 (2.1)	27.7 (2)	0.11
Tremor severity (FMTRS)	0.38 (0.20)	NA	NA
MDS-UPDRS III	6.2 (3)	NA	NA

The data are presented as mean (standard deviation). MOCA refers to the Montreal Cognitive Assessment, FMTRS refers to the Fahn–Tolosa–Marin Tremor Rating Scale, and MDS-UPDRS III refers to the Movement Disorder Society Unified Parkinson's Disease Rating Scale. NA stands for not applicable.

Table 4: Kinematic variables of finger tapping in patients with essential tremor (ET) and healthy subjects (HS)

	ET	HS	p-value
N° Movements	41.00 (13.36)	54.65 (13.76)	**0.0043**
Rhythm	0.12 (0.05)	0.09 (0.09)	>0.05
Amplitude	47.49 (8.61)	53.41 (8.05)	0.0389
Amplitude slope	-0.12 (0.16)	-0.15 (0.11)	>0.05
Velocity	951.51 (187.51)	1126.35 (142.92)	**0.0034**
Velocity slope	5.36 (2.94)	5.57 (2.97)	>0.05

The amplitude is expressed in degrees. The amplitude slope is expressed in degrees per number of movements. The speed is expressed in degrees per second. The speed slope is expressed in degrees per second per number of movements. The rhythm is expressed as the coefficient of variation of the inter-tap intervals. The data are presented as means (standard deviation). Significant p values are in bold.

Table 5: Volumes of brain structures in patients with essential tremor (ET) and healthy subjects (HS)

	ET	HS	p-value
Whole GM [ml]	640.70 (52.6)	642.33 (54.3)	0.99
Whole WM [ml]	723.38 (64.5)	704.49 (66.6)	0.58
Left Pallidum [ml]	1.56 (0.22)	1.72 (0.15)	0.05
Right Pallidum [ml]	1.58 (0.28)	1.70 (0.17)	0.09
Left Dentate nucleus [ml]	1.07 (0.32)	1.09 (0.31)	0.78
Right Dentate nucleus [ml]	1.26 (0.47)	1.20 (0.35)	0.87
Left Cerebellum [ml]	60.93 (9.69)	63.18 (5.97)	0.32
Right Cerebellum [ml]	58.73 (9.61)	60.78 (5.97)	0.33

The data are presented as means (standard deviation). GM refers to Gray Matter, and WM refers to White Matter. To assess differences between groups in terms of GM and WM volumes, volumes of deep grey matter structures, DN volumes and left and right cerebellar volumes, non-parametric tests (Mann-Whitney U test) with Bonferroni correction were performed.

Table 6: Brain regions showing significant dorsal and ventral dentate nucleus (DN) functional connectivity differences between patients with essential tremor (ET) and healthy subjects (HS) ($p < 0.05$, false discovery rate corrected, minimum cluster extent set at 100 voxels). Anatomical localizations of peak MNI coordinates were established according to Harvard-Oxford cortical and subcortical structural atlases and the cerebellar atlas included in FMRIB's Software Library.

Cluster size (voxels)	T	MNI coordinates X	y	z	Cluster location (local maxima)
Dorsal DN FC					
ET > HS					
ET > HS					
1231	4.46	62	-24	20	R Parietal Operculum Cortex
	4.24	50	-2	32	R Precentral Gyrus
	3.96	66	-24	14	R Planum Temporale
	3.64	64	-38	16	R Supramarginal Gyrus
	3.17	62	-12	16	R Central Opercular Cortex
772	4.66	32	2	8	R Putamen
	4.03	36	4	12	R Central Opercular Cortex
	3.49	38	-4	-8	R Insular Cortex
	3.36	46	-18	-4	R Superior Temporal Gyrus, posterior division
	2.56	26	-4	-10	R Amygdala
503	3.30	-62	-20	18	L Postcentral Gyrus
	3.30	-62	0	6	L Precentral Gyrus
	3.12	-68	-24	8	L Superior Temporal Gyrus
	3.10	-58	-26	22	L Supramarginal Gyrus, anterior division
	2.92	-58	-22	18	L Central Opercular Cortex
	2.90	-62	-14	6	L Planum Temporale
	2.71	-56	-42	12	L Supramarginal Gyrus, posterior division
	2.51	-52	-26	14	L Parietal Operculum Cortex
293	3.68	-12	-64	-52	L Cerebellar Lobule VIIIa
	3.09	-16	-76	-50	L Cerebellar Lobule VIIb
	2.47	-24	-46	-52	L Cerebellar Lobule VIIIb
	2.42	-34	-76	-38	L Cerebellar Crus II
	2.29	-28	-70	-36	L Cerebellar Crus I
219	3.55	-4	-2	6	L Thalamus
	2.81	-20	14	0	L Putamen
	2.60	-30	8	12	L Insular Cortex
	2.22	-10	4	10	L Caudate
	2.02	2	-6	8	R Thalamus
215	3.08	-2	-66	-2	L Lingual Gyrus
	2.69	2	-60	-8	R Cerebellar Lobule V
	2.67	-8	-66	-12	L Cerebellar Lobule VI
	2.01	-4	-72	-18	Vermis Lobule VI
177	3.27	-52	-2	-6	L Planum Polare
	3.16	-38	-10	-4	L Insular Cortex
	2.76	-50	-10	-6	L Superior Temporal Gyrus, anterior division
	2.75	-52	8	-2	L Temporal Pole
	1.98	-48	6	-2	L Central Opercular Cortex
174	3.36	-36	-58	-12	L Temporal Occipital Fusiform Cortex
	3.20	-34	-66	-18	L Occipital Fusiform Gyrus
	2.93	-28	-62	-18	L Cerebellar Lobule VI
	2.83	-44	-58	0	L Middle Temporal Gyrus, temporooccipital part
158	3.07	48	-54	4	R Middle Temporal Gyrus, temporooccipital part
	2.86	62	-62	-6	R Lateral Occipital Cortex, inferior division
	2.48	46	-54	-6	R Inferior Temporal Gyrus, temporooccipital part
	2.44	36	-64	-12	R Occipital Fusiform Gyrus
127	2.71	22	-30	-30	R Cerebellar Lobule I-IV
	2.70	22	-32	-34	Brainstem
	2.69	22	-26	-28	R Parahippocampal Gyrus, posterior division
	2.59	28	-36	-32	R Cerebellar Lobule V
116	3.93	56	4	6	R Central Opercular Cortex
	2.57	58	6	-2	R Planum Polare

112	3.23	20	-34	68	R Postcentral Gyrus
	3.10	18	-28	66	R Precentral Gyrus
111	3.18	44	44	0	R Frontal Pole
108	3.20	6	-20	-36	Brainstem
103	2.81	10	26	26	R Cingulate Cortex, anterior division
	1.97	8	34	26	R Paracingulate Gyrus, anterior division
HS > ET					
868	3.62	-40	-72	38	L Lateral Occipital Cortex, superior division
452	4.42	32	-68	54	R Lateral Occipital Cortex, superior division
360	3.02	-6	-62	36	L Precuneous Cortex
	2.38	6	-60	22	R Precuneous Cortex
302	4.01	56	-8	-28	R Middle Temporal Gyrus, posterior division
	2.71	50	-10	-34	R Inferior Temporal Gyrus, posterior division
	2.56	60	0	-30	R Middle Temporal Gyrus, anterior division
245	2.88	4	28	-22	R Subcallosal Cortex
	2.86	14	42	-18	R Frontal Pole
	2.68	10	32	-18	R Frontal Medial Cortex
	2.64	14	24	-14	R Frontal Orbital Cortex
187	3.02	12	68	18	R Frontal Pole
	3.00	8	48	22	R Paracingulate Gyrus
	2.76	6	54	22	R Superior Frontal Gyrus
145	3.12	-36	2	36	L Middle Frontal Gyrus
113	2.69	28	-60	58	R Lateral Occipital Cortex, superior division
	2.63	40	-50	54	R Superior Parietal Lobule
103	3.82	26	28	48	R Middle Frontal Gyrus
VENTRAL DN FC					
ET > HS					
ET > HS					
1680	4.02	-2	34	16	L Cingulate Gyrus, anterior division
	3.81	-42	22	50	L Middle Frontal Gyrus
	3.62	4	66	4	R Frontal Pole
	3.37	-36	44	-8	L Frontal Pole
1177	3.39	-24	-68	-40	L Cerebellar Crus II
	3.29	-32	-74	-38	L Cerebellar Crus I
	3.28	-28	-52	-24	L Cerebellar Lobule VI
	3.14	0	-64	-48	Vermis Lobule VIIIb
	2.84	-24	-72	-46	L Cerebellar Lobule VIIb
825	3.37	34	-84	-38	R Cerebellar Crus II
	3.35	34	-54	-40	R Cerebellar Crus I
	2.87	28	-68	-26	R Cerebellar Lobule VI
	2.77	30	-72	-16	R Occipital Fusiform Gyrus
366	3.09	-36	14	-12	L Insular Cortex
	2.87	-40	10	-18	L Temporal Pole
	2.87	-18	12	16	L Caudate
	2.77	-30	8	-2	L Putamen
	2.73	-40	18	-12	L Frontal Orbital Cortex
	2.67	-12	2	-4	L Pallidum
319	3.43	-6	-38	-18	Brainstem
	2.77	4	-44	-12	R Cerebellar Lobule I-IV
	2.30	18	-40	-18	R Cerebellar Lobule V
211	3.76	-66	-50	-6	L Middle Temporal Gyrus, temporooccipital part
	3.42	-58	-62	-14	L Inferior Temporal Gyrus, temporooccipital part
	3.35	-52	-66	-26	L Cerebellar Crus I
	2.72	-46	-64	-28	L Cerebellar Crus I
	2.18	-64	-38	0	L Middle Temporal Gyrus, posterior division
	1.88	-60	-42	4	L Superior Temporal Gyrus, posterior division
192	3.22	-50	-2	-6	L Planum Polare
	2.89	-38	-16	-8	L Insular Cortex
	2.74	-54	-6	-20	L Middle temporal Gyrus, anterior division
	2.48	-52	-10	-22	L Middle Temporal Gyrus, posterior division
	2.01	-48	4	-14	L Temporal Pole

188	3.03	8	8	8	R Caudate
	2.72	16	-4	16	R Thalamus
	2.37	28	4	12	R Putamen
	2.25	36	0	10	R Insular Cortex
	1.79	20	2	4	R Pallidum
166	4.50	58	-44	20	R Supramarginal Gyrus
	2.66	54	-50	20	R Angular Gyrus
132	3.23	42	8	-16	R Temporal Pole
	3.10	38	14	-10	R Insular Cortex
	2.61	44	0	-10	R Planum Polare
	2.33	32	20	-16	R Frontal Orbital Cortex
126	3.89	-36	-16	14	L Insular Cortex
	2.85	-28	-8	12	L Putamen
124	2.98	-60	-22	22	L Postcentral Gyrus
	2.89	-58	-28	14	L Parietal Operculum Cortex
	2.14	-58	-32	28	L Supramarginal Gyrus
	1.83	-56	-36	10	L Superior Temporal Gyrus, posterior division
122	3.40	16	70	0	R Frontal Pole
120	2.82	-4	-10	-4	L Thalamus
	2.73	4	-8	2	R Thalamus
	2.03	14	0	-4	R Pallidum
106	3.25	-50	-44	46	L Supramarginal Gyrus, posterior division
	2.89	-44	-40	22	L Parietal Operculum Cortex
104	2.89	26	-36	-32	R Cerebellar Lobule V
	1.99	34	-38	-34	R Cerebellar Lobule VI
HS > ET					
160	3.50	24	6	-38	R Temporal Pole
	3.40	20	4	-34	R Parahippocampal Gyrus, anterior division
121	3.69	-6	-30	-6	Brainstem
	2.80	-14	-34	-8	L Parahippocampal Gyrus, posterior division
	2.50	-18	-30	-8	L Hippocampus
111	2.68	-44	-32	-22	L Inferior Temporal Gyrus, posterior division
	2.67	-38	-30	-20	L Temporal Fusiform Cortex, posterior division

Table 7: Brain regions showing significant external and internal segments of the globus pallidus (GPe, GPi) functional connectivity differences between patients with essential tremor (ET) and healthy subjects (HS) ($p < 0.05$, false discovery rate corrected, minimum cluster extent set at 100 voxels). Anatomical localizations of peak MNI coordinates were established according to Harvard-Oxford cortical and subcortical structural atlases and the cerebellar atlas included in FMRIB's Software Library.

		MNI coordinates			
Cluster size (voxels)	**T**	**x**	**y**	**z**	**Cluster location (local maxima)**
GPe FC					
ET > HS					
646	3.69	50	24	14	R Inferior Frontal Gyrus, pars triangularis
	3.46	42	14	0	R Insular Cortex
	3.26	30	6	-4	R Putamen
	3.05	54	38	0	R Frontal Pole
325	3.34	34	48	34	R Frontal Pole
	2.80	8	52	28	R Superior Frontal Gyrus
	2.77	10	44	32	R Paracingulate Gyrus
299	3.91	52	-30	46	R Supramarginal Gyrus, anterior division
	2.98	36	-34	40	R Postcentral Gyrus
	2.71	36	-42	42	R Superior Parietal Lobule
	2.46	46	-36	54	R Supramarginal Gyrus, posterior division
251	3.36	6	-40	-36	Brainstem
	2.46	-20	-36	-50	L Cerebellar Lobule X
	2.35	6	-48	-48	R Cerebellar Lobule IX
197	4.06	-52	32	-4	L Inferior Frontal Gyrus, pars triangularis
	2.94	-38	52	-4	L Frontal Pole
187	3.24	-54	-62	20	L Lateral Occipital Cortex, superior division
	2.91	-52	-48	28	L Supramarginal Gyrus, posterior division
	2.76	-54	-56	14	L Angular Gyrus
	2.76	-62	-62	8	L Middle Temporal Gyrus, temporooccipital part
153	2.73	48	-52	-34	R Cerebellar Crus I
	2.33	46	-48	-26	R Temporal Occipital Fusiform Cortex
135	2.83	58	-32	6	R Superior Temporal Gyrus, posterior division
	2.21	62	-30	14	R Planum Temporale
127	2.67	-32	12	-38	L Temporal Pole
	2.36	-42	26	-20	L Frontal Orbital Cortex
119	3.26	-22	-30	-18	L Parahippocampal Gyrus, posterior division
	2.97	-24	-32	-8	L Hippocampus
108	2.95	-40	10	2	L Frontal Operculum Cortex
	2.89	-40	8	6	L Central Opercular Cortex
	2.56	-50	10	2	L Inferior Frontal Gyrus, pars opercularis
100	3.30	28	-96	12	R Occipital Pole
	2.13	34	-84	18	R Lateral Occipital Cortex
HS > ET					
935	4.12	16	18	-20	R Frontal Orbital Cortex
	3.64	-2	6	-8	L Subcallosal Cortex
	3.39	-8	38	-28	L Frontal Pole
	3.12	14	50	-20	R Frontal Pole
	2.90	0	24	-22	R Subcallosal Cortex
	2.86	-10	32	-22	L Frontal Medial Cortex
185	2.99	34	-66	-50	R Cerebellar Lobule VIIb
	2.72	32	-74	-48	R Cerebellar Crus II
	2.26	52	-68	-40	R Cerebellar Crus I
185	3.44	36	-24	-26	R Temporal Fusiform Cortex, posterior division
	2.99	30	-22	-26	R Parahippocampal Gyrus, anterior division
	2.50	52	-8	-26	R Middle Temporal Gyrus, anterior division
	2.49	44	-30	-24	R Inferior Temporal Gyrus, posterior division
142	3.45	12	-32	-16	Brainstem

	1.96	10	-40	-4	R Lingual Gyrus
120	3.19	-6	-84	-40	L Cerebellar Crus I
	2.40	-4	-86	-28	L Cerebellar Crus II
112	2.87	-26	4	56	L Superior Frontal Gyrus
	2.64	-30	14	56	L Middle Frontal Gyrus
GPi FC					
ET > HS					
3639	4.75	30	-40	60	R Superior Parietal Lobule
	4.69	22	-62	60	R Lateral Occipital Cortex, superior division
	3.72	16	-44	72	R Postcentral Gyrus
	3.51	10	-56	62	R Precuneous Cortex
	3.36	40	-84	-2	R Lateral Occipital Cortex, inferior division
2271	4.35	-36	-64	-58	L Cerebellar Lobule VIIb
	4.30	10	-26	-40	Brainstem
	4.22	6	-72	-50	R Cerebellar Lobule VIIb
	4.13	10	-46	-50	R Cerebellar Lobule IX
	3.66	-24	-48	-46	L Cerebellar Lobule VIIIb
	3.65	16	-50	-56	R Cerebellar Lobule VIIIb
	3.61	-16	-40	-46	L Cerebellar Lobule X
	3.39	-18	-66	-60	L Cerebellar Lobule VIIIa
683	3.19	6	60	4	R Frontal Pole
523	4.14	-44	44	-2	L Frontal Pole
	3.65	-54	30	-2	L Inferior Frontal Gyrus, pars triangularis
	3.44	-56	16	4	L Inferior Frontal Gyrus, pars opercularis
	2.62	-52	38	2	L Frontal Pole
466	3.50	-38	-84	-4	L Lateral Occipital Cortex, inferior division
	3.08	-34	-94	-4	L Occipital Pole
	2.92	-16	-86	-20	L Occipital Fusiform Gyrus
	2.48	-10	-78	-18	L Cerebellar Lobule VI
403	4.09	-18	-70	10	L Intracalcarine Cortex
	3.27	-16	-86	42	L Lateral Occipital Cortex, superior division
	3.11	-20	-70	18	L Cuneal Cortex
333	3.48	-20	-60	68	L Lateral Occipital Cortex, superior division
	3.28	-28	-42	54	L Superior Parietal Lobule
	2.72	-26	-38	68	L Postcentral gyrus
	2.56	-12	-54	58	L Precuneous Cortex
317	3.36	54	4	-14	R Superior Temporal Gyrus, anterior division
	3.27	54	10	-6	R Temporal Pole
	3.08	46	20	-10	R Frontal Orbital Cortex
	2.74	56	22	0	R Inferior Frontal Gyrus, pars triangularis
	2.73	40	18	-2	R Insular Cortex
	2.72	30	6	-4	R Putamen
	2.70	54	18	-2	R Inferior Frontal Gyrus, pars opercularis
	2.59	48	22	-4	R Frontal Operculum Cortex
269	3.46	-50	2	46	L Precentral Gyrus
	3.36	-44	14	40	L Middle Frontal Gyrus
	2.72	-44	12	26	L Inferior Frontal Gyrus, pars opercularis
241	3.73	-22	-52	-30	L Cerebellar Lobule VI
	3.26	-32	-60	-40	L Cerebellar Crus II
	3.25	-40	-70	-12	L Occipital Fusiform Gyrus
	2.11	-36	-58	-28	L Cerebellar Crus I
220	3.50	56	8	32	R Precentral Gyrus
	2.71	46	6	44	R Middle Frontal Gyrus
	2.07	52	14	30	R Inferior Frontal Gyrus, pars opercularis
183	3.08	-60	-10	2	L Planum Temporale
	2.76	-58	-30	-4	L Middle Temporal Gyrus, posterior division
	2.50	-54	-16	2	L Heschl's Gyrus (includes H1 and H2)
	2.38	-64	-30	0	L Superior Temporal Gyrus, posterior division
153	3.62	32	-50	-38	R Cerebellar Crus I
	2.84	30	-42	-50	R Cerebellar Lobule VIIIb
	2.76	32	-42	-44	R Cerebellar Lobule VIIIa

	2.37	38	-38	-38	R Cerebellar Lobule VI
104	3.22	-6	-56	-50	L Cerebellar Lobule IX
	2.24	2	-52	-44	R Cerebellar Lobule IX
HS > ET					
160	3.68	52	-4	-26	R Middle Temporal Gyrus, anterior division
	2.63	52	6	-42	R Temporal Pole
	2.56	46	-6	-32	R Inferior Temporal Gyrus, anterior division
	2.26	50	-16	-24	R Inferior Temporal Gyrus, posterior division
119	3.16	20	-16	-26	R Parahippocampal Gyrus, anterior division
	2.98	14	-24	-20	Brainstem

Table 8: Brain regions showing significant correlations between dorsal dentate nucleus (DN) and the external and internal segments of globus pallidus (GPe and GPi) functional connectivity maps and velocity of finger tapping, in healthy subjects (HS) and ET patients ($p < 0.05$, false discovery rate corrected, minimum cluster extent set at 100 voxels). Anatomical localizations of peak MNI coordinates were established according to Harvard-Oxford cortical and subcortical structural atlases and the cerebellar atlas included in FMRIB's Software Library.

Cluster size (voxels)	T	MNI coordinates x	y	z	Cluster location (local maxima)
HS					
Dorsal DN FC – velocity of finger tapping ↑					
276	2.77	-10	-74	-16	L Cerebellar Lobule VI
	2.16	-20	-36	-28	L Cerebellar Lobule V
	1.89	-10	-42	-28	L Cerebellar Lobule I-IV
	1.83	-10	-38	-30	Brainstem
	1.64	-6	-82	-16	L Lingual Gyrus
224	2.67	6	-68	-12	R Cerebellar Lobule VI
	2.59	30	-66	-16	R Occipital Fusiform Gyrus
	2.58	12	-60	-8	R Lingual Gyrus
	2.41	0	-70	-10	Vermis Lobule VI
	2.19	4	-62	-10	R Cerebellar Lobule V
121	3.49	-26	-78	-36	L Cerebellar Crus I
	1.80	-24	-74	-22	L Cerebellar Lobule VI
	1.52	-34	-80	-34	L Cerebellar Crus II
HS					
Dorsal DN FC – velocity of finger tapping ↓					
372	3.41	-34	-62	50	L Lateral Occipital Cortex
257	3.19	-20	64	16	L Frontal Pole
225	3.19	-6	-12	8	L Thalamus
179	2.70	-10	-44	38	L Cingulate Gyrus, posterior division
	1.67	-2	-44	44	L Precuneous Cortex
174	3.60	-46	18	32	L Middle Frontal Gyrus
	2.01	-40	20	22	L Inferior Frontal Gyrus, pars opercularis
164	3.04	-18	34	50	L Superior Frontal Gyrus
106	3.28	34	-72	46	R Lateral Occipital Cortex, superior division
ET					
Dorsal DN FC – velocity of finger tapping ↑					
354	2.77	-66	-20	12	L Superior Temporal Gyrus, posterior division
	2.54	-58	-26	18	L Parietal Operculum Cortex
	2.10	-58	-8	6	L Central Opercular Cortex
	2.09	-62	-26	24	L Supramarginal Gyrus, anterior division
	2.05	-64	-10	6	L Planum Temporale
	2.01	-62	-22	28	L Postcentral Gyrus
272	3.30	20	-38	-18	R Cerebellar Lobule V
	2.94	14	-26	-28	Brainstem
	2.75	10	-46	-8	R Cerebellar Lobule I- IV
	2.33	0	-50	-10	L Cerebellar Lobule I-IV
224	3.42	54	-20	14	R Parietal Operculum Cortex
	3.21	66	-22	24	R Supramarginal Gyrus, anterior division
	2.45	62	-18	22	R Postcentral Gyrus
	2.39	58	-16	16	R Central Opercular Cortex
	1.96	68	-18	12	R Superior Temporal Gyrus, posterior division
220	3.01	56	-40	6	R Supramarginal Gyrus, posterior division
	2.73	48	-28	0	R Superior Temporal Gyrus, posterior division
	2.39	54	-34	16	R Planum Temporale
	2.00	58	-36	-2	R Middle Temporal Gyrus, posterior division
	1.91	54	-40	-6	R Middle Temporal Gyrus, temporooccipital part
192	3.20	-18	10	-6	L Putamen
	2.88	-22	10	0	L Accumbens
	2.68	-6	0	0	L Thalamus
	1.82	-8	2	10	L Caudate
140	2.53	-10	-98	2	L Occipital Pole
138	2.85	26	-6	0	R Pallidum
	2.70	26	6	12	R Putamen
	2.03	34	-16	4	R Insular Cortex

130	3.06	-52	4	28	L Precentral Gyrus
	2.29	-54	10	24	L Inferior Frontal Gyrus
	1.83	-50	18	30	L Middle Frontal Gyrus
122	3.37	-44	-30	6	L Planum Temporale
	2.94	-44	-24	6	L Heschl's Gyrus (includes H1 and H2)
	2.91	-36	-8	8	L Insular Cortex
	2.68	-28	-14	8	L Putamen
118	3.20	68	-28	0	R Superior Temporal Gyrus, posterior division
	2.36	70	-42	4	R Middle Temporal Gyrus, temporooccipital part
	2.16	64	-38	8	R Supramarginal Gyrus, posterior division
HS					
GPe FC – velocity of finger tapping ↑					
175	2.63	-32	0	-6	L Putamen
	2.20	-34	-10	6	L Insular Cortex
HS					
GPe FC – velocity of finger tapping ↓					
476	3.75	-20	16	8	L Caudate
	2.72	-10	2	-6	L Pallidum
	2.48	0	12	0	Subcallosal Cortex
	2.04	-6	-20	6	L Thalamus
329	2.91	-4	16	44	L Paracingulate Gyrus
	2.85	2	8	60	R Juxtapositional Lobule Cortex (formerly Supplementary Motor Cortex)
	2.60	2	18	58	R Superior Frontal Gyrus
193	2.77	56	-2	4	R Central Opercular Cortex
	2.50	62	2	10	R Precentral Gyrus
	2.10	66	-4	4	R Superior Temporal Gyrus, anterior division
	2.04	66	-12	8	R Planum Temporale
	1.96	52	-4	2	R Planum Polare
178	2.66	24	8	-12	R Putamen
	2.54	20	-6	-10	R Amygdala
	2.27	18	-16	-14	R Hippocampus
	1.80	10	8	-6	R Accumbens
	1.74	28	18	-10	R Insular Cortex
	1.55	34	22	-10	R Frontal Orbital Cortex
ET					
GPe FC – velocity of finger tapping ↑					
1296	3.30	-58	-44	46	L Supramarginal Gyrus, posterior division
	3.23	-56	-36	38	L Supramarginal Gyrus, anterior division
	3.13	-46	-34	16	L Parietal Operculum Cortex
	2.95	-40	-42	50	L Superior Parietal Lobule
	2.87	-66	-36	18	L Superior Temporal Gyrus, posterior division
	2.76	-40	-38	46	L Postcentral Gyrus
816	3.87	46	6	-2	R Insular Cortex
	3.55	30	2	8	R Putamen
	3.38	56	16	-2	R Inferior Frontal Gyrus, pars opercularis
	3.11	60	6	-10	R Superior Temporal Gyrus, anterior division
	2.65	54	22	-6	R Inferior Frontal Gyrus, pars triangularis
717	3.16	58	-30	36	R Supramarginal Gyrus, anterior division
	3.05	50	-28	8	R Planum Temporale
	3.03	64	-18	34	R Postcentral Gyrus
	3.00	66	-40	12	R Supramarginal Gyrus, posterior division
	2.62	58	-18	-6	R Superior Temporal Gyrus, posterior division
290	2.86	-14	-50	58	L Precuneous Cortex
	2.22	-14	-40	50	L Postcentral Gyrus
	2.19	-12	-26	38	L Cingulate Gyrus, posterior division
	1.96	-26	-48	64	L Superior Parietal Lobule
159	2.52	-36	46	28	L Frontal Pole
	2.36	-30	36	34	L Middle Frontal Gyrus
251	2.78	6	-8	58	R Juxtapositional Lobule Cortex (formerly Supplementary Motor Cortex)
	2.45	4	20	34	R Cingulate Gyrus, anterior division
	2.15	6	-16	58	R Precentral Gyrus
	2.05	8	12	44	R Paracingulate Gyrus
	1.99	-4	0	58	L Juxtapositional Lobule Cortex (formerly Supplementary Motor Cortex)
236	3.42	-54	-58	8	L Middle Temporal Gyrus, temporooccipital part

	3.10	-60	-66	10	L Lateral Occipital Cortex, inferior division
195	2.50	52	46	4	R Frontal Pole
	2.39	56	28	12	R Inferior Frontal Gyrus, pars triangularis
184	2.29	-46	18	-4	L Frontal Operculum Cortex
	2.07	-34	8	-14	L Insular Cortex
	1.95	-52	30	-10	L Frontal Orbital Cortex
183	3.16	-48	2	28	L Precentral Gyrus
	2.35	-46	12	28	L Inferior Frontal Gyrus, pars opercularis
180	2.59	36	48	34	R Frontal Pole
168	2.78	12	-44	-24	R Cerebellar Lobule I-IV
	2.71	-6	-40	-28	Brainstem
	2.30	-10	-40	-26	L Cerebellar Lobule I-IV
	2.21	-2	-58	-16	L Cerebellar Lobule V
136	3.20	-14	-72	-46	L Cerebellar Lobule VIIb
	3.07	-16	-74	-42	L Cerebellar Crus II
	3.00	-16	-70	-58	L Cerebellar Lobule VIIIa
	2.05	-20	-68	-30	L Cerebellar Lobule VI
130	2.71	36	-48	52	R Superior Parietal Lobule
	2.39	38	-42	38	R Supramarginal Gyrus, posterior division
	1.80	42	-34	48	R Postcentral Gyrus
119	3.19	50	-2	36	R Precentral Gyrus
	1.70	52	6	50	R Middle Frontal Gyrus
115	2.95	-26	-12	8	L Putamen
	2.48	-30	-4	2	L Caudate
	2.20	-34	-6	10	L Insular Cortex
71	2.05	-14	10	-2	L Caudate
	1.74	-20	10	-6	L Putamen
40	1.94	-20	6	10	L Putamen
ET					
GPe FC – velocity of finger tapping ↓					
140	2.40	10	58	2	R Frontal Pole
	2.37	8	54	6	R Paracingulate Gyrus
	2.18	4	42	8	R Cingulate Gyrus, anterior division
129	2.69	-8	44	30	L Superior Frontal Gyrus
	2.43	-6	58	32	L Frontal Pole
	1.89	-6	38	36	L Paracingulate Gyrus
100	2.35	-10	46	-6	L Paracingulate Gyrus
	2.19	-8	44	8	L Cingulate Gyrus, anterior division
	1.93	-4	30	-2	L Subcallosal Cortex
HS					
GPi FC – velocity of finger tapping ↑					
159	2.88	-36	10	0	L Insular Cortex
	2.60	-30	4	-2	L Putamen
	1.57	-16	0	-4	L Pallidum
110	2.86	-4	42	28	L Paracingulate Gyrus
	2.38	2	28	28	R Cingulate Gyrus, anterior division
	1.89	8	40	26	R Paracingulate Gyrus
ET					
GPi FC – velocity of finger tapping ↑					
365	3.15	32	22	-10	R Frontal Orbital Cortex
	2.84	40	22	-2	R Frontal Operculum Cortex
	2.61	56	10	-4	R Temporal Pole
	2.49	48	6	-2	R Central Opercular Cortex
	2.22	48	2	-10	R Planum Polare
	2.09	38	16	-10	R Insular Cortex
	1.88	60	10	-4	R Temporal Pole
326	2.88	-46	18	-4	L Frontal Operculum Cortex
	2.55	-52	30	-6	L Inferior Frontal Gyrus, pars triangularis
	2.53	-50	8	-4	L Temporal Pole
	2.50	-34	24	-6	L Frontal Orbital Cortex
	1.97	-56	14	0	L Inferior Frontal Gyrus, pars opercularis
	1.89	-34	18	-8	L Insular Cortex
185	3.03	26	10	2	R Putamen
	2.26	34	0	8	R Insular Cortex
122	2.76	40	-40	-22	R Temporal Occipital Fusiform Cortex
	2.57	46	-50	-36	R Cerebellar Crus I
	2.49	34	-44	-34	R Cerebellar Lobule VI

	2.16	38	-48	-42	R Cerebellar Crus II
119	2.70	-40	-38	46	L Postcentral Gyrus
	2.41	-32	-54	42	L Superior Parietal Lobule
	1.99	-44	-32	40	L Supramarginal Gyrus, anterior division
	1.94	-48	-44	54	L Supramarginal Gyrus, posterior division
116	3.37	30	18	60	R Middle Frontal Gyrus
	2.76	20	10	60	R Superior Frontal Gyrus
100	2.63	14	-32	-30	Brainstem
100	2.49	-10	-66	-16	L Cerebellar Lobule VI
	1.91	-22	-70	-30	L Cerebellar Crus I

8. FIGURES

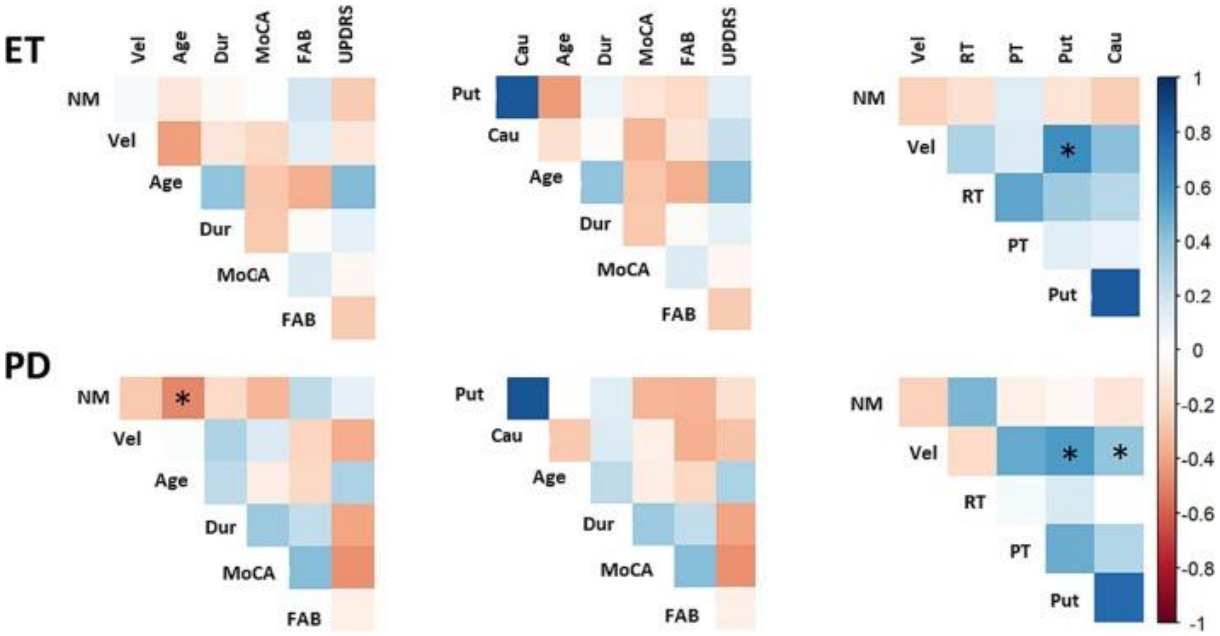

Figure 1: Correlation matrices for Essential tremor (ET) and Parkinson's disease (PD) patients. The colour map indicates matrices of Pearson's correlations and coefficients, and significant p-values adjusted for false discovery rate (FDR) are indicated by asterixis. Cau: caudate striatal binding ratio; Dur: disease duration, FAB: Frontal Assessment Battery; MoCA: Montreal Cognitive Assessment; NM: finger tapping number of movements; PT: postural tremor root-mean-square; Put: putamen striatal binding ratio, RT: resting tremor root-mean-square, UPDRS: Movement Disorder Society Unified Parkinson's Disease Rating Scale; Vel: velocity of finger tapping.

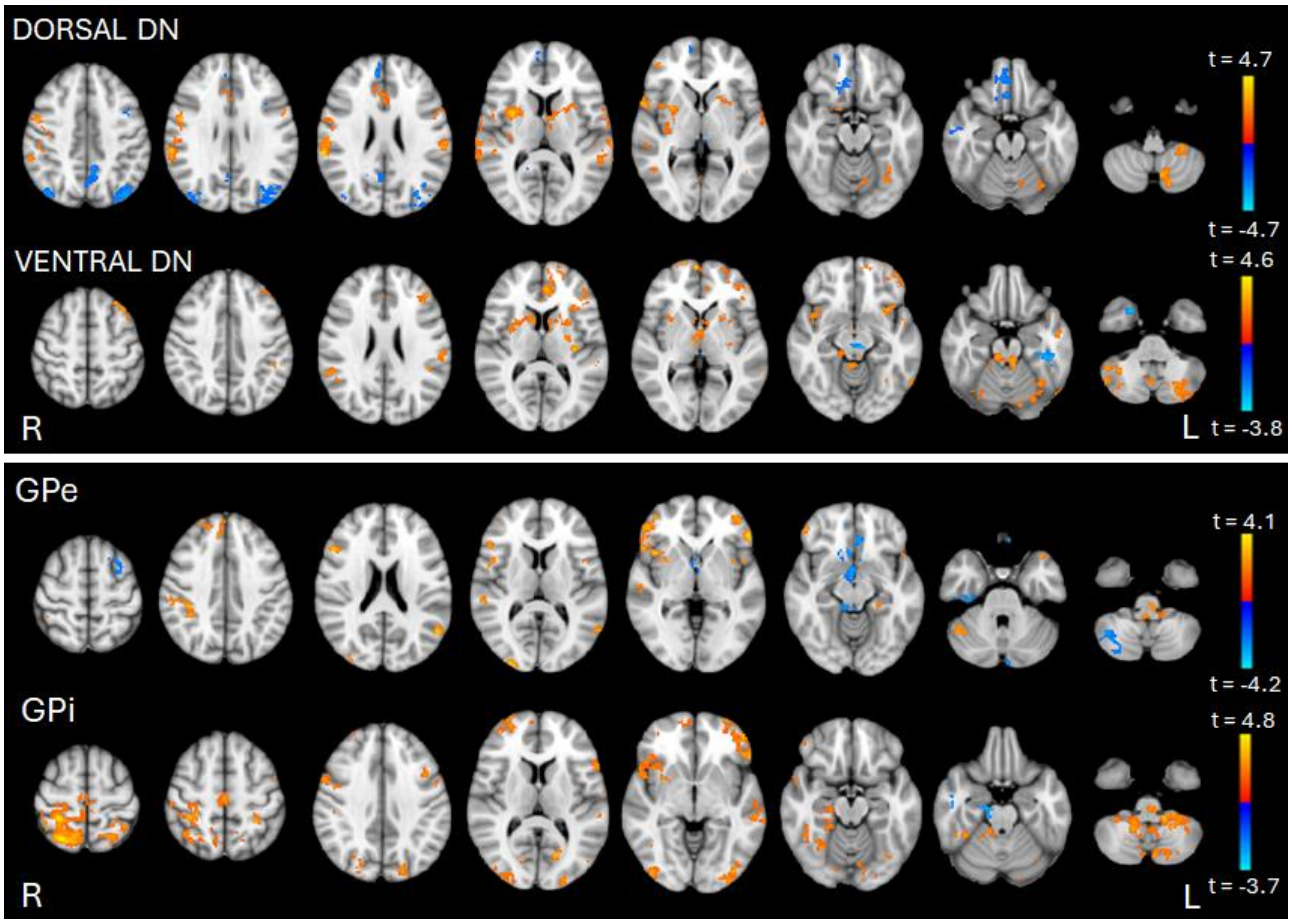

Figure 2: Resting-state functional connectivity (rsFC) maps of dorsal and ventral portions of the dentate nucleus (DN) and external and internal segments of the globus pallidus (GPe and GPi) comparing essential tremor (ET) patients with healthy subjects (HS). The color bar represents the *t* statistic of FC differences between the two groups. Red-yellow areas indicate where FC was significantly higher in ET patients than in HS, and blue-light blue areas indicate where FC was significantly lower in ET patients than in HS. Statistical significance was considered at $p<0.05$, False Discovery Rate (FDR) corrected.

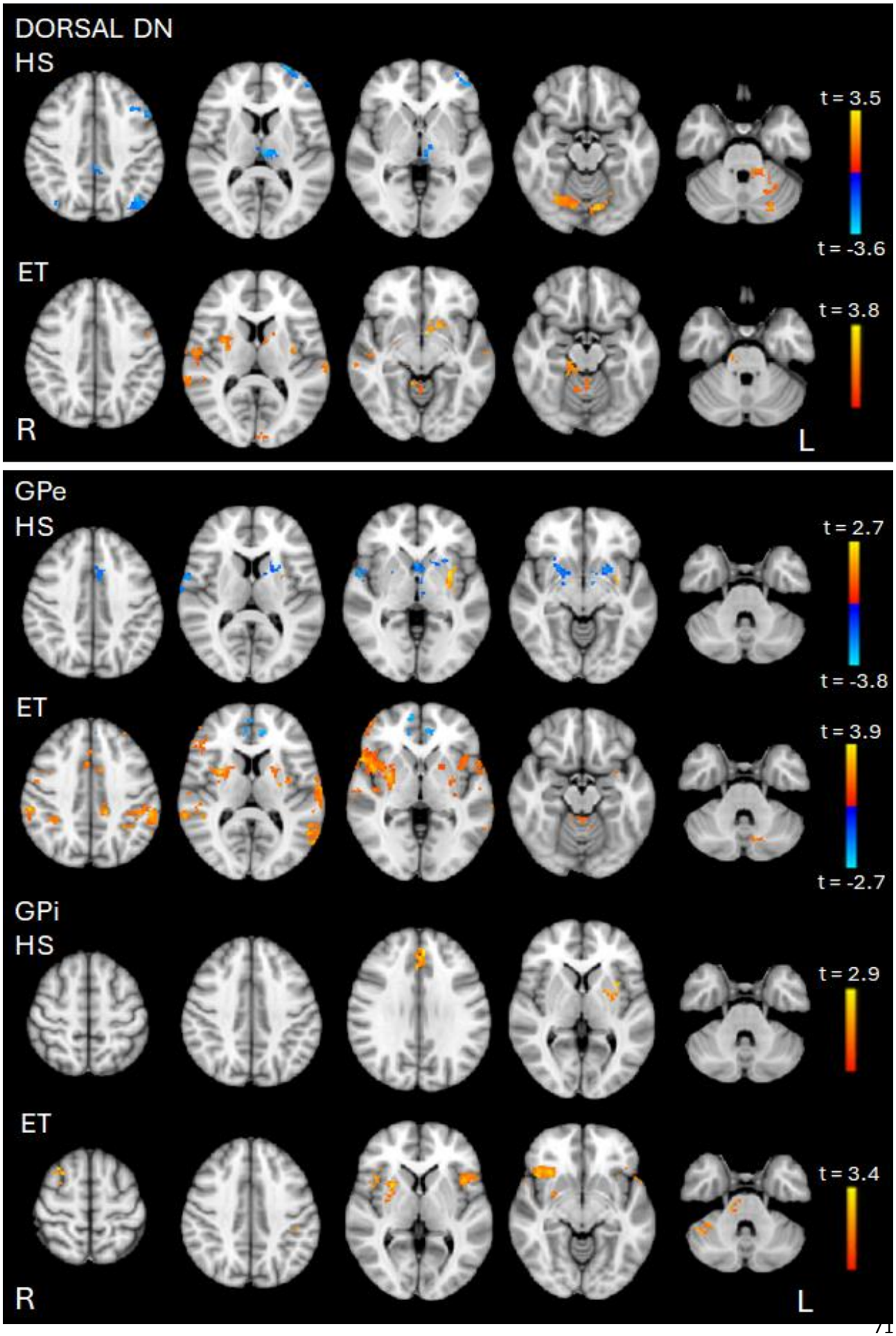
DORSAL DN
HS
t = 3.5
t = -3.6
ET
t = 3.8
R
L
GPe
HS
t = 2.7
t = -3.8
ET
t = 3.9
t = -2.7
GPi
HS
t = 2.9
ET
t = 3.4
R
L

Figure 3: Correlation maps between velocity of finger tapping and dorsal portion of the dentate nucleus (DN) rsFC and external and internal segments of the globus pallidus (GPe and GPi) rsFC in HS and ET patients. Positive correlations are shown in red-yellow color, and negative correlations are shown in blue-light blue color. The color bar represents the *t* statistic of correlation between rsFC of the ROIs and clinical data. Significant correlation was reached if $p < 0.05$ (FDR corrected).

9. SUPPLEMENTARY MATERIALS

Supplementary Table 1. Pharmacological treatment in patients with essential tremor (ET).

ET	Treatment
1	Propranolol 40mg
2	-
3	Bromazepam 1.5mg
4	-
5	-
6	-
7	Propranolol 40mg; Clonazepam 0.5mg
8	Propranolol 40mg
9	Clonazepam 0.3mg
10	Clonazepam 0.3mg
11	-
12	Propranolol 80mg
13	-
14	Propranolol 60mg
15	-
16	Propranolol 60mg; Clonazepam 3mg

Data are expressed as daily dose.

Supplementary Table 2 Correlations of clinical, kinematic, and DaTQUANT data in Parkinson's disease patients.

	Age	Duration	MOCA	FAB	MDS-UPDRS III	Rest tremor RMS	Postural tremor (P2) RMS	Putamen SBR	Caudate SBR
Velocity									
Coef	0.00	0.36	0.15	0.04	-0.39	-0.18	0.51	0.59	0.49
P-adj	1.00	0.16	0.58	0.87	0.12	0.57	0.07	**0.01**	**0.05**
N° Movemements									
Coef	-0.45	-0.30	-0.16	0.32	0.15	0.45	-0.14	-0.06	-0.13
P-adj	**0.07**	0.25	0.54	0.21	0.56	0.14	0.64	0.81	0.62
Putamen SBR									
Coef	0.05	0.19	-0.31	-0.25	-0.16	0.16	0.43	-	-
P-adj	0.84	0.48	0.22	0.34	0.54	0.62	0.13	-	-
Caudate SBR									
Coef	-0.11	0.28	-0.14	-0.30	-0.19	-0.01	0.28	-	-
P-adj	0.67	0.27	0.60	0.24	0.46	0.98	0.33	-	-

Results of Pearson's correlations are presented as coefficient and p-adjusted for false discovery rate (FDR). FAB: Frontal Assessment Battery; MOCA: Montreal Cognitive Assessment; MDS-UPDRS III: Movement Disorder Society Unified Parkinson's Disease Rating Scale; P2: posture 2, RMS: root-mean-square; SBR: striatal binding ratio.

Supplementary Table 3 Correlations of clinical, kinematic, and DaTQUANT data in Essential Tremor patients.

	Age	Duration	MOCA	FAB	MDS-UPDRS III	Rest tremor RMS	Postural tremor (P2) RMS	Putamen SBR	Caudate SBR
Velocity									
Coef	-0.29	-0.06	-0.05	0.14	-0.17	0.20	0.14	0.53	0.35
P-adj	0.28	0.84	0.85	0.72	0.53	0.46	0.63	**0.03**	0.18
N° Movemements									
Coef	-0.19	-0.09	-0.05	0.14	0.01	-0.21	0.14	-0.25	-0.32
P-adj	0.49	0.74	0.86	0.72	0.96	0.43	0.64	0.36	0.23
Putamen SBR									
Coef	-0.25	0.12	-0.13	0.02	0.14	0.34	0.12	-	-
P-adj	0.66	0.34	0.95	0.62	0.61	0.20	0.68	-	-
Caudate SBR									
Coef	-0.16	0.14	-0.38	0.04	0.25	0.29	0.08	-	-
P-adj	0.63	0.57	0.98	0.15	0.35	0.27	0.78	-	-

Results of Pearson's correlations are presented as coefficient and p-adjusted for false discovery rate (FDR). FAB: Frontal Assessment Battery; MOCA: Montreal Cognitive Assessment; MDS-UPDRS III: Movement Disorder Society Unified Parkinson's Disease Rating Scale; P2: posture 2, RMS: root-mean-square; SBR: striatal binding ratio.

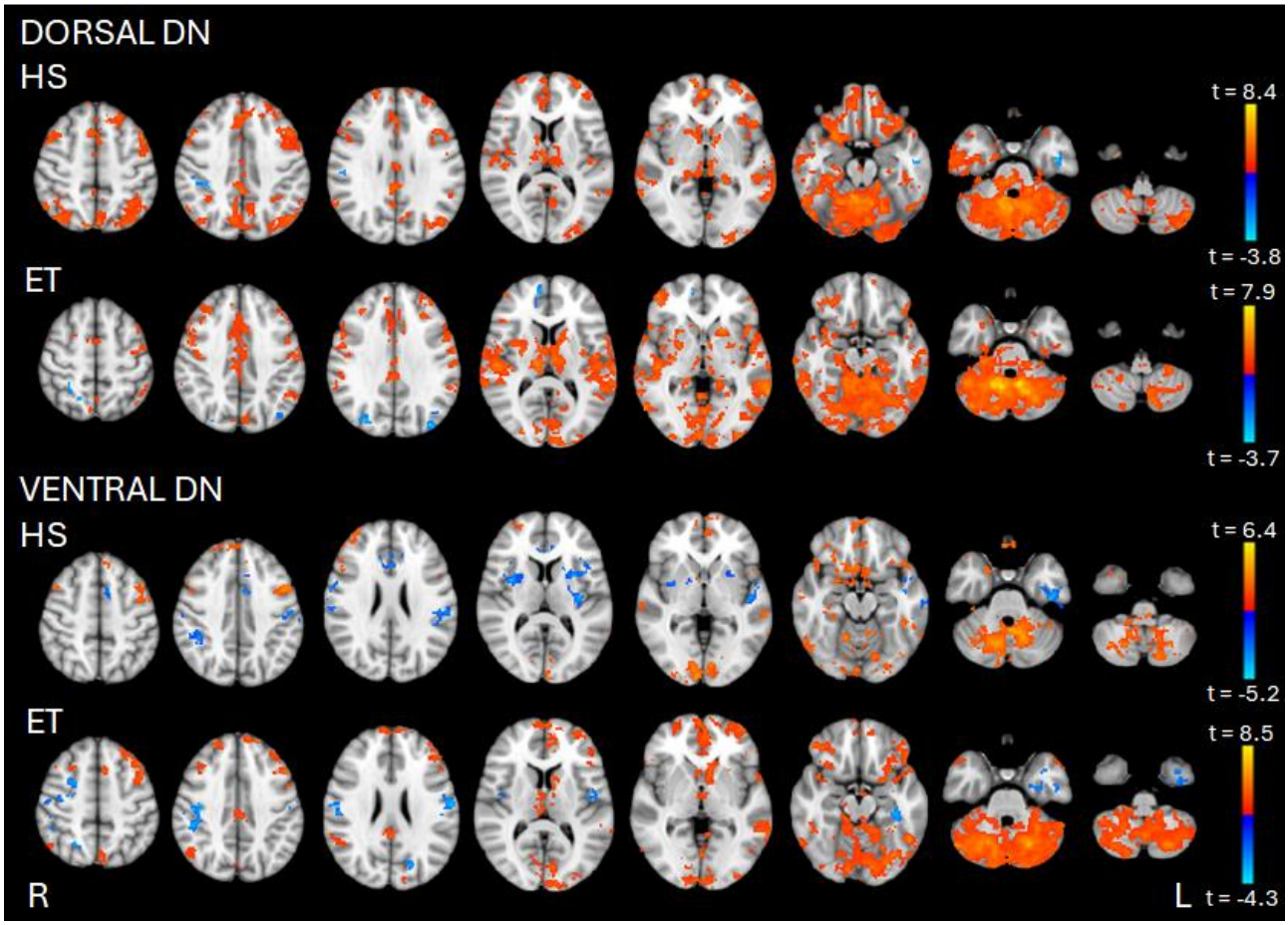

Supplementary Figure 1: Maps of dorsal and ventral portions of the dentate nucleus (DN) rsFC in HS and in ET patients. The color bars represent *t* values. Red-yellow and blue-light blue areas indicate respectively regions positively and negatively correlated with dorsal and ventral DN. Statistical significance was considered at $p<0.05$, False Discovery Rate (FDR) corrected.

Supplementary Table 4: Dorsal and ventral DN rsFC in the single groups of HS and ET patients (one-sample t-test, p <0.05, false discovery rate corrected, minimum cluster extent set at 100 voxels). Positive and negative correlations in rsFC maps were reported. Anatomical localizations of peak MNI coordinates were established according to Harvard-Oxford cortical and subcortical structural atlases and the cerebellar atlas included in FMRIB's Software Library.

		MNI coordinates			
Cluster size (voxels)	**T**	**x**	**y**	**z**	**Cluster location (local maxima)**
HS					
Dorsal DN FC – positive					
29682	8.36	12	-56	-26	R Cerebellar Lobule V
	6.90	10	-50	-22	R Cerebellar Lobule I-IV
	6.41	26	12	-16	R Frontal Orbital Cortex
	6.24	4	-60	-30	Vermis Lobule VIIIa
	6.04	4	-60	-26	Vermis Lobule VI
	5.78	10	-56	-32	R Cerebellar Lobule IX
	5.36	-14	-60	-26	L Cerebellar Lobule VI
	5.26	-8	-54	-22	L Cerebellar Lobule V
664	3.42	50	-58	52	R Lateral Occipital Cortex, superior division
	3.18	38	-52	54	R Superior Parietal Lobule
	3.06	56	-56	48	R Angular Gyrus
643	3.38	54	10	36	R Precentral Gyrus
	3.33	52	30	24	R Middle Frontal Gyrus
	3.01	48	12	24	R Inferior Frontal Gyrus, pars opercularis
	2.90	54	36	14	R Frontal Pole
487	4.98	44	-26	14	R Heschl's Gyrus (includes H1 and H2)
	3.32	36	-12	16	R Insular Cortex
	3.32	54	-20	6	R Planum Temporale
	3.02	56	-16	14	R Central Opercular Cortex
	2.98	34	-18	-4	R Putamen
289	3.69	14	62	22	R Frontal Pole
167	3.27	-2	-20	26	L Cingulate Gyrus, posterior division
	3.06	4	-12	46	R Cingulate Gyrus, anterior division
	2.12	-2	0	48	L Juxtapositional Lobule Cortex (formerly Supplementary Motor Cortex)
137	3.69	58	12	-6	R Temporal Pole
	2.98	30	26	-6	R Frontal Orbital Cortex
	2.75	40	24	2	R Frontal Operculum Cortex
	2.08	46	26	6	R Inferior Frontal Gyrus, pars triangularis
	1.84	36	20	0	R Insular Cortex
HS					
Dorsal DN FC – negative					
123	3.80	-44	-2	-40	L Inferior Temporal Gyrus, anterior division
	3.20	-42	-10	-30	L Inferior Temporal Gyrus, posterior division
	2.80	-54	-16	-20	L Middle Temporal Gyrus, posterior division
	2.27	-48	-8	-22	L Middle Temporal Gyrus, anterior division
	1.83	-38	0	-34	L Temporal Fusiform Cortex, anterior division
101	3.18	52	-22	32	R Supramarginal Gyrus, anterior division
	3.05	34	-36	40	R Postcentral Gyrus
	2.29	58	-22	22	R Parietal Operculum Cortex
ET					
Dorsal DN FC – positive					
33633	6.00	-16	-62	-30	L Cerebellar Lobule VI
	5.10	8	-90	-8	R Occipital Pole
	4.98	-66	-48	-2	L Middle Temporal Gyrus, temporooccipital part
	4.94	-24	-70	-28	L Cerebellar Crus I
	4.89	-24	-70	-40	L Cerebellar Crus II
	4.87	14	-18	8	R Thalamus
	4.84	30	-64	-24	R Cerebellar Lobule VI

	4.79	-40	-92	-6	L Occipital Pole
	4.60	12	-50	-20	R Cerebellar Lobule V
	4.51	42	-56	-34	R Cerebellar Crus I
	4.38	-18	14	0	L Putamen
	4.32	28	-6	6	R Putamen
419	3.5	-48	-46	50	L Supramarginal Gyrus
	3.29	-48	-60	48	L Lateral Occipital Cortex, superior division
	3.29	-38	-50	60	L Superior Parietal Lobule
	2.84	-54	-56	48	L Angular Gyrus
401	3.42	50	6	42	R Precentral Gyrus
	2.69	48	12	36	R Middle Frontal Gyrus
	2.33	42	-18	38	R Postcentral Gyrus
252	3.57	0	-60	62	R Precuneous Cortex
	3.06	-10	-66	66	L Lateral Occipital Cortex, superior division
	2.77	-12	-48	76	L Postcentral Gyrus
	2.72	-6	-62	64	L Precuneous Cortex
223	4.35	46	50	8	R Frontal Pole
201	3.40	32	28	44	R Middle Frontal Gyrus
	2.79	36	38	20	R Frontal Pole
176	3.70	28	38	-12	R Frontal Pole
	2.63	40	26	-20	R Frontal Orbital Cortex
134	3.77	-4	-82	42	L Precuneous Cortex
	3.16	4	-78	46	R Precuneous Cortex
116	3.08	0	52	-24	R Frontal Medial Cortex
	2.81	-14	58	-16	L Frontal Pole
	2.57	-6	48	-24	L Frontal Medial Cortex
	2.20	4	58	-24	R Frontal Pole
110	4.37	-22	-2	-34	L Parahippocampal Gyrus, anterior division
	2.60	-32	2	-44	L Temporal Pole
	2.20	-24	0	-46	L Temporal Fusiform Cortex, anterior division
ET					
Dorsal DN FC – negative					
182	3.48	8	60	18	R Frontal Pole
	2.83	12	54	10	R Paracingulate Gyrus
	2.29	12	52	-4	R Frontal Medial Cortex
	2.12	14	42	8	R Cingulate Gyrus, anterior division
128	3.13	30	-78	32	R Lateral Occipital Cortex, superior division
126	3.62	22	-52	56	R Superior Parietal Lobule
	3.09	18	-60	54	R Lateral Occipital Cortex, superior division
125	3.34	-40	-84	30	L Lateral Occipital Cortex, superior division
HS					
Ventral DN FC – positive					
4682	6.34	18	-68	-40	R Cerebellar Lobule VIIb
	5.04	-16	-62	-32	L Cerebella Lobule VI
	5.00	-14	-62	-40	L Cerebellar Lobule VIIIb
	4.61	-26	-70	-42	L Cerebellar Crus II
	4.53	4	-50	-24	R Cerebellar Lobule I-IV
	4.46	14	-56	-42	R Cerebellar Lobule IX
	4.39	-4	-54	-28	L Cerebellar Lobule I-IV
	4.39	-14	-66	-44	L Cerebellar Lobule VIIIa
1782	4.49	16	-94	-12	R Occipital Pole
	3.77	12	-88	0	R Intracalcarine Cortex
	3.70	32	-76	-22	R Cerebellar Crus I
	3.56	4	-88	-16	R Lingual Gyrus
	3.42	50	-68	-20	R Lateral Occipital Cortex, inferior division
	3.38	-8	-84	-2	L Lingual Gyrus
	3.37	-2	-94	12	L Occipital Pole
	3.36	-24	-84	-20	L Occipital Fusiform Gyrus
991	4.32	-6	30	-28	L Subcallosal Cortex
	3.83	-4	38	-14	L Frontal Medial Cortex
	3.43	4	16	-18	R Subcallosal Cortex
	3.36	26	24	-22	R Frontal Orbital Cortex
	3.34	4	32	-30	R Frontal Medial Cortex
	3.05	46	20	-24	R Temporal Pole
523	4.04	-44	16	50	L Middle Frontal Gyrus
	3.84	-40	-4	62	L Precentral Gyrus
	2.58	-54	14	28	L Inferior Frontal Gyrus, pars opercularis

503	3.36	54	36	18	R Frontal Pole
277	3.38	60	22	18	R Inferior Frontal Gyrus, pars opercularis
	3.22	50	16	44	R Middle Frontal Gyrus
	2.39	52	18	26	R Inferior Frontal Gyrus, pars opercularis
261	5.41	-42	18	-22	L Temporal Pole
	4.61	-36	20	-20	L Frontal Orbital Cortex
230	4.79	24	6	-38	R Temporal Pole
224	3.69	-4	38	46	L Superior Frontal Gyrus
	3.05	8	52	42	R Frontal Pole
	2.43	-8	32	36	L Paracingulate Gyrus
186	3.52	-66	-38	6	L Superior Temporal Gyrus, posterior division
	3.20	-66	-50	0	L Middle Temporal Gyrus, temporooccipital part
157	3.96	38	-32	-26	R Temporal Fusiform Cortex, posterior division
	3.29	26	-34	-18	R Parahippocampal Gyrus
126	4.26	-8	-34	-38	Brainstem
120	3.52	64	-30	-8	R Middle Temporal Gyrus, posterior division
	2.21	64	-20	-2	R Superior Temporal Gyrus, posterior division
105	3.40	-12	50	-8	L Frontal Medial Cortex
	3.13	6	44	6	R Cingulate Gyrus, anterior division
	2.60	2	48	2	R Paracingulate Gyrus
	2.29	-4	56	-2	L Frontal Pole
101	2.55	-6	16	68	L Superior Frontal Gyrus
HS					
Ventral DN FC – negative					
445	3.87	-46	-18	-30	L Inferior Temporal Gyrus, posterior division
	3.80	-42	-20	-30	L Temporal Fusiform Cortex, posterior division
	3.76	-46	-8	-18	L Superior Temporal Gyrus, anterior division
	2.79	-36	-10	-30	L Temporal Fusiform Cortex, anterior division
	2.56	-50	-10	-22	L Middle Temporal Gyrus, anterior division
398	5.19	6	26	18	R Cingulate Gyrus, anterior division
	3.09	-4	20	36	L Paracingulate Gyrus
	3.04	-4	32	16	L Cingulate Gyrus, anterior division
	2.68	12	30	30	R Paracingulate Gyrus
379	4.09	-30	8	10	L Insular Cortex
	2.86	-36	-14	20	L Central Opercular Cortex
	2.80	-38	10	12	L Frontal Operculum Cortex
	2.46	-28	-16	4	L Putamen
	2.29	-20	16	8	L Caudate
331	3.24	-58	-28	26	L Supramarginal Gyrus, anterior division
	3.10	-50	-26	22	L Parietal Operculum Cortex
	2.99	-54	-16	40	L Postcentral Gyrus
309	4.36	34	2	12	R Insular Cortex
	2.60	30	0	-4	R Putamen
	2.54	44	8	14	R Inferior Frontal Gyrus, pars opercularis
	2.22	42	6	8	R Central Opercular Cortex
	2.05	20	0	2	R Pallidum
249	3.18	16	-56	64	R Superior Parietal Lobule
	3.10	12	-60	66	R Lateral Occipital Cortex, superior division
	3.10	20	-42	74	R Postcentral Gyrus
	2.76	12	-54	56	R Precuneous Cortex
199	4.00	40	-42	38	R Supramarginal Gyrus, posterior division
	3.91	52	-22	30	R Supramarginal Gyrus, anterior division
	2.82	54	-34	34	R Parietal Operculum Cortex
	2.68	40	-48	38	R Angular Gyrus
	2.12	60	-18	32	R Postcentral Gyrus
199	3.20	24	4	66	R Superior Frontal Gyrus
	3.12	10	-12	58	R Juxtapositional Lobule Cortex (formerly Supplementary Motor Cortex)
175	3.34	-48	-14	-2	L Planum Polare
	3.05	-46	-20	0	L Heschl's Gyrus (includes H1 and H2)
	2.48	-52	0	2	L Central Opercular Cortex
	2.28	-50	4	-14	L Temporal Pole
136	3.62	68	-18	20	R Postcentral Gyrus
	2.99	58	2	22	R Precentral Gyrus
	2.51	60	-24	24	R Supramarginal Gyrus, anterior division
	2.25	52	-22	12	R Planum Temporale
119	4.12	-4	8	46	L Paracingulate Gyrus

	3.65	-10	4	46	L Juxtapositional Lobule Cortex (formerly Supplementary Motor Cortex)
	2.93	-8	4	34	L Cingulate Gyrus, anterior division
ET					
Ventral DN FC – positive					
17719	8.21	14	-70	-36	R Cerebellar Crus II
	7.03	-20	-66	-34	L Cerebellar Lobule VI
	6.75	-20	-68	-38	L Cerebellar Crus II
	5.81	20	-66	-32	R Cerebellar Lobule VI
	5.30	-14	-66	-38	L Cerebellar Lobule VIIb
	5.29	32	-70	-36	R Cerebellar Crus I
3735	4.49	-42	24	48	L Middle Frontal Gyrus
	4.08	-40	56	2	L Frontal Pole
	4.03	-8	10	-6	L Accumbens
	3.95	-8	10	-2	L Caudate
	3.84	-24	2	-20	L Amygdala
	3.68	-32	16	-14	L Frontal Orbital Cortex
2639	5.24	4	64	2	R Frontal Pole
	4.25	-6	62	4	L Frontal Pole
	4.18	2	44	2	R Cingulate Gyrus, anterior division
	4.16	-2	44	2	L Cingulate Gyrus, anterior division
	3.85	-4	54	2	L Paracingulate Gyrus
	3.82	-10	50	-8	L Frontal Medial Cortex
498	4.01	-16	22	62	L Superior Frontal Gyrus
	3.90	12	26	64	R Superior Frontal Gyrus
	3.35	-6	16	52	L Paracingulate Gyrus
346	3.93	42	10	-16	R Temporal Pole
	3.76	44	6	-10	R Insular Cortex
	3.36	34	26	-22	R Frontal Orbital Cortex
	3.22	42	-10	-8	R Planum Polare
221	3.48	-8	-36	32	L Cingulate Gyrus, posterior division
	3.05	0	-44	24	R Cingulate Gyrus, posterior division
213	3.96	-2	-70	56	L Precuneous Cortex
	2.62	-10	-66	66	L Lateral Occipital Cortex, superior division
172	3.31	-8	-24	34	L Cingulate Gyrus, posterior division
170	3.31	46	24	44	R Middle Frontal Gyrus
	2.56	24	18	50	R Superior Frontal Gyrus
149	2.62	48	-64	48	R Lateral Occipital Cortex, superior division
	1.74	52	-54	36	R Angular Gyrus
142	3.11	56	-52	18	R Angular Gyrus
	2.56	54	-44	20	R Supramarginal Gyrus, posterior division
ET					
Ventral DN FC-negative					
564	4.30	36	-14	46	R Precentral Gyrus
	3.78	36	-22	44	R Postcentral Gyrus
	3.40	48	-34	44	R Supramarginal Gyrus, anterior division
	3.19	48	-38	44	R Supramarginal Gyrus, posterior division
	3.14	42	4	56	R Middle Frontal Gyrus
	2.73	24	4	48	R Superior Frontal Gyrus
373	3.71	-44	-8	14	L Central Opercular Cortex
	3.30	-60	-14	26	L Postcentral Gyrus
	2.44	-52	-2	28	L Precentral Gyrus
245	3.26	46	-18	16	R Central Opercular Cortex
	2.78	54	-20	24	R Postcentral Gyrus
	2.77	32	-20	16	R Insular Cortex
226	3.29	-36	-30	-20	L Temporal Fusiform Cortex, posterior division
	2.80	-38	-22	-14	L Hippocampus
	1.84	-46	-38	-18	L Inferior Temporal Gyrus, posterior division
195	2.80	-38	-4	-44	L Temporal Fusiform Cortex, anterior division
	2.71	-32	4	-48	L Temporal Pole
	2.47	-42	-16	-40	L Inferior Temporal Gyrus, posterior division
193	3.16	22	-62	54	R Lateral Occipital Cortex, superior division
	2.82	16	-56	62	R Superior Parietal Lobule
	2.75	12	-42	62	R Postcentral Gyrus
152	3.27	-10	-20	64	L Precentral Gyrus
122	3.33	-26	-10	-26	L Hippocampus
	2.23	-34	-4	-28	L Parahippocampal Gyrus, anterior division

105	3.14	-20	-78	26	L Cuneal Cortex
	2.28	-14	-70	20	L Precuneous Cortex
	2.07	-16	-68	16	L Supracalcarine Cortex

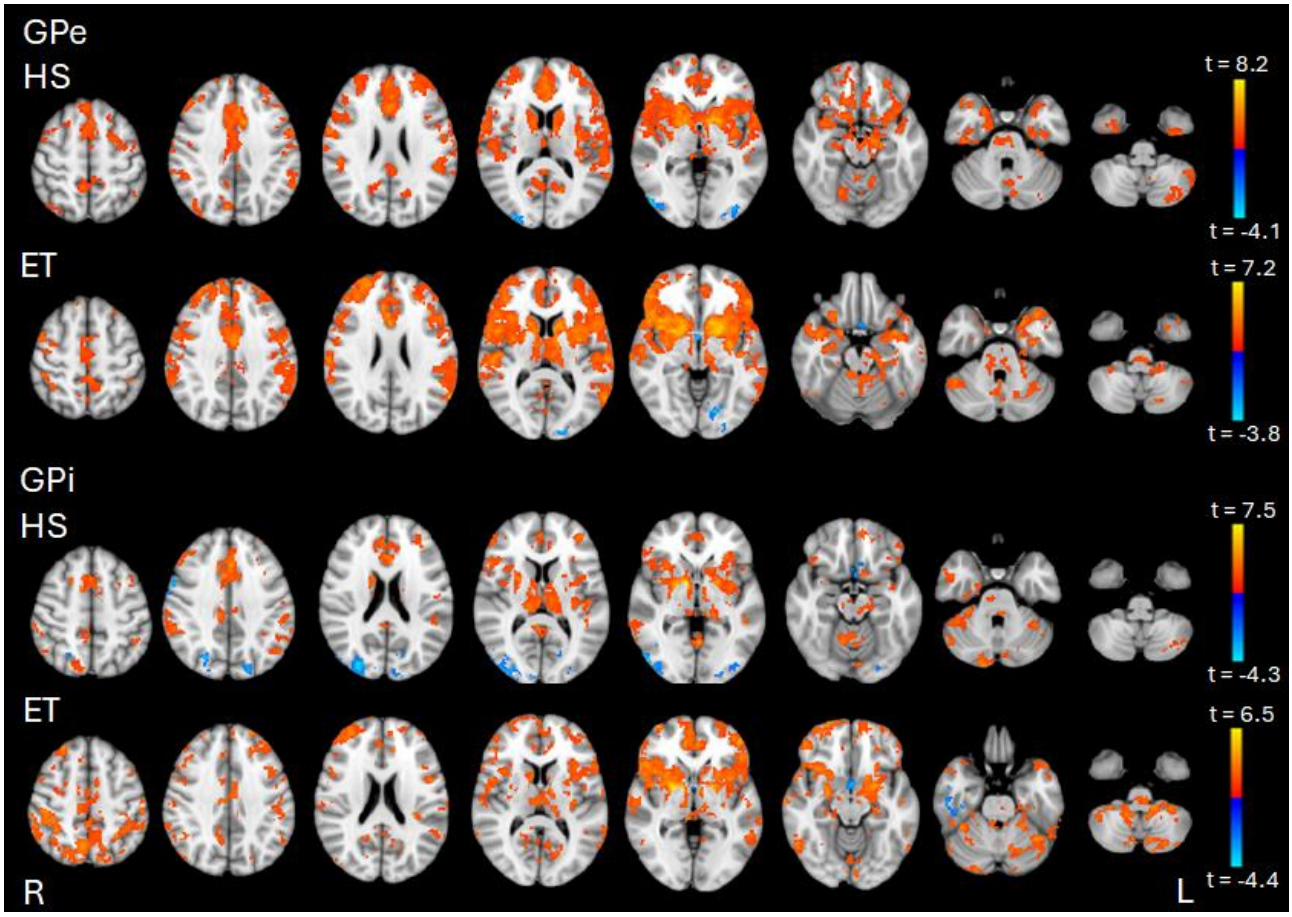

Supplementary Figure 2: Maps of external and internal segments of the globus pallidus (GPe and GPi) rsFC in HS and ET patients. The color bars represent *t* values. Red-yellow and blue-light blue areas indicate respectively regions positively and negatively correlated with GPe and GPi. Statistical significance was considered at $p<0.05$, False Discovery Rate (FDR) corrected.

Supplementary Table 5: GPe and GPi rsFC in the single groups of HS and ET patients (one-sample t-test, p <0.05, false discovery rate corrected, minimum cluster extent set at 100 voxels). Positive and negative correlations in rsFC maps were reported. Anatomical localizations of peak MNI coordinates were established according to Harvard-Oxford cortical and subcortical structural atlases and the cerebellar atlas included in FMRIB's Software Library.

		MNI coordinates			
Cluster size (voxels)	**T**	**x**	**y**	**z**	**Cluster location (local maxima)**
HS					
GPe FC – positive					
32181	7.30	-14	6	-2	L Pallidum
	6.90	-8	4	-2	L Caudate
	6.25	18	2	0	R Pallidum
	5.85	-36	16	-20	R Frontal Orbital Cortex
	5.71	-8	12	38	L Paracingulate Gyrus
	5.64	4	26	20	R Cingulate Gyrus, anterior division
	5.62	40	12	-6	R Insular Cortex
	5.47	20	8	2	R Putamen
1614	4.47	-6	-76	-26	L Cerebellar Lobule VI
	3.89	-46	-52	-48	L Cerebellar Crus II
	3.67	-22	-76	-56	L Cerebellar Lobule VIIb
	3.66	-52	-60	-32	L Cerebellar Crus I
	3.59	-12	-52	-12	L Cerebellar Lobule V
	3.42	-26	-64	-56	L Cerebellar Lobule VIIIa
	3.25	-4	-66	-34	Vermis Lobule VIIIa
318	3.22	44	-76	22	R Lateral Occipital Cortex, superior division
125	3.54	22	-66	-16	R Cerebellar Lobule VI
HS					
GPe FC – negative					
266	4.02	50	-78	0	R Lateral Occipital Cortex, inferior division
	2.26	40	-90	6	R Occipital Pole
142	3.74	-34	-86	-4	L Lateral Occipital Cortex, inferior division
	2.54	-36	-74	-12	L Occipital Fusiform Gyrus
	1.99	-24	-92	-10	L Occipital Pole
108	3.41	26	-98	8	R Occipital Pole
ET					
GPe FC – positive					
39864	7.12	-22	8	-2	L Putamen
	6.56	26	4	-4	R Putamen
	6.40	16	16	-2	R Caudate
	6.23	52	10	4	R Inferior Frontal Gyrus, pars opercularis
	6.10	60	8	14	R Precentral Gyrus
	5.98	34	16	-6	R Insular Cortex
	5.86	-14	12	-4	L Caudate
329	3.38	46	-50	-32	R Cerebellar Crus I
	2.95	52	-50	-24	R Inferior Temporal Gyrus, temporooccipital part
	2.40	46	-60	-20	R Temporal Occipital Fusiform Cortex
	2.24	36	-58	-28	R Cerebellar Lobule VI
	2.17	44	-38	-26	R Temporal Fusiform Cortex, posterior division
172	4.21	34	-44	-54	R Cerebellar Lobule VIIIa
	2.56	20	-46	-56	R Cerebellar Lobule VIIIb
	2.45	26	-36	-42	R Cerebellar Lobule X
	2.43	32	-36	-40	R Cerebellar Lobule VI
ET					
GPe FC - negative					
311	3.15	-18	-94	12	L Occipital Pole
	3.03	-16	-76	-4	L Lingual Gyrus
	2.74	-28	-68	-14	L Occipital Fusiform Gyrus
249	2.77	0	16	-6	R Subcallosal Cortex
	2.36	-4	12	-20	L Subcallosal Cortex

	2.24	-10	18	-26	L Frontal Orbital Cortex
HS					
GPi FC – positive					
10654	7.39	12	0	-2	R Pallidum
	7.26	0	26	24	R Cingulate Gyrus
	5.41	34	14	-6	R Insular Cortex
	5.33	-16	-18	8	L Thalamus
	5.00	-22	-6	-10	L Amygdala
	4.91	-40	50	8	L Frontal Pole
	4.85	6	12	36	R Cingulate Gyrus, anterior division
	4.75	24	12	6	R Putamen
911	4.39	-30	-22	8	L Putamen
	4.08	-50	-42	16	L Planum Temporale
	3.78	-46	-40	8	L Superior temporal Gyrus, posterior division
	3.61	-52	-12	18	L Central Opercular Cortex
	3.60	-34	-28	8	L Heschl's Gyrus (includes H1 and H2)
	3.22	-52	-34	36	L Supramarginal Gyrus, anterior division
	3.21	-48	-40	-2	L Middle Temporal Gyrus, posterior division
	3.16	-56	-16	28	L Postcentral Gyrus
	3.13	-34	-24	12	L Insular Cortex
	3.06	-64	-44	34	L Supramarginal Gyrus, posterior division
596	3.80	58	-34	52	R Supramarginal Gyrus, posterior division
	3.46	64	-26	44	R Supramarginal Gyrus, anterior division
	2.93	48	-56	46	R Angular Gyrus
	2.79	38	-50	42	R Superior Parietal Lobule
470	3.83	12	-28	36	R Cingulate Gyrus, posterior division
	2.89	10	-42	48	R Precuneous Cortex
	2.78	4	-12	28	R Cingulate Gyrus, anterior division
356	3.90	44	-46	-34	R Cerebellar Crus I
	3.64	28	-34	-28	R Cerebellar Lobule V
	2.93	38	-56	-24	R Cerebellar Lobule VI
254	3.54	-24	-74	-22	L Cerebellar Lobule VI
	3.26	-20	-70	-34	L Cerebellar Crus I
	3.09	-24	-74	-44	L Cerebellar Crus II
209	3.21	-22	12	58	L Superior Frontal Gyrus
	3.05	-34	10	62	L Middle Frontal Gyrus
185	3.38	62	-50	-4	R Middle Temporal Gyrus, temporooccipital part
	2.64	58	-58	-12	R Inferior Temporal Gyrus, temporooccipital part
	2.50	66	-34	2	R Superior Temporal Gyrus, posterior division
177	3.06	12	-74	58	R Lateral Occipital Cortex, superior division
	2.30	14	-74	40	R Precuneous Cortex
150	3.49	-4	-82	-16	L Lingual Gyrus
	2.72	-10	-78	-32	L Cerebellar Crus II
	2.65	-8	-78	-28	L Cerebellar Crus I
	2.20	6	-76	-20	Vermis Lobule VI
	1.95	0	-78	-34	Vermis Crus II
	1.85	-12	-74	-42	L Cerebellar Lobule VIIb
150	4.15	16	-92	-30	R Cerebellar Crus II
	4.13	20	-86	-26	R Cerebellar Crus I
144	3.32	-32	-50	-32	L Cerebellar Lobule VI
	3.12	-40	-62	-24	L Cerebellar Crus I
125	3.28	52	-4	-28	R Middle Temporal Gyrus, anterior division
	2.88	54	10	-24	R Temporal Pole
	2.63	58	-6	-36	R Inferior Temporal Gyrus, anterior division
121	3.38	50	28	36	R Middle Frontal Gyrus
	2.64	38	36	34	R Frontal Pole
111	3.14	-40	16	56	L Middle Frontal Gyrus
103	3.19	-44	-46	50	L Supramarginal Gyrus, posterior division
	2.76	-44	-52	54	L Angular Gyrus
HS					
GPi FC – negative					
1043	4.23	42	-64	-10	R Lateral Occipital Cortex, inferior division
	4.15	30	-84	20	R Lateral Occipital Cortex, superior division
	3.36	36	-90	14	R Occipital Pole
497	3.96	12	-40	72	R Postcentral Gyrus
	3.35	22	-60	58	R Lateral Occipital Cortex, superior division
	3.01	20	-56	56	R Superior Parietal Lobule
349	3.11	-20	-84	36	L Lateral Occipital Cortex, superior division

	2.93	-18	-70	16	L Cuneal Cortex
	2.71	-10	-96	18	L Occipital Pole
275	3.47	-38	-82	2	L Lateral Occipital Cortex, inferior division
	3.28	-26	-80	-10	L Occipital Fusiform Gyrus
	2.52	-24	-92	-2	L Occipital Pole
	2.44	-16	-78	-12	L Lingual Gyrus
155	3.17	-10	18	-26	L Frontal Orbital Cortex
	2.82	-10	18	-22	L Subcallosal Cortex
	2.77	-12	28	-22	L Frontal Orbital Cortex
	2.60	2	16	-16	R Subcallosal Cortex
141	3.99	24	-72	36	R Occipital Cortex, superior division
128	3.48	58	2	30	R Precentral Gyrus
	2.56	62	-8	30	R Postcentral Gyrus
ET					
GPi FC – positive					
27413	6.43	22	-2	0	R Pallidum
	6.21	-18	-2	-4	L Pallidum
	5.76	24	4	-4	R Putamen
	5.13	8	-62	62	R Precuneous Cortex
	5.08	10	-62	66	R Lateral Occipital Cortex, superior division
	5.08	-24	2	-10	L Putamen
	4.99	10	-26	-34	Brainstem
	4.95	10	-2	-2	R Thalamus
	4.90	26	-8	-10	R Amygdala
	4.85	26	-42	60	R Superior Parietal Lobule
	4.64	-36	-44	-42	L Cerebellar Crus II
577	3.68	-50	4	20	L Precentral Gyrus
	3.03	-50	12	26	L Inferior Frontal Gyrus, pars opercularis
	3.02	-38	16	40	L Middle Frontal Gyrus
490	3.58	2	-58	4	R Lingual Gyrus
	3.51	-8	-60	12	L Precuneous Cortex
	3.02	-18	-70	10	L Intracalcarine Cortex
	2.65	2	-56	8	R Precuneous Cortex
	2.33	-20	-70	22	L Cuneal Cortex
	2.28	-6	-60	2	L Lingual Gyrus
	2.27	14	-70	14	R Intracalcarine Cortex
424	3.57	56	-58	-12	R Inferior Temporal Gyrus, temporooccipital part
	3.22	50	-70	-30	R Cerebellar Crus I
	3.01	64	-58	-6	R Middle Temporal Gyrus, temporooccipital part
	2.29	48	-62	-18	R Lateral Occipital Cortex, inferior division
	2.17	42	-66	-16	R Occipital Fusiform Gyrus
381	4.03	10	-46	-50	R Cerebellar Lobule IX
	3.71	18	-50	-58	R Cerebellar Lobule VIIIb
	3.48	4	-44	-56	Brainstem
	2.97	14	-40	-46	R Cerebellar Lobule X
229	3.85	-54	-14	-8	L Superior Temporal Gyrus, posterior division
	3.31	-58	-14	-10	L Middle Temporal Gyrus, posterior division
	2.90	-50	-8	0	L Planum Polare
	2.66	-48	-4	6	L Central Opercular Cortex
	2.48	-56	-14	2	L Planum Temporale
	2.38	-56	-12	6	L Heschl's Gyrus (includes H1 and H2)
138	3.00	28	-84	-22	R Cerebellar Crus I
	2.04	16	-92	-28	R Cerebellar Crus II
137	3.32	-14	58	-10	L Frontal Pole
	2.16	-4	52	-12	L Frontal Medial Cortex
134	3.07	46	-72	32	R lateral Occipital Cortex, superior division
114	3.52	8	26	48	R Superior Frontal Gyrus
	2.72	8	30	28	R Paracingulate Gyrus
103	2.80	-56	-48	-30	L Inferior Temporal Gyrus, temporooccipital part
	2.61	-62	-38	-24	L Inferior Temporal Gyrus, posterior division
ET					
GPi FC-negative					
152	3.54	34	-22	-30	R Temporal Fusiform Cortex, posterior division
	3.47	52	-20	-26	R Inferior Temporal Gyrus, posterior division
	3.05	52	-4	-26	R Middle Temporal Gyrus, anterior division
	2.99	56	-10	-20	R Middle Temporal Gyrus, posterior division

Correlation of FC with clinical scores.

Methods

In patients' group, voxel-wise correlations between either dorsal and ventral portions of the DN or external and internal segments of the GP FC maps and clinical scores (FMTRS scores) were non parametrically performed (FSL randomise, 5000 permutations), with age and gender as covariates of no interest. Results were corrected using false discovery rate (FDR) correction [Benjamini et al. 1995] for multiple comparisons ($p < 0.05$). The minimum cluster extent was set at 100 voxels.

Results

DN

In ET patients, dorsal DN-FC with the left inferior and middle temporal gyri exhibited a positive correlation with tremor severity (Suppl. Fig. 3, Suppl. Table 3), while dorsal DN-FC with cingulate and paracingulate cortices and occipital fusiform, lingual and intracalcarine regions showed a negative correlation with tremor severity (Suppl. Fig. 3, Suppl. Table 3). Ventral DN-FC with the cerebellum (right lobule VI, crus I and II), bilateral frontal pole and paracingulate cortex was positively correlated with tremor severity (Suppl. Fig. 3, Suppl. Table 3).

GP

In ET patients, GPe-FC with the left putamen, pallidum and insular cortex showed a positive correlation with tremor severity, while GPe-FC with pre and post central gyri, anterior cingulate cortex, inferior and middle fontal gyri and orbitofrontal regions exhibited a negative correlation with tremor severity (Suppl. Fig. 3, Suppl. Table 3). Finally, GPi-FC with postcentral gyri, precuneus, left superior parietal lobule and angular gyrus exhibited a negative correlation with tremor severity (Supplementary Fig. 3).

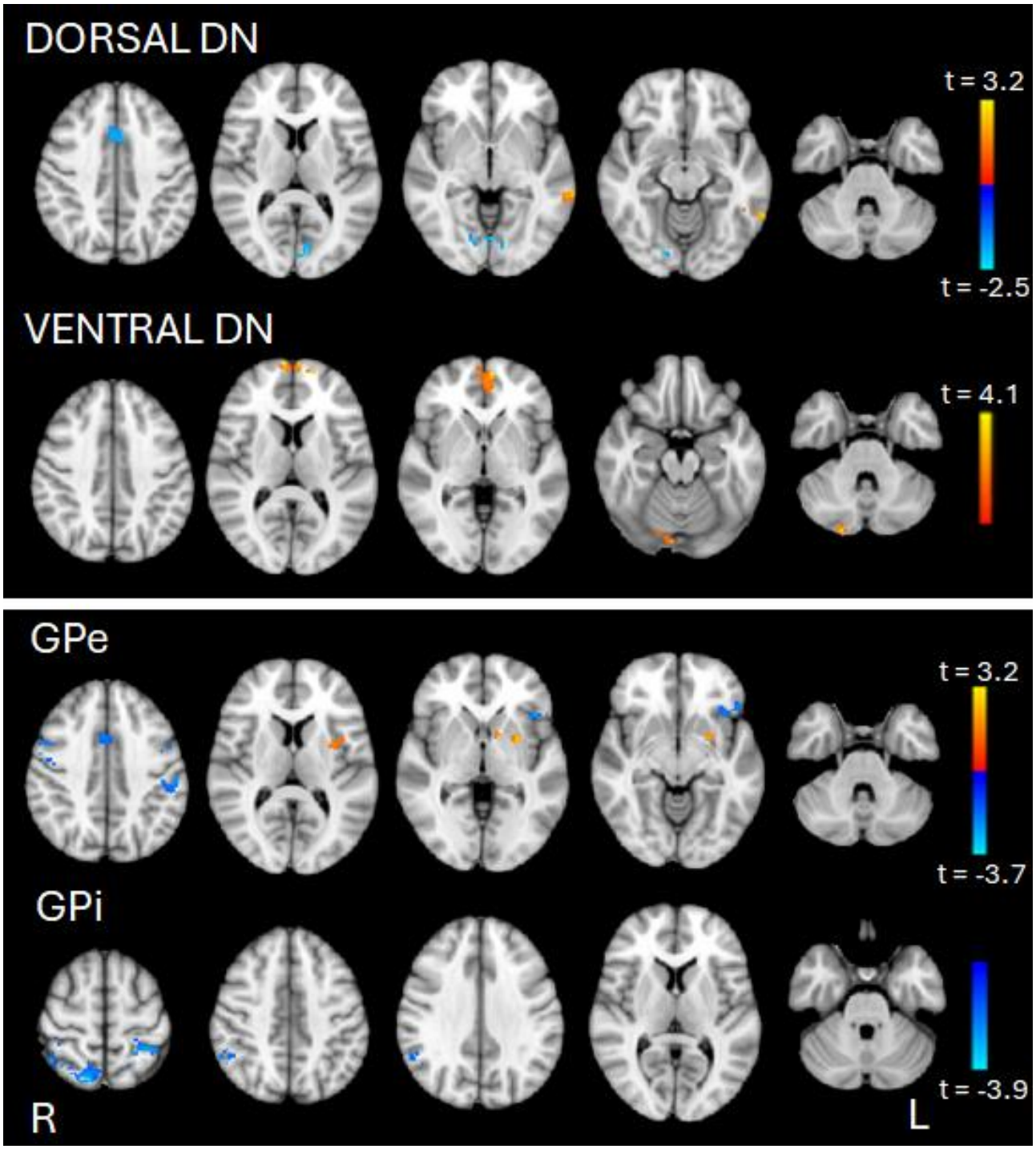

Supplementary Figure 3: Correlation maps of dorsal and ventral portions of the dentate nucleus (DN) rsFC and external and internal segments of the globus pallidus (GPe and GPi) rsFC with tremor severity in ET patients. Positive correlations are shown in red-yellow color, and negative correlations are shown in blue-light blue color. Statistical significance was considered at $p < 0.05$ (FDR corrected).

Supplementary Table 6: Brain regions showing significant correlations between dorsal and ventral portions of the dentate nucleus (DN) and external and internal segments of the globus pallidus (GPe and GPi) functional connectivity maps and tremor severity in ET patients ($p < 0.05$, false discovery rate corrected, minimum cluster extent set at 100 voxels). Anatomical localizations of peak MNI coordinates were established according to Harvard-Oxford cortical and subcortical structural atlases and the cerebellar atlas included in FMRIB's Software Library

		MNI coordinates			
Cluster size (voxels)	**T**	**x**	**y**	**z**	**Cluster location (local maxima)**
ET					
Dorsal DN FC – tremor severity ↑					
154	3.19	-54	-46	-16	L Inferior Temporal Gyrus, temporooccipital part
	2.71	-68	-36	-6	L Middle Temporal Gyrus, posterior division
ET					
Dorsal DN FC – tremor severity ↓					
170	2.44	-2	-78	-2	L Lingual Gyrus
	2.30	10	-76	4	R Intracalcarine Cortex
	2.21	-8	-82	10	L Intracalcarine Cortex
	2.11	16	-70	0	R Lingual Gyrus
	2.02	18	-82	-12	R Occipital Fusiform Gyrus
165	2.17	-4	16	34	L Cingulate Gyrus, anterior division
	1.98	0	6	34	R Cingulate Gyrus, anterior division
	1.86	2	14	42	R Paracingulate Gyrus
ET					
Ventral DN FC – tremor severity ↑					
387	4.01	8	68	10	R Frontal Pole
	3.89	-6	58	0	L Frontal Pole
	2.33	-6	54	-12	L Frontal Medial Cortex
	2.23	-6	42	-2	L Paracingulate Gyrus
121	3.27	20	-90	-34	R Cerebellar Crus II
	2.85	26	-82	-24	R Cerebellar Crus I
	2.57	8	-84	-18	R Lingual Gyrus
	1.70	20	-76	-20	R Cerebellar Lobule VI
ET					
GPe FC – tremor severity ↑					
255	3.19	-28	4	2	L Putamen
	2.07	-40	8	12	L Central Opercular Cortex
	2.01	-36	-2	8	L Insular Cortex
	1.91	-16	2	-6	L Pallidum
	1.66	-26	0	-14	L Amygdala
ET					
GPe FC – tremor severity ↓					
238	3.67	38	-12	66	R Precentral Gyrus
	2.09	52	6	50	R Middle Frontal Gyrus
131	2.34	-42	22	0	L Frontal Operculum Cortex
	2.08	-38	22	-4	L Frontal Orbital Cortex
	1.57	-54	22	6	L Inferior Frontal Gyrus, pars triangularis
	1.48	-52	18	-2	L Inferior Frontal Gyrus, pars opercularis
	1.43	-32	22	2	L Insular Cortex
128	2.39	-2	2	28	L Cingulate Gyrus, anterior division
127	2.66	-54	-26	42	L Postcentral Gyrus
	2.33	-54	-32	42	L Supramarginal Gyrus, anterior division
124	2.59	-40	-48	60	L Superior Parietal Lobule
101	2.62	-52	-2	30	L Precentral Gyrus
ET					
GPi FC – tremor severity ↓					
585	3.86	14	-68	58	R Lateral Occipital Cortex, superior division
	2.72	42	-54	54	R Angular Gyrus
	2.71	40	-38	56	R Superior Parietal Lobule
	2.53	8	-46	68	R Precuneous Cortex
	2.50	18	-42	72	R Postcentral Gyrus
360	2.80	-24	-46	58	L Superior Parietal Lobule

	2.41	-26	-62	64	L Lateral Occipital Cortex, superior division
	2.40	-22	-34	68	L Postcentral Gyrus
	2.38	-10	-62	50	L Precuneous Cortex
144	3.03	60	-52	44	R Angular Gyrus

Benjamini Y, Hochberg Y (1995) Controlling the false discovery rate: a practical and powerful approach to multiple testing. J Roy Stat Soc: Ser B (Methodol) 57:289–300. https:// doi. org/ 10. 1111/j. 2517- 6161.995. tb020 31.x